University of Dundee

University of Dundee

DOCTOR OF PHILOSOPHY

Functions and Mechanisms of the ERK5 MAP Kinase in Pluripotent Stem Cells

Brown, Helen

Award date:
2021

Awarding institution:
University of Dundee

Link to publication

General rights
Copyright and moral rights for the publications made accessible in the public portal are retained by the authors and/or other copyright owners and it is a condition of accessing publications that users recognise and abide by the legal requirements associated with these rights.

- Users may download and print one copy of any publication from the public portal for the purpose of private study or research.
- You may not further distribute the material or use it for any profit-making activity or commercial gain
- You may freely distribute the URL identifying the publication in the public portal

Take down policy
If you believe that this document breaches copyright please contact us providing details, and we will remove access to the work immediately and investigate your claim.

Download date: 21. May. 2025

Functions and Mechanisms of the ERK5 MAP Kinase in Pluripotent Stem Cells

Helen A. Brown

A THESIS SUBMITTED FOR THE DEGREE OF DOCTOR OF PHILOSOPHY.

MRC PROTEIN PHOSPHORYLATION AND UBIQUITYLATION UNIT,

UNIVERSITY OF DUNDEE.

OCTOBER 2021

Contents

List of Figures

List of Tables

List of Abbreviations

ABBREVIATION	MEANING
2C	2-cell stage
ACVR	activin receptor
AGC	automatic gain control
ALK	anaplastic lymphoma kinase
ANXA2	annexin a2
AP2	apetala 2
APS	ammonium persulphate
ATP	adenosine triphosphate
ATP	adenosine triphosphate
BCA	bicinchoninic acid
BET	bromo and extra terminal
BME	2-mercaptoethanol
BMK	big MAP kinase
BMP	bone morphogenic protein
BSA	bovine serum albumen
CCM	cerebral caverous malformations
CDC37	cell division control protein 37
CDK1	cyclin-dependent kinase 1
CHIP	chromatin immunoprecipitation
CHX	cycloheximide
C-MYC	myelocytomatosis
CRISPR	clustered regularly interspaced short palindromic repeats
DMEM	dulbecco's modified eagle medium
DMSO	dimethyl sulphoxide
DNA	deoxyribonucleic acid
DNMT	DNA methyl transferase
DPPA3	developmental pluripotency-associated 3
DTT	dithiothreitol
DUSP	dual-specificity phosphatase
DUX	double homeobox protein
E. COLI	Escherichia coli
E3.5	embryonic day 3.5
ECM	extracellular matrix
EDTA	ethylenediamine tetraacetic acid
EGF	epidermal growth factor
EGTA	ethylene glycol tetraacetic acid
EMT	epithelial-mesenchymal transition
EPHA2	ephrin a2
EPISC	epi stem cell
ERK	extracellular signal-regulated kinase
ESC	embryonic stem cell

ESRRB	steroid hormone receptor ERR2
FAK	focal adhesion kinase
FBS	foetal bovine serum
FBW7	F-box and WD repeat domain-containing 7
FGF	fibroblast growth factor
GAPDH	glyceraldehyde 3-phosphate dehydrogenase
GDP	guanine diphosphate
GFP	green fluorescent protein
GO TERM	gene ontology term
GP130	glycoprotein 130
GRB	growth factor receptor-bound
GSK	glycogen synthase kinase
GST	glutathione S-transferase
GTP	guanine triphosphate
HA	hemagglutinin
HCD	higher energy collisional dissociation
HER2	human epidermal growth factor receptor 2
HIF1	hypoxia-inducible factor 1
HPLC	high-performance liquid chromatography
HPRT1	hypoxanthine phosphoribosyl transferase 1
HRP	horseradish peroxidase
HSP90	heat-shock protein 90
ICM	inner cell mass
ID	inhibitor of differentiation
IGF1	insulin-like growth factor
INH	inhibin
IP	immunoprecipitation
IPSC	induced pluripotent stem cell
IRS	insulin receptor substrate
JAK	Janus kinase
JNK	JUN N-terminal kinase
KCTD10	potassium channel tetramerisation domain 10
KLF	Kruppel-like factor
LAD/RIBP	Lck-associated adapter/Rlk- and Itk-binding protein
LB	Luria-Bertani
LC-MS	liquid chromatography-mass spectrometry
LDS	lithium dodecyl sulphate
LIF	leukaemia inhibitory factor
MAPK	mitogen-activated protein kinase
MAPKK	mitogen-activated protein kinase kinase
MAPKKK	mitogen-activated protein kinase kinase kinase
MEF2	myocyte enhancer factor 2
MEK	MAPK/ERK Kinase
MEKK	MAPK/ERK kinase kinase
MESC	mouse embryonic stem cell

MESC	mouse embryonic stem cell
MKK7	mitogen-activated protein kinase kinase 7
MTOR	mechanistic target of rapamycin
MTORC	mechanistic target of rapamycin complex
MUERVL	murine endogenous retrovirus-L
NCAM1	neural cell adhesion molecule 1
NF-KB	nuclear factor kappa light chain enhancer of activated B cells
NGF	neural growth factor
NP-40	nonidet P-40
OCT4	octamer-binding transcription factor 4
PAGE	polyacrylamide gel electrophoresis
PB1	Phox and Bem1 domain
PBS	phosphate-buffered saline
PDGF	platelet-derived growth factor
PDK1	phosphoinositide-dependent kinase 1
PE	primitive endoderm
PFA	perfluoroalkoxy polymer
PH	pleckstrin homology
PI3K	phosphoinositide 3-kinase
PIP2	phosphatidylinositol 4,5-bisphosphate
PKC	protein kinase C
PMSF	phenylmethylsulphonyl fluoride
PRO	proline
PTEN	phosphatase and tensin homolgy
PVDF	polyvinylidene fluoride
QRT-PCR	quantitative reverse transcriptase polymerase chain reaction
RAS	rat sarcoma
REX	reduced expression 1
RNA	ribonucleic acid
RTK	receptor tyrosine kinase
SDS	sodium dodecyl sulphate
SH2	SRC homology domain 2
SOS	son of sevenless
SOX2	(sex determinin region Y)-box 2
SPS	system performance specification
STAT	signal transducer and activator of transcription
TBS	tris-buffered saline
TCF3	transcription factor 3
TDPOZ3	TRAF and POZ/BTB domain containing protein 3
TEMED	tetramethylethylenediamine
TET	ten-eleven translocation
TFA	trifluoroacetic acid
TGF	transforming growth factor
TMT	tandem mass tag
TRF2	telomeric repeat-binding factor 2

TRIS	tris(hydroxymethyl)aminomethane
T-SCE	telomere sister chromatid exchange
TUBE	tandem ubiquitin-binding entities
UB	ubiquitin
UHRF1	ubiquitin-like containing PHD and RING finger domains 1
VEGF	vascular endothelial growth factor
WNT	wingless-related integration site
XAF1	X-linked inhibitor of apoptosis-associated factor 1
ZFP352	zinc finger protein 352
ZSCAN4	zinc finger and SCAN domain containing 4

Amino Acid Code

AMINO ACID	SINGLE LETTER	THREE LETTER
ALANINE	A	Ala
CYSTEINE	C	Cys
ASPARTIC ACID	D	Asp
GLUTAMIC ACID	E	Glu
PHENYLALANINE	F	Phe
GLYCINE	G	Gly
HISTIDINE	H	His
ISOLEUCINE	I	Ile
LYSINE	K	Lys
LEUCINE	L	Leu
METHIONINE	M	Met
ASPARAGINE	N	Asn
PROLINE	P	Pro
GLUTAMINE	Q	Gln
ARGININE	R	Arg
SERINE	S	Ser
THREONINE	T	Thr
VALINE	V	Val
TRYPTOPHAN	W	Trp
TYROSINE	Y	Tyr

Acknowledgements

This thesis could not have been completed without the help of many others. I would firstly like to thank my supervisor Dr. Greg Findlay for offering me this position, and for the opportunities to discuss ideas and mentor students which have helped develop my skills in both project conception and execution. Furthermore, the support of the past and present members of the Findlay lab has been invaluable, and I am so glad to have had the opportunity to work with all of them.

Within the MRC PPU, I was very fortunate to have access to an incredible support system of lab management and technical staff, without whom I would not have been able to get so much done.

Finally, I would like to express my appreciation and gratitude to my family and friends, but particularly to my parents, grandparents and sister for all their encouragement during my PhD. Last but not least, to Kyle who has had to put up with me every day throughout the whole thing: thank you so much, I could not have done it without you.

Declaration

I hereby declare that the following thesis is based on the results of investigations conducted by myself and that this thesis is of my own composition. Work other than my own is clearly indicated in the text by reference to the researchers or their publications. This dissertation has not in whole, or in part, been previously presented for a higher degree.

I certify that Helen A. Brown has spent the equivalent of at least nine terms in research work in the School of Life Sciences, University of Dundee, and that she has fulfilled the conditions of the Ordinance General No. 14 of the University of Dundee and is qualified to submit the accompanying thesis in application for the degree of Doctor of Philosophy.

List of publications

Brown, H. A.; Williams, C. A. C.; Zhou, H.; Rios-Szwed, D.; Fernandez-Alonso, R.; Mansoor, S.; McMulkin, L.; Toth, R.; Gourlay, R.; Peltier, J.; Dieguez-Martinez, N.; Trost, M.; Lizcano, J. M.; Stavridis, M. P.; Findlay, G. M.; An ERK5-KLF2 signalling module regulates early embryonic gene expression dynamics and stem cell rejuvenation (bioRxiv 2021). Doi: https://doi.org/10.1101/2021.03.29.435803

Summary

ERK5 is a MAPK which is an important regulator of stem cell pluripotency, maintaining naïve pluripotency and suppressing differentiation. Interestingly, ERK5 differs from other MAPKs as it possesses an extended C-terminal domain containing a transcriptional activation domain. However, the biological functions of the ERK5 signalling pathway have not been systematically investigated. In this thesis, I employed quantitative proteomics to identify novel targets of ERK5 signalling, which I subsequently validated biochemically. This screen identified two projects to pursue. Firstly, ANNEXIN A2 and S100A10, which form a heterotetrameric membrane-bound complex, were upregulated in response to ERK5 signalling, implicating ERK5 in membrane dynamics. Secondly, ZSCAN4 isoforms were upregulated by ERK5 signalling, suggesting a role for ERK5 in regulating early embryonic genes and stem cell rejuvenation.

I next dissected the signalling pathway controlling expression of these proteins, and found that ERK5 regulates expression of *Anxa2*, *S100a10*, and *Zscan4* mRNA through KLF2, a transcription factor key to naïve pluripotency and known to be induced downstream of ERK5. I also confirmed a role for ERK5 regulating cell morphology and telomere elongation through these novel targets. Furthermore, I identified a feedback mechanism by which ERK5 transcriptionally induces KLF2, but also post-translationally regulates KLF2, through phosphorylation which promotes ubiquitylation and subsequent degradation. As such, ERK5 can both switch on and switch off the expression of downstream targets, such as ZSCAN4, consistent with the dynamic expression profile of these genes.

1. Introduction

1.1 Pluripotent Stem Cells

1.1.1 The Origin of Pluripotent Stem Cells

Embryogenesis is the process by which an organism is generated from one cell, which has the potential to generate all cells of the organism. As the embryo progresses through a series of cell divisions, more cells are produced, but the number of potential cell types that each daughter cell can generate decreases. The fertilised egg (zygote) represents the point in organism development where the cells have the greatest potential, meaning they can form the greatest number of different cell types (Figure 1.1). As cells deriving from any developmental stage prior to trophoblast lineage commitment can form not only cells of all three germ layers of the embryo proper, but also extra-embryonic tissues of the trophectoderm, these cells are referred to as totipotent (Smith, 2006).

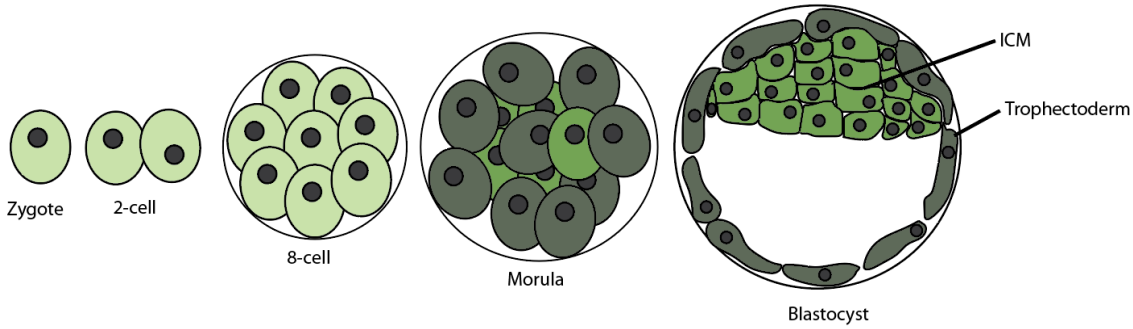

Figure 1.1: Early embryonic development. *The zygote has the capacity to generate all cells of an adult organism and is thus termed totipotent. During a series of divisions, where the embryo becomes clusters of 2, 4, and 8 cells, the cells begin to lose totipotency until they commit to either trophoblast lineage or remain as pluripotent cells in the inner cell mass (ICM) (Panksy, 1982).*

The zygote then undergoes several rounds of cell division to produce a cluster of cells known as the morula by embryonic day 3 (E3) (Panksy, 1982). At this point, cells either polarise to form the trophectoderm (an outer epithelial later) or persist as apolar cells, forming the inner cell mass (ICM) within (Johnson & Ziomek, 1981). The whole structure of trophectoderm and ICM is known as the blastocyst (Johnson & Ziomek, 1981). The cells of the ICM are referred to as pluripotent, as they can differentiate into all three germ layers of the embryo proper, but are unable to form trophoblasts (Smith, 2006).

1.1.2 Types of Pluripotent Cells

1.1.2.1 Embryonic Carcinoma Cells

The study of pluripotency began with the discovery of teratocarcinomas, tumours which contain multiple tissue types, in the 1950s. Cells from these tumours could be serially transplanted, allowing for continuous propagation. This suggested that the tumour contained cells which could not only divide to continue a population of the continuously dividing tumour cells, but could also generate cells for multiple different tissues (Stevens & Little, 1954). Furthermore, isolation of the cells, known as embryonic carcinoma cells, and transplantation into embryos allowed for the generation of chimera organisms, where cells in all tissues could be genetically traced back to the transplanted cells (Papaioannou et al., 1975). As such, pluripotent cells are defined by the ability to differentiate into all three germ layers, whilst retaining the capacity to self-renew indefinitely (Smith, 2006). This dual nature of pluripotency provides a window of opportunity for differentiation into all cell types, meanwhile safeguarding the maintenance of the stem cell population through self-renewal. A number of different categories of pluripotent cells have been identified.

1.1.2.2 Embryonic Stem Cells

The first identified type of pluripotent cell, mouse embryonic stem cells (ESCs) are derived from the ICM of the blastocyst at E3.5 (Evans & Kaufman, 1981). While these cells are unable to form the extra-embryonic trophoblast lineage when transplanted into the embryo (Rossant & Lis, 1979), they retain the capacity to generate all three germ layers (Smith, 2006). Once removed from the embryo, ESCs can be cultured *ex vivo*, kept indefinitely in a state of pluripotency (Evans & Kaufman, 1981). ESCs have been isolated from other organisms including human (as well as sheep, rabbit, cattle, rat, and pig) (Cherny et al., 1994; Giles et al., 1993; Handyside et al., 1987; M. Li et al., 2003; P. Li et al., 2008; Thomson et al., 1998), although human ESCs display different characteristics compared to mouse ESCs, and are more similar to mouse epiblast stem cells (EpiSCs) which are found at E4.5 despite being derived from pre-implantation embryos (Tesar et al., 2007).

1.1.2.3 Induced Pluripotent Stem Cells

In addition to ESCs produced during development, pluripotent cells have been generated by reprogramming adult cells. Known as induced pluripotent stem cells (iPSCs), they can be generated in several ways. Forced expression of pluripotency factors OCT4, SOX2, KLF4, and c-MYC, which coordinate the expression of other stem cell genes, results in the reprogramming of somatic cells back to a pluripotent state (Takahashi & Yamanaka, 2006). Since the discovery of these so called Yamanaka factors, other combinations of factors have been used for reprogramming, including LIN28 + NANOG, and ESRRB amongst others replacing one or more of the Yamanaka factors (Feng et al., 2009; Yu et al., 2007). Alternatively, chemical reprogramming can be used to reproducibly alter somatic cell fate to a desired lineage using different cocktails of potent small molecules, including inhibitors of histone deacetylases, histone methyltransferases, and kinases such as MEK and GSK3 (Biswas & Jiang, 2016; Hou et al., 2013; Lin et al., 2009).

1.1.3 Therapeutic Applications

The study of pluripotent stem cells presents many exciting applications, as they are able to indefinitely self-renew and can generate any differentiated cell type. Firstly, pluripotent stem cells offer the opportunity for tissue regeneration which, particularly in the case of iPSCs, can be used as an alternative to transplant of organs from donors which reduces the risk of tissue rejection. Additionally, stem cell therapy can be used to treat a variety of degenerative diseases and injuries, including hematopoietic disorders, injuries to the spinal cord or musculoskeletal tissue, and liver damage (Liu et al., 2011; Nori et al., 2011; Suzuki et al., 2013; Tan et al., 2012).

Secondly, pluripotent stem cells can be used to model the genotype-phenotype relationship in disease. For example, ESCs were used to characterise the disease phenotype associated with Lesch-Nyhan syndrome, which is caused by disruption of the *Hprt1* gene (A. Urbach, 2004). Furthermore, chromosomal diseases such as Down and Turner syndromes and complex disorders such as autism spectrum disorder and schizophrenia have also been successfully modelled in pluripotent stem cells (Brennand et al., 2011; Briggs et al., 2013; DeRosa et al., 2012; Achia Urbach & Benvenisty, 2009).

Finally, pluripotent stem cells are useful for testing drug toxicity. Pluripotent stem cells have the benefit of being inexpensive compared to animal models or human clinical trials, and so can be used for early detection of drug toxicity to prevent the costly and time consuming process of drug manufacture. Furthermore, by employing differentiation studies alongside toxicity assays, potential side effects can be identified for specific tissues (Choi et al., 2013; Liang et al., 2013).

1.1.4 Molecular Basis of Pluripotency

Pluripotency is characterised by transcription factors which coordinate the expression of genes required for self-renewal. These transcription factors are known as pluripotency factors. Amongst the best characterised of these are OCT4, NANOG, and SOX2. As knock out of these factors prevents ICM formation due to all cells adopting trophoblast lineage, OCT4, NANOG and SOX2 are essential for pluripotency (Avilion et al., 2003; Chambers et al., 2003; Nichols et al., 1998). OCT4, NANOG, and SOX2 share binding sites at promoter sequences for genes involved in maintaining the pluripotency transcriptional programme, including their own promoters, leading to an autoregulatory transcriptional pluripotency network (Loh et al., 2006; Rodda et al., 2005). In addition to these core pluripotency factors, other transcription factors are also markers of pluripotency. These include ESRRB, which is expressed in a NANOG-dependent manner and regulates expression of OCT4, KLF2 and REX1 (Ivanova et al., 2006; Yeo et al., 2014; Zhang et al., 2008). Kruppel-like factors (KLFs) are also critical transcription factors for pluripotency, with KLF2, KLF4, and KLF5 required for stem cell self-renewal (Jiang et al., 2008). REX1 is a transcriptional repressor and marker of pluripotency, and, while key for pluripotency acquisition, is not required for pluripotency maintenance (Gontan et al., 2012; Masui et al., 2008; Scotland et al., 2008). In summary, pluripotency is coordinated by a hierarchical circuitry of transcription factors.

1.1.5 Distinct Pluripotent States have been Identified

During development, the number of cell types that a stem cell can give rise to decreases. As such, there exists a developmental continuum from totipotency through pluripotency to differentiated cells. Additionally, distinct states within pluripotency have been

identified which add more complexity to this scale. In mESCs, naïve-like cells represent ESCs derived from the ICM at E3.5, primed-like cells represent post-implantation EpiSCs around E4.5, and formative pluripotency represents a state between naïve and primed.

1.1.5.1 Naïve pluripotency

Culturing ESCs in the presence of inhibitors of the MEK1/2 and GSK3 kinases (2i media) maintains cells in a homogenous naïve-like "ground" state (Ying et al., 2008). This represents the earliest developmental state, at E3.5 in mice, which can give rise to the three germ layers of the embryo proper but not the trophectoderm (Ying et al., 2008). Alternatively, ESCs can be cultured in the presence of Leukaemia Inhibitory Factor and foetal bovine serum (LIF/Serum). In LIF/Serum, ESCs exist in a dynamic equilibrium between naïve, primed and formative pluripotency (Nichols & Smith, 2009) (Figure 1.2). Naïve stem cells can be derived from the ICM of E3.5 mouse embryos (Nichols & Smith, 2009).

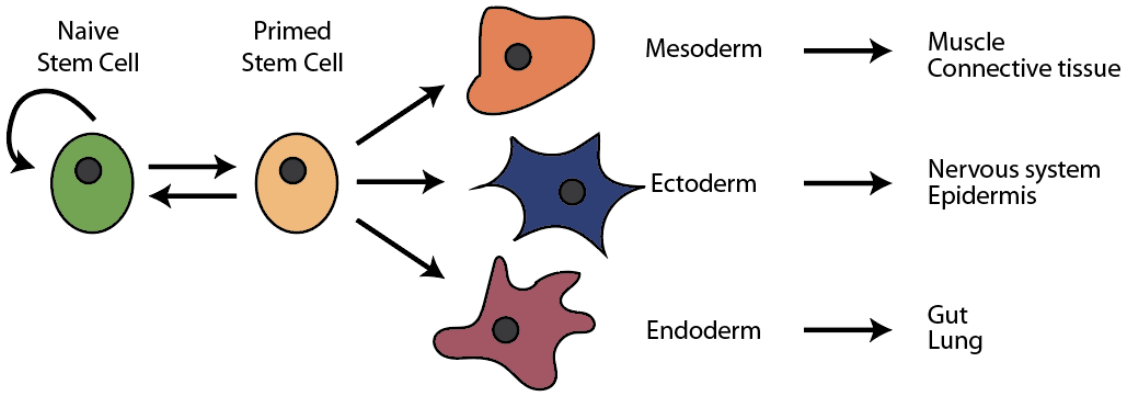

Figure 1.2: Distinct pluripotent states represent different stages in developmental continuum. *Pluripotent ESCs exist in a dynamic equilibrium between different states, which allows differentiation into any germ layer while safeguarding self-renewal. Naïve-like cells efficiently self-renew, whereas primed cells are poised for differentiation, which leads to the generation of any tissue in the adult body (Nichols & Smith, 2009).*

Naïve pluripotency encompasses ground state pluripotency; however, cells can only be described as ground state if they are defined by the 2i culture condition, or the transcriptional and epigenomic landscape arising from 2i (Ying et al., 2008). Naïve-like cells in culture exhibit a domed morphology, efficiently self-renew and are characterised by the expression of key pluripotency markers, including transcription factors OCT4,

NANOG, and SOX2, which coordinate the expression of other pluripotency factors characteristic of naïve pluripotent cells including ESRRB, REX1, and KLFs (Chambers et al., 2003; Dunn et al., 2014). The KLF family contains 17 members, of which KLF2, KLF4, and KLF5 are required for self-renewal (Jiang et al., 2008), although KLF2 alone is reportedly sufficient to sustain the naïve state (Yeo et al., 2014).

1.1.5.2 Primed pluripotency

The term primed pluripotency is used to describe cells which still express pluripotency markers such as OCT4, but have reduced expression of others including NANOG and SOX2, and instead express early lineage markers such as BRACHYURY, DNMT3B, and FGF5 (Ficz et al., 2011; Nichols & Smith, 2009). Human ESCs derived from the equivalent pre-implantation developmental timepoint as mouse E3.5 are found in the primed state, although they differ from mouse EpiSCs in that they express high levels of NANOG (Darr et al., 2006). The primed state can represent both cells in the early stages of specification towards the primitive endoderm (PE) at mouse E4.5 and EpiSCs derived from mice at E5.5 (Tesar et al., 2007). However, mESCs do not efficiently differentiate to PE cells *in vitro*. Primed-like cells exhibit a flattened morphology and are poised towards differentiation (Nichols & Smith, 2009). Unlike naïve cells, primed cells display increased mobility and cell adhesion, reminiscent of the epithelial-mesenchymal transition (EMT) process during development (Kalkan et al., 2017). EMT allows a polarised epithelial cell to become a mesenchymal cell by gaining increased migratory capacity and resistance to apoptosis resistance, as well as the production of extracellular matrix (ECM) components and ECM-degrading agents. EMT is characterised by the expression of specific cell surface proteins and reorganisation of the cytoskeleton (Kalluri & Neilson, 2003; Kalluri & Weinberg, 2009).

1.1.5.3 Formative pluripotency

Recently, a state on the developmental continuum between naïve and primed pluripotency was described, termed formative pluripotency (Smith, 2017). This is hypothesised to entail transcriptional, epigenetic, signalling and metabolic remodelling required to

facilitate the response to lineage specification cues and maintain multi-lineage competence (Smith, 2017). Formative pluripotency represents cells found in the ICM between E4.5 and E5.5 (Kalkan et al., 2017). Molecularly, formative cells express OCT4, but are devoid of both naïve markers and early lineage markers, and are hence distinct from both naïve and primed pluripotency (Kalkan & Smith, 2014).

1.1.5.4 Totipotent-like stem cells and pluripotency

Interestingly, an additional transient state has been identified whereby naïve-like ESCs in LIF/Serum revert back to a 2-cell stage (2C) phenotype, and can therefore be considered totipotent-like (T. Amano et al., 2013). In this 2C phase, cells do not show any changes in morphology relative to the naïve state, but change their transcriptional programme. This totipotent state is characterised by the expression of factors including ZSCAN4, which bring about the global DNA demethylation necessary for this stage of development (Eckersley-Maslin et al., 2016). This is achieved by ZSCAN4 recruiting E3 ubiquitin ligase UHRF1 to DNA methyltransferase DNMT1, resulting in the ubiquitylation and degradation of both UHRF1 and DNMT1 (Dan et al., 2017). In cultured ESCs, ZSCAN4-dependent DNA demethylation creates a permissive environment for recombination events, which results in telomerase-independent rapid telomere extension (Dan et al., 2017; Falco et al., 2007). Telomeres are non-coding regions at the ends of chromosomes, which prevent the degradation of coding DNA during cell division. Therefore, telomere extension protects genome stability of ESCs in long term culture, and this process is therefore known as stem cell rejuvenation. Evidence that this 2C state differs from pluripotency comes from expression of OCT4, a universal marker of pluripotency, which is downregulated as the cells enter this transient state, and is subsequently re-expressed upon leaving this state (Hirata et al., 2012). In addition to being a critical process in cultured ESCs, expression of ZSCAN4 has potential for improving iPSC generation efficiency, as a key barrier to reprogramming is reversing DNA methylation found in somatic cells (Jiang et al., 2013).

In summary, pluripotent stem cells can self-renew indefinitely but retain the capacity to differentiate into any of the germ layers of the embryo proper. This makes pluripotent stem cells vital in development as well as offering exciting opportunities for therapeutic application. However, pluripotency is not a homogenous state, and instead consists of a number of molecularly distinct states which exist along a developmental continuum. A network of transcription factors regulates the pluripotency transcriptional programme.

1.2 Signalling Pathways are Key Regulators of Stem Cell Pluripotency

The transition from totipotency through pluripotency to differentiation is a key event during development and is therefore tightly regulated by signalling pathways. Signalling pathways transduce stimuli from outside and within the cell to downstream effectors, frequently transcription factors, resulting in a change of cellular activity in response to the stimulus (Matthews & Gerritsen, 2010). Post-translational modifications are often used to propagate these signals. Protein kinases, which phosphorylate substrates, are one of the most common components of signalling pathways, although most studies into kinase regulation have studied approximately 10% of the kinome (Fedorov et al., 2010). This leaves a large number of kinases understudied and significant potential therapeutic applications untapped (Fedorov et al., 2010).

1.2.1 An Overview of Phosphorylation

Phosphorylation involves the modification of a hydroxyl group-containing residue (eg serine, threonine or tyrosine) with a phosphate group. This large negative charge then alters protein characteristics, leading to conformational changes, change of interaction partners, or changes in activity (Fischer & Krebs, 1955; Sutherland & Wosilait, 1955). The phosphate group is taken from the γ phosphate of ATP and transferred to the substrate via a transesterification reaction (Figure 1.3).

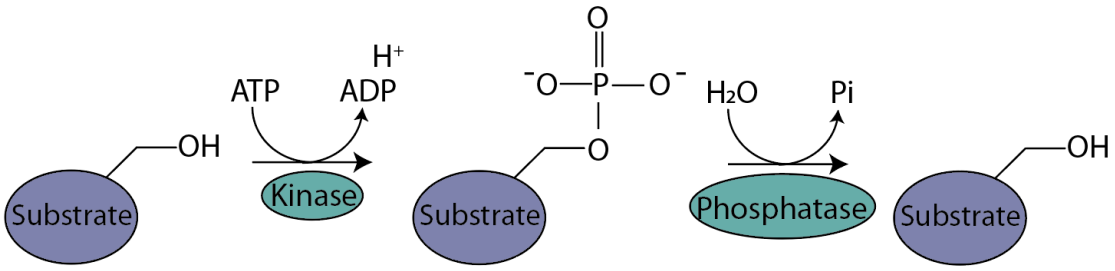

Figure 1.3: Phosphorylation and Dephosphorylation. *A kinase catalyses the transfer of phosphate onto a hydroxyl-containing residues. A phosphatase reverses this by hydrolysing the phosphodiester bond.*

1.2.1.1 Kinases

Protein kinases can broadly be grouped into those which phosphorylate serine/threonine, those that phosphorylate tyrosine, and dual specificity kinases. Mitogen-activated protein kinases (MAPKs) are examples of serine/threonine kinases, and have been extensively studied in many cellular systems (Cargnello & Roux, 2011). Receptor tyrosine kinases (RTKs) represent some of the best characterised members of the tyrosine kinase class, and function as transmembrane kinases by receiving a signal via ligand binding on the extracellular surface of the membrane which leads to activation of the kinase domain inside the cell (Lemmon & Schlessinger, 2010). This leads to phosphorylation of intracellular substrates, and hence signal propagation. There are also protein kinases which phosphorylate other residues, such as histidine (Wolanin et al., 2002), although histidine kinases are thought to be more common in non-animal species.

1.2.1.1.1 Regulation of Kinases

Kinases must be regulated by the cell to ensure they are only functional when necessary. This can be achieved through binding of activator or inhibitor proteins or small molecules, by controlling their cellular location in relation to their substrates, or through their own phosphorylation status (Cargnello & Roux, 2011). MAPKs in particular require phosphorylation on their activation loop for activity. Prior to phosphorylation, the activation loop resides within the kinase active site (Huse & Kuriyan, 2002; Zhang et al., 1995). Upon dual phosphorylation on the conserved T-X-Y motif, the activation loop is

expelled from the active site, enabling substrate and ATP binding, and hence substrate phosphorylation to occur (Figure 1.4) (Huse & Kuriyan, 2002; Zhang et al., 1995).

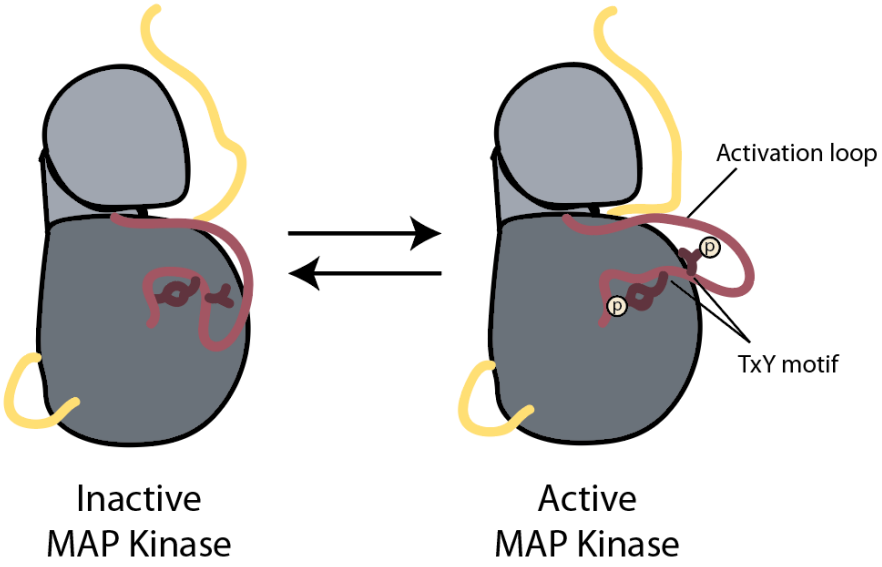

Figure 1.4: Phosphorylation of the activation loop of kinases causes a conformational change resulting in the revelation of the kinase active site. *ERK2 (shown above as a representative of other MAPKs) is phosphorylated at a TXY motif in its activation loop. As a result, the loop shifts, providing access to the active site. Adapted from (Huse & Kuriyan, 2002).*

Phosphatases are responsible for the removal of phosphate groups. Phosphatase activity is vital in cells as it facilitates the switching off of a pathway when it is no longer needed, for example when the stimulus has been removed (Cohen, 1989). There are fewer phosphatases than kinases, but again they are classed according to the residues they dephosphorylate, namely those which dephosphorylate serine and threonine, those which dephosphorylate tyrosine, and dual specificity phosphatases (Chen et al., 2017). Phosphatases are significantly understudied compared to kinases as they are highly structurally divergent and promiscuous, which makes genetic approaches as well as the development of specific and selective inhibitors challenging (M. J. Chen et al., 2017).

1.2.1.1.2 Kinases as drug targets

Due to the conserved nature of the kinase active site, and the necessity to bind ATP, specific kinase inhibitors can be readily designed (Gashaw et al., 2011). This makes them important candidates for therapeutic applications for diverse diseases, with approximately 30% of current R&D spending in pharmaceutical companies focused on kinase inhibitor

development. Examples of clinically approved kinase inhibitors include trametinib (a MEK1/2 inhibitor used to treat skin cancer), upadacitinib (a JAK inhibitor used to treat rheumatoid arthritis) and sirolimus/rapamune (an mTOR inhibitor used to treat kidney transplants) (Flaherty et al., 2012; Sehgal, 1998; Serhal & Edwards, 2019). The kinase active site has several key residues, mutation of which results in deletion of kinase activity. These include an aspartate residue, responsible for hydrogen bonding and orientating the substrate hydroxyl, and a lysine and glutamate pair which polarise the active site, making it more energetically favourable to transfer the phosphate to the substrate (Zhang et al., 1995). A hydrophobic patch also plays an important role in reaction intermediate stabilisation.

1.2.2 Kinase Regulation of Pluripotency

Kinases can be activated through a number of different mechanisms, including growth factors, cytokines and chemical signals, and through mechanical signals and interactions with the cellular environment (such as contacts with neighbouring cells or the extracellular matrix). Most signalling pathways culminate in transcriptional regulation. This occurs through target gene transcription, induced by a combination of transcription factors and epigenetic regulation. This is particularly true in pluripotency – the major pluripotency markers, namely OCT4, NANOG, and SOX2, are transcription factors which coordinate the expression of other pluripotency genes (Chambers & Tomlinson, 2009). This is similarly true of KLFs including KLF2 (Yeo et al., 2014). Although transcriptional targets of different signalling pathways are well characterised, the precise mechanism of transcriptional activation is challenging to elucidate due to the interplay of transcription and epigenetic factors. Kinases play an important role in the regulation of pluripotency, with a number of pathways studied extensively.

1.2.2.1 Leukaemia Inhibitory Factor Receptor (LIFR)

One of the most studied signalling pathways regulating pluripotency is LIF signalling, which promotes self-renewal and pluripotency in mESCs. LIF is a member of the interleukine-6 cytokine family, and binds to its receptor (LIFR) and glycoprotein-130

(gp130), both of which contain a proline-rich region. These receptors heterodimerise but lack intrinsic kinase activity. However, Janus kinases (JAKs) which associate with the proline-rich regions of both LIFR and gp130 are brought together by the receptor dimerisation, resulting in trans-autophosphorylation and kinase activation (Davis et al., 1993; Neil Stahl et al., 1994). Although LIF can activate JAKs including JAK1, JAK2, and TYK2, JAK1 is critical for the maintenance of pluripotency, with RNA inhibition of JAK1 resulting in mESC differentiation (Ernst et al., 1996; Guschin et al., 1995). JAKs then phosphorylates Y-x-x-Q motifs on gp130 and LIFR, which recruit STAT3 to the receptor complex in an SH2 domain-dependent manner (Stahl et al., 1995). This results in STAT3 phosphorylation by JAK at Tyr705, which allows for STAT3 dimerisation and hence nuclear translocation (Heinrich et al., 1998; Niwa et al., 1998). Once in the nucleus, STAT3 acts as a transcription factor for pluripotency genes including *Klf4* (Bourillot et al., 2009).

1.2.2.2 Bone Morphogenic Protein (BMP)

Despite the importance of LIF signalling in pluripotency maintenance, it is insufficient to sustain self-renewal, requiring serum in addition, which supplies mESCs with further growth factors (Ying et al., 2003). Of particular note is BMP, a member of the TGFβ family. The TGFβ family consists of 33 members in mammals, including agonists such as TGFβ, Activin, and BMP, and antagonists such as Inhibins and LEFTYs. BMP binds to the type II receptor Bone Morphogenic Protein Receptor Type-2. (Miyazono et al., 2010; Ying et al., 2003). This leads to the recruitment of recruits and phosphorylates a type I receptor, such as ALK3 or ALK6 (Miyazono et al., 2010). Upon phosphorylation and activation, ALK phosphorylates SMADs 1, 5, and 8, leading to complex formation with SMAD4, and nuclear translocation of this complex, whereupon transcription of BMP target genes such as *Oct4*, *Sox2* and *Nanog* can be induced (Chen et al., 2008). The Inhibitor of Differentiation (ID) proteins are important downstream targets of BMP signalling, which allow for mESC maintenance in the absence of serum or BMP (Shi & Massagué, 2003; Ying et al., 2003).

1.2.2.3 Fibroblast Growth Factor Receptor/Extracellular-signal Regulated Kinase 1/2 (FGFR-ERK1/2)

Kinases not only support pluripotency, but can also promote differentiation. Fibroblast growth factor 4 (FGF4) signalling is one such pathway which is instrumental in differentiation (Feldman et al., 1995). FGF4 primarily binds FGF receptor 2 (FGFR2) in mESCs, resulting in receptor autophosphorylation and SH2 domain-dependent recruitment of Growth factor Receptor-Bound protein 2 (GRB2) (Arman et al., 1998). GRB2 then recruits RAS guanine nucleotide exchange factor SOS which catalyses GDP-GTP exchange on RAS GTPase (Cheng et al., 1998). This exchange activates RAF kinases, which then lead to the sequential phosphorylation and activation cascade of MEK1/2 and ERK1/2 (Payne et al., 1991). ERK1/2 can then phosphorylate substrates such as ELK1, C-FOS, P53 and C-JUN, the downstream transcriptional programme of which leads to mESC transition to the primed state (Kunath et al., 2007). Inhibition of MEK1/2 promotes the conversion of mouse epiSCs to ESC-like cells, and the combined treatment of ESCs with MEK1/2 and GSK3 inhibitors supports naïve pluripotency (Ying et al., 2008; Zhou et al., 2010). Physiologically, ERK1/2 is important for development, particularly of neural tissue, with *Erk2*$^{-/-}$ resulting in deficiencies in neural crest development and microcephaly (Newbern et al., 2008; Samuels et al., 2008).

1.2.2.4 Glycogen Synthase Kinase 3 (GSK3)

Additionally, Glycogen Synthase Kinase 3 (GSK3) promotes the ubiquitylation and subsequent degradation of β-CATENIN by phosphorylating β-CATENIN (Yost et al., 1996). WNT and PI3K signalling act in opposition to this pathway by inhibiting GSK3 (Sokol, 2011). This leads to β-CATENIN accumulation, which inhibits T Cell Factor 3 (TCF3), a repressor of pluripotency genes (Hikasa et al., 2010). As such, WNT signalling is a promoter of naïve pluripotency and GSK3 primes mESCs for differentiation. The role of GSK3 in promoting pluripotency exit is further confirmed by the phenotype of *Gsk3α*$^{-/-}$ *Gsk3β*$^{-/-}$ double knockout mESCs, which display enhanced self-renewal (Bone et al., 2009). The use of 2i media demonstrates the importance of the GSK3 and ERK1/2

signalling pathways in pluripotency, as inhibition of these pathways is sufficient to suppress differentiation and maintain naïve pluripotency (Ying et al., 2008).

1.2.2.5 Phosphoinositide 3-kinase/AKT (PI3K/AKT)

PI3K/AKT signalling also has vital roles in pluripotency maintenance, with knock out or inhibition of any of the key components of the pathway resulting in embryonic lethality (Bi et al., 1999; Murakami et al., 2004; Peng et al., 2003). PI3K is canonically activated through IGF1/insulin stimulation via the receptor regulatory subunit or adaptor molecules such as the insulin receptor substrate (IRS) proteins (Harrington et al., 2004). PI3K phosphorylates phosphatidylinositol-(3,4)-bisphosphate (PIP2) to make phosphatidylinositol-(3,4,5)-trisphosphate (PIP3), a process which can be reversed by Phosphatase and Tensin Homologue (PTEN) which thereby inhibits this pathway (Li et al., 1997). AKT is recruited through its pleckstrin homology (PH) domain to the plasma membrane by PIP3, where it is phosphorylated at Thr308 by PDK1 and at Ser473 by mTORC2, a kinase complex responsible for metabolic sensing and regulation (Alessi et al., 1997; Sarbassov et al., 2005). Once activated, AKT can phosphorylate a number of different substrates, including GSK3 (Cross et al., 1995). PI3K is thought to maintain pluripotency by inhibiting ERK1/2 and GSK3 signalling, as indicated by its dispensability in culture with 2i media (Hishida et al., 2015). Furthermore, PI3K has been implicated in the regulation of stem cell rejuvenation factor ZSCAN4, as an upstream signalling pathway inducing its expression (Storm et al., 2009).

1.2.2.6 Other Kinases

Protein Kinase C (PKC) and SRC also promote pluripotent exit, the former through activation of NF-κB, and the latter which promotes the epithelial-mesenchymal transition upon upregulation by ERK1/2 signalling (Dutta et al., 2011; Li et al., 2011). Inhibition of PKC signalling is sufficient to derive and maintain ESCs and further facilitates the reprogramming of somatic cells to iPSCs (Dutta et al., 2011). Similarly, inhibition of SRC abolishes mESC differentiation (Li et al., 2011).

1.2.2.7 Extracellular-signal Regulated Kinase 5 (ERK5)

ERK5 is another MAPK which regulates ESC pluripotency. However, in contrast to closely-related kinases ERK1/2, ERK5 promotes naïve pluripotency and suppresses differentiation (Figure 1.5) (Williams et al., 2016). The ERK5 signalling pathway is activated by growth factors and extracellular stress stimuli, which activate MAPK/ERK Kinase Kinases 2 and 3 (MEKK2/3) (Figure 1.6) (Chao et al., 1999; Sun et al., 2001). MEKK2/3 then phosphorylate and activate MAPK/ERK Kinase 5 (MEK5), which selectively activates ERK5 (Chao et al., 1999; Sun et al., 2001; Zhou et al., 1995). ERK5 regulates pluripotency through the induction of KLFs, particularly KLF2 and KLF4 (Sunadome et al., 2011; Williams et al., 2016).

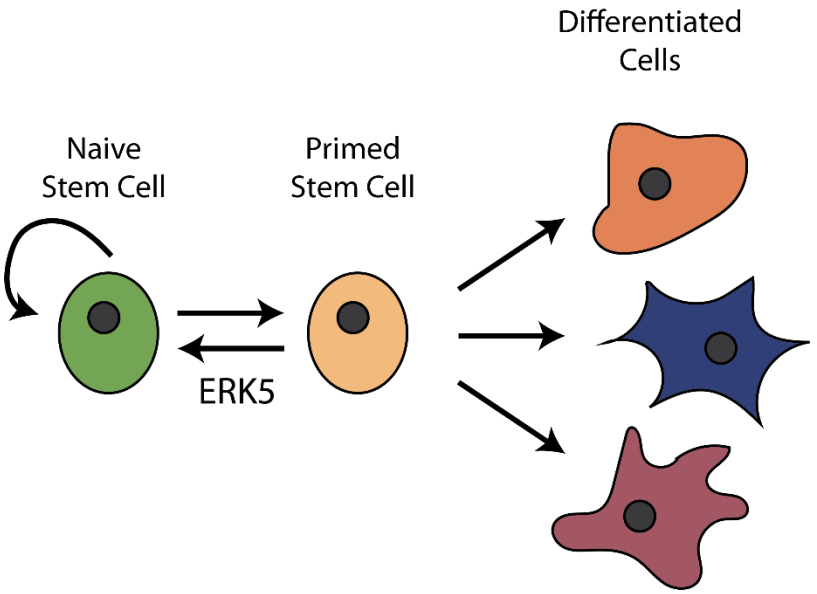

Figure 1.5: ERK5 identified as a promoter of naïve pluripotency by screen for kinases regulating the naïve-primed transition. *A screen of kinase inhibitors was used to identify kinases which regulated the transition between naïve and primed pluripotency. ERK5 was identified as a kinase which promoted naïve pluripotency (Williams et al., 2016).*

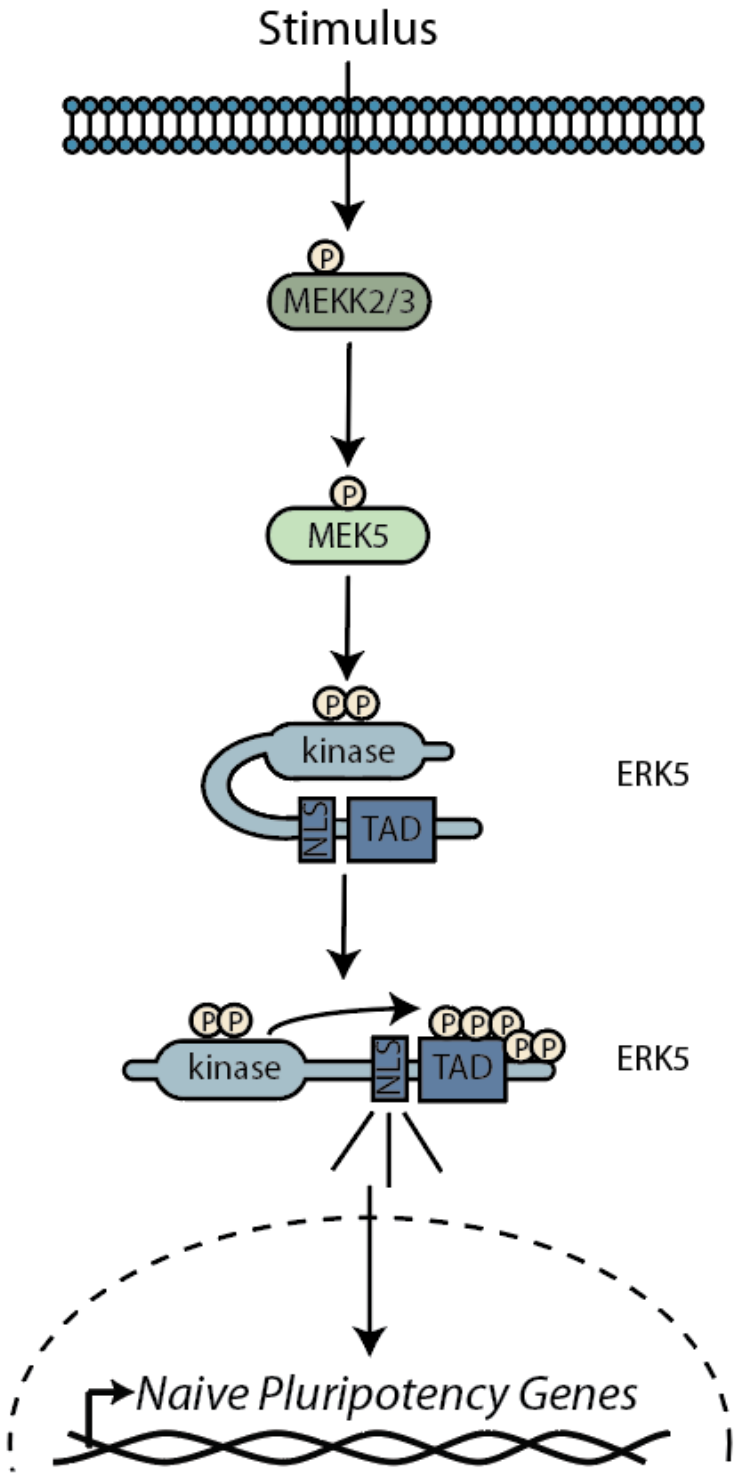

Figure 1.6: ERK5 signalling pathway. *An external stimulus triggers the activation of MEKK2/3. MEKK2/3 phosphorylate and activate MEK5, the only known upstream kinase of ERK5. MEK5 phosphorylates and activates ERK5 at its activation loop, leading to activation of ERK5 kinase activity. ERK5 then phosphorylates its C-terminal region, resulting in a conformational change, exposing the nuclear localisation signal (NLS) and activating the transcriptional activation domain (TAD). ERK5 then translocates to the nucleus, where it can regulate the expression of stem cell genes such as Klf2 through its kinase and/or transcriptional activation activities.*

Previous work in the Findlay lab identified ERK5 in a screen to identify kinases which regulate the transition between naïve and primed pluripotency, and as an understudied kinase was prioritised for further investigation (Williams et al., 2016).

1.3 The ERK5/BMK1 MAP Kinase

1.3.1 Discovery of ERK5

ERK5 was initially discovered in 1995, by two independent methods. Firstly, ERK5 was identified as a binding partner for the newly identified MEK5 through a yeast two-hybrid screen (G. Zhou et al., 1995). Additionally, a novel MAPK gene was identified in a screen in human placental cDNA, which was termed Big MAPK 1 (BMK1) as it was found to be much larger than other MAPKs such as ERK1/2 (Lee et al., 1995). BMK1 and ERK5 were subsequently found to be the same species.

1.3.2 ERK5 structure

ERK5 is a unique MAPK as it contains not only the canonical kinase domain, but also an extended C-terminal region (G. Zhou et al., 1995). This region contains a nuclear localisation signal and a transcriptional activation domain (Buschbeck & Ullrich, 2005; Kasler et al., 2000). These two activities, kinase and transcriptional activity, suggest that ERK5 can modulate target gene transcription through either phosphorylation of transcription factor substrates or alternatively through direct transcriptional activation (for example interacting with gene promoters either alone or in combination with transcription factors).

1.3.3 Regulation of ERK5 pathway

1.3.3.1 ERK5 pathway activation

ERK5 can be activated by several extracellular signals including hyperosmolarity, oxidative stress, and growth factors such as EGF, VEGF, NGF, PDGF, and BMP (Abe et

al., 1996; Finegan et al., 2009; Holmes et al., 2007; Kato et al., 1998; Lennartsson et al., 2010; Morikawa et al., 2016; Razumovskaya et al., 2011; Roberts et al., 2010). Like the closely related ERK1/2 kinases, ERK5 is the effector kinase in a canonical MAPK cascade. The only known upstream MAPKKKs of the ERK5 pathway are MEKK2 and MEKK3 (Chao et al., 1999; Sun et al., 2001). These kinases share 94% sequence identity in their C-terminal moiety, but differ significantly within their N-terminal regions (65% homologous) to allow for differential regulation of the pathway (Blank et al., 1996). This allows MEKK2 and MEKK3 to perform overlapping but distinct cellular functions. For example, MEKK2 but not MEKK3 binds the SH2-domain containing adaptor protein Lad/RIBP which is involved in T cell antigen presentation (Sun et al., 2001), whereas MEKK3 mediates EGF receptor-dependent activation of the ERK5 pathway (Chao et al., 1999), demonstrating that although both MEKK2 and MEKK3 mediate signal transduction, they are subject to differential stimulus- and cell type-specific regulation.

MEKK2 and MEKK3 contain PB1 domains, which allow for complex formation with the PB1 domain of MEK5, resulting in a heterotrimer of all three hierarchical tiers of the MAPK cascade (MEKK-MEK5-ERK5) (Nakamura & Johnson, 2003). MEKK2 and MEKK3 also transduce signals to other MAPK pathways, including JNK (Nakamura & Johnson, 2007). The ability of MEKK2/3 to preferentially activate JNK or ERK5 signalling pathways is based on the phosphorylation status of MEKK2, as quiescent MEKK2 preferentially binds MEK5, whereas activated MEKK2 engages MKK7, the specific upstream kinase of JNK (Nakamura & Johnson, 2007). MEKK3 can be functionally inhibited by cerebral cavernous malformation (CCM) proteins, with CCM proteins sterically disrupting the formation of the MEKK3-MEK5-ERK5 complex and thereby disrupting ERK5 signalling (Cuttano et al., 2016; Zhou et al., 2015).

1.3.3.2 MEK5

MEK5 is the only identified upstream MAPKK that phosphorylates ERK5, and does not phosphorylate and activate any other MAPK family members such as ERK1/2 (Lee et al., 2017; Lee et al., 1995; Ohnesorge et al., 2010). As per canonical MAPK signal

cascades, MEK5 is phosphorylated and activated by upstream kinases MEKK2 or MEKK3, and then in turn phosphorylates and activates ERK5 (Chao et al., 1999; Sun et al., 2001; Zhou et al., 1995). This phosphorylation occurs at Thr218/Tyr220 within the TEY motif in the activation loop of ERK5 (Mody et al., 2003). Upon ERK5 kinase activation, ERK5 can not only autophosphorylate, but it can also phosphorylate MEK5 in a feedback mechanism (Mody et al., 2003). This decreases the affinity of the interaction between MEKK2/3 and MEK5 (Mody et al., 2003).

1.3.3.3 ERK5 nuclear translocation

Before cells are stimulated, ERK5 is found complexed to chaperone protein HSP90 in the cytoplasm. HSP90 maintains ERK5 in an autoinhibited state, obscuring the nuclear localisation signal, and tethering ERK5 to the cytoplasm (Gomez et al., 2016). When a stimulus is applied, MEKK2/3 phosphorylate and activate MEK5 (Chao et al., 1999; Sun et al., 2001). MEK5 then phosphorylates and activates ERK5 on its activation loop (Mody et al., 2003). With ERK5 kinase now active, ERK5 autophosphorylates its C-terminal region (Morimoto et al., 2007). This leads to a conformational change, dissociation of HSP90, relief of autoinhibition, and nuclear localisation signal revelation (Kondoh et al., 2006). ERK5 therefore translocates to the nucleus, where it can achieve its transcriptional roles, including phosphorylation of transcription factor substrates and direct transcriptional regulation.

Alternatively, ERK5 may enter the nucleus through another mechanism, independent of its own kinase activity (Figure 1.7). The ERK5 C-terminal region may be phosphorylated by other kinases, such as CDK1, which causes the same conformational change and subsequent nuclear localisation (Iñesta-Vaquera et al., 2010). Again, ERK5 can perform all its transcriptional roles in this case. Additionally, CDC37 overexpression, such as occurs in some cancers, can eject HSP90 from its complex with ERK5 (Erazo et al., 2013). With HSP90 uncomplexed, ERK5 conformational change can occur, leading to nuclear localisation.

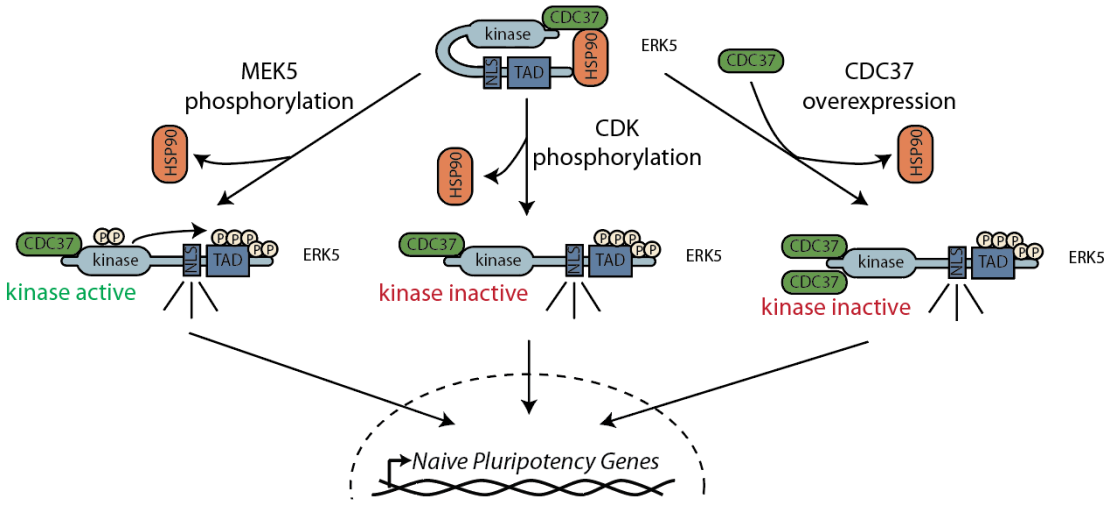

Figure 1.7: ERK5 can translocate to the nucleus via ERK5 kinase activity-independent mechanisms. *To regulate transcription, ERK5 must localise to the nucleus. For this to occur, ERK5 must dissociate from chaperone HSP90 which tethers ERK5 to the cytoplasm. This can occur through phosphorylation of the C-terminal region by ERK5 kinase activity (as described above), by CDK phosphorylation during mitosis, or by a kinase-independent mechanism in the case of CDC37 overexpression (such as under cancerous conditions). Adapted from (Gómez, Erazo, & Lizcano, 2016).*

1.3.3.4 ERK5 phosphatases

MAPKs are typically dephosphorylated and inactivated by the action of dual specificity phosphatases (DUSPs) that target the TXY motif in the activation loop. However, a DUSP has yet to be identified for ERK5, although PTP-SL, a phosphotyrosine-specific phosphatase, is able to dephosphorylate and thereby deactivate ERK5 at Tyr220 (Buschbeck et al., 2002). Whilst ERK5 can phosphorylate PTP-SL, this does not seem to influence phosphatase activity, whereas complex formation between ERK5 and PTP-SL stimulates phosphatase activity (Buschbeck et al., 2002).

1.3.4 Molecular Functions of ERK5

1.3.4.1 ERK5 inhibitors

ERK5 inhibitors have been employed to identify ERK5-specific functions. The first was XMD8-92 which, despite being very selective for ERK5, also inhibits BET family

bromodomain activity (acetylated histone binding) (Lin et al., 2016). As bromodomains are significantly involved in gene regulation, an additional compound was required to study ERK5 protein and gene targets. Therefore XMD8-92 derivatives were designed by modification of the R_1 and R_3 groups (Figure 1.8), generating the JWG series of compounds which selectively inhibit ERK5 and have no reactivity for bromodomains (Wang et al., 2018). Later, AX15836, another derivative of XMD8-92 with reduced bromodomain affinity, was produced by ActivX Biosciences Inc, and as the most readily available and highly selective inhibitor, this is now the most commonly used ERK5 inhibitor (E. C. K. Lin et al., 2016).

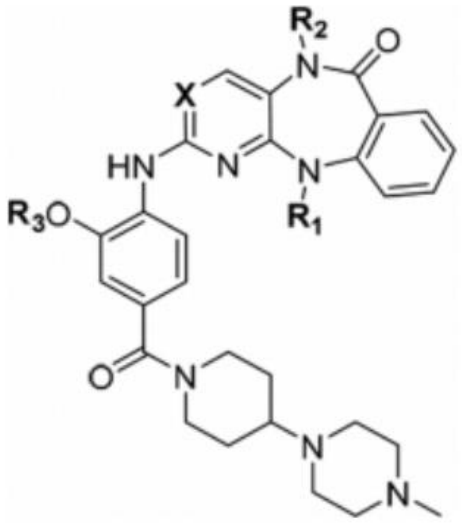

Compound	R1	R2	R3
XMD8-92	Me	Me	Et
JWG-071	s-Bu	Me	Me
AX15836	SO_2Me	Me	Et

Figure 1.8: Structures of ERK5 inhibitors. *Modification of key functional groups (denoted R_1, R_2, and R_3 has allowed the development of potent ERK5-selective inhibitors which lack cross-reactivity with BET family bromodomains. (Wang et al., 2018)*

1.3.4.2 Substrates

Most MAPKs preferentially phosphorylate Ser/Thr residues which immediately precede Pro. While ERK5 also phosphorylates proline-directed residues, this is not a requirement, with four autophosphorylated Ser residues in the ERK5 C-terminal region undergoing non-Pro-directed phosphorylation (Mody et al., 2003). This indicates that ERK5 differs in substrate specificity compared to other MAPK family members.

1.3.4.2.1 MEF2

ERK5 contains a MEF2-binding region (residues 440-501), and can phosphorylate members of the MEF2 transcription factor family (Y. Kato, 1997). MEF2A, C, and D are ERK5 substrates, or which MEF2D is an ERK5-specific substrate, whereas MEF2A and C are downstream targets of p38 in addition (Kato et al., 2000; Yang et al., 1998). ERK5 phosphorylates MEF2C on Ser387, leading to increased transcriptional activity, resulting in the induction of c-JUN, a target gene of MEF2C (Kato, 1997). ERK5 may also act as a transcriptional co-regulator with MEF2 transcription factors, through the formation of a transcription factor complex (Yan et al., 2001).

1.3.4.2.2 c-FOS

Phosphorylation of c-FOS can be performed by both ERK5 and ERK1/2 on Ser387 (Terasawa et al., 2003). However, ERK5 is additionally able to phosphorylate alternative sites on c-FOS, and this allows for maximal transactivation of c-FOS (Terasawa et al., 2003). Interestingly, phosphorylation of these sites is dependent not only on the ERK5 kinase domain, but also the C-terminal domain of ERK5.

1.3.4.3 Transcriptional targets

In ESCs, ERK5 functions in opposition to related MAPKs ERK1 and ERK2, which promote differentiation (Kunath et al., 2007). Due to the high similarity of their kinase domains, it appears that the ERK5 C-terminal region is largely responsible for the functional differences between these kinases. Indeed, the transcriptional activity attributed to ERK5 regulates expression of key stem cell genes, including KLF2, and KLF2 expression is dependent on both ERK5 kinase activity and presence of the ERK5 transcriptional domain (Morikawa et al., 2016; Williams et al., 2016). The ERK5-KLF2 signalling axis is important for development, especially in myoblast fusion (Sunadome et al., 2011). In this system, ERK5 activates the transcription factor SP1, which transcriptionally upregulates KLF2 and KLF4, which in turn regulate target genes such as *Nephronectin*.

1.3.4.4 ERK5 mechanism of gene regulation

ERK5 does not share homology with any known transcription factor and does not possess a DNA-binding domain. However, expression of the C-terminal region of ERK5 alone is sufficient to drive expression of MEF2-dependent genes (Kasler et al., 2000). This raises the question of how ERK5 can directly regulate transcription. ERK5 can act as a potent transcriptional co-activator with other transcription factors such as the MEF2 family members, and therefore may direct these transcription factors to ERK5 target genes (Sohn et al., 2005). ERK5 may also bind chromatin or transcription machinery to facilitate access of intermediate transcription factors, such as MEF2 family members or KLF2, to promoter or enhancer regions of target genes (Madak-Erdogan et al., 2014; Pearson et al., 2020; Tusa et al., 2018).

Since ERK5 possesses these two distinct activities, ERK5 can modulate the transcriptional programme either through phosphorylation of transcription factor substrates or through direct transcriptional regulation. However, as ERK5 transcriptional activity relies on a conformational change most commonly brought about through autophosphorylation, there is a degree of interplay between the two activities. Indeed, it has been demonstrated that phosphorylation of the C-terminal region is required for transcriptional activation, as mutation of these phosphorylation sites to alanine ablates this function, whereas phosphomimetic mutants relieve the need for kinase activity (Morimoto et al., 2007). The best illustrated example of this is ERK5's regulation of MEF2 family members. ERK5 can phosphorylate MEF2 family members, which leads to their activation (Kasler et al., 2000). Additionally, ERK5 C-terminal region contains a MEF2-interaction domain, which allows ERK5 to complex with MEF2 family members, enhancing their transcriptional activity (Sunadome et al., 2011). However, complex formation between ERK5 and MEF2 family members necessitates ERK5 kinase activity for relief of ERK5 autoinhibition. Hence, ERK5 utilises multiple mechanisms to regulate its targets.

1.3.5 Physiological functions of ERK5

1.3.5.1 ERK5 signalling in development

In addition to its importance in embryonic stem cells, ERK5 is essential in the early stages of development, with *Erk5*$^{-/-}$ mice failing to survive past E9.5 due to failure to form cardiac vasculature (Hayashi & Lee, 2004). Vasculogenesis occurs, however embryonic blood vessels fail to mature and myocardium-lining endothelial cells display a rounded and disorganised morphology (Regan et al., 2002). Conditional ERK5 mutants mice have also been generated, with *Erk5* deletion in endothelial cells of adult mice resulting in lethality within 2-4 weeks due to poor blood vessel integrity and multi-organ haemorrhaging (Hayashi et al., 2004). Interestingly, although endothelial-specific *Erk5*$^{-/-}$ recapitulates the phenotype of whole body *Erk5*$^{-/-}$, cardiomyocyte-specific deletion of *Erk5* did not display any apparent defects (Hayashi et al., 2004). Furthermore, ERK5 prevents differentiation specifically to cardiomyocyte lineage, as *Erk5*$^{-/-}$ mESCs preferentially differentiate to this lineage (Williams et al., 2016). These phenotypes are interesting in relation to pluripotency, as it might be expected that deletion of a key pluripotency factor could result in lethality at an earlier developmental timepoint. However, as deletion of a pluripotency factor results in ESCs differentiating, this explains why *Erk5*$^{-/-}$ mice display a phenotype at later stages of development, and suggests that ERK5 has distinct roles in different biological contexts.

Additionally, *Mekk2*$^{-/-}$ and *Mekk3*$^{-/-}$ mice display different phenotypes: *Mekk2*$^{-/-}$ mice are viable and fertile, but exhibit attenuated right ventricle hypertrophy and altered myocardial inflammatory gene expression in response to hypoxia (Brown et al., 2013), whereas *Mekk3*$^{-/-}$ mice are embryonic lethal at E11, showing arrested blood vessel development and angiogenesis from E9.5 (Yang et al., 2000). Interestingly, a *Ccm* loss-of-function mutation in patients results in enlarged and disordered vasculature, predominantly in the central nervous system and retina, reflecting the phenotype of ERK5 pathway dysregulation in mouse models (Tomlinson et al., 1994).

The MEF2 family regulate differentiation and calcium-dependent gene expression in muscle cells, with genetic knock outs of MEF2 family members associated with poor cardiac development. For example, *Mef2a*$^{-/-}$ mice suffer from sudden death within the first week of life resulting from right ventricle dilation, myofibrillar fragmentation, and foetal cardiac gene programme activation (Naya et al., 2002). Similarly *Mef2c*$^{-/-}$ mice are embryonic lethal by E10.5 due to failure of looping morphogenesis in the heart, formation of right ventricle and expression of cardiac muscle genes (Lin et al., 1997). *Klf2*$^{-/-}$ mice are embryonic lethal between E10.5 and E14.5 (dependent on genetic background) due to haemorrhaging and poor smooth muscle integrity around blood vessels (Kuo et al., 1997). These phenotypes closely reflect those of *Erk5*$^{-/-}$ mice.

1.3.5.2 ERK5 signalling in cancer

ERK5 expression is also implicated in cancer, playing a role in tumour drug resistance and particularly vigorous forms of cancer. For example, oncogenic SRC isoforms in fibroblasts activate ERK5 resulting in podosome (invasive adhesion) formation (Barros & Marshall, 2005; Schramp et al., 2008). Additionally, MEK5 activation in breast cancer cells leads to hyperphosphorylation of FAK, complex formation between ERK5/FAK/$\alpha_v\beta_3$ intergrin, and regulation of adhesion and migration (Rajinder et al., 2009). ERK5 signalling is also upregulated in HER2-overexpressing cells, and ERK5 levels in HER2-overexpressing cells are inversely proportional to disease-free survival time. Trastuzumab, which is used to treat HER2-overexpressing cancers, has little effect on ERK5 activation, although administration of trastuzumab with dominant-negative (activation loop mutated: AEF) ERK5 decreases cancer cell proliferation (Hayashi & Lee, 2004; Montero et al., 2009). ERK5-overexpressing prostate cancer cells are more proliferative, motile and invasive, as well as more efficient in tumour formation, suggesting ERK5 correlates with prostate cancer aggressiveness (McCracken et al., 2008). In the advanced stages of cancer, ERK5 signalling drives proliferation of macrophages in human tumours, contributing to a tumour microenvironment which facilitates tumour growth and malignancy (Giurisato et al., 2020).

1.3.5.2.1 ERK5 signalling in cancer stem cells

ERK5-expressing cancers may be particularly aggressive due to the presence of cancer stem cells. Cancer stem cells are tumour cells which revert to a stem cell-like phenotype, for example through expression of pluripotency factors such as OCT4 (Liu et al., 2013). This allows the cell to continually self-renew, generating more tumour cells, while also gaining the capacity to generate cells of other lineages. This facilitates tumour survival by, for instance, providing a blood supply via generation of a new blood vessel, and by promoting tumour heterogeneity. Therefore, cancer stem cell prevalence correlates strongly with treatment-resistant tumours and correspondingly poor survival (Prieto-Vila et al., 2017). As such, identifying druggable targets in cancer stem cells is key to designing more effective treatments for these particularly aggressive cancers. ERK5 drives cancer stem cell generation in a number of systems including colon cancer, breast cancer, and leukaemia, through the induction of downstream target genes (Pereira et al., 2019; Tusa et al., 2018; Ucar et al., 2019).

1.4 Aims

ERK5 is an important regulator of developmental processes including stem cell pluripotency, with significant potential as a drug target in the treatment of cancer and other diseases. Comprehensively elucidating ERK5 functions in ESCs will deepen our understanding of how development is regulated, and how ERK5 signalling goes awry in disease states. Additionally, ERK5 was identified in a screen to identify kinases which regulate the naïve-primed transition in pluripotency. As an understudied kinase with a unique structure among MAPKs, ERK5 represents an interesting target to investigate. However, a systematic analysis of ERK5-dependent genes and proteins in ESCs has not yet been performed, and the mechanism by which ERK5 regulates these targets is not fully understood. Therefore, the aims of this thesis are:

1. To identify the ERK5-dependent proteome in mESCs
2. To dissect the pathways by which ERK5 regulates its target genes and proteins
3. To interrogate the downstream biology associated with novel target proteins.

2. Materials and Methods

2.1 Materials

2.1.1 Commercial Reagents

(3-Aminopropyl) triethoxysilane solution, Acetonitrile (HPLC grade), Adenosine 5'-triphosphate sodium salt (ATP), ammonium bicarbonate, ammonium persulphate (APS), Agarose, Ampicillin, anti-FLAG (M2) agarose, Bovine Serum Albumin (BSA), Dimethyl Sulphoxide (DMSO), Glycerol, Glycine, Hoechst 34580, Hydrogen Peroxide, Iodoacetamide, Kanamycin, Magnesium Acetate, Tetramethylethylenediamine (TEMED), NBT/BCIP Stock Solution, Polyethylene glycol sorbitan monolaurate (Tween-20), Ponceau S Solution, Puromycin, Sodium 2-glycerophosphate, Sodium Azide, Sodium Chloride, Sodium Dodecyl Sulphate (SDS), Sodium Ethylene Glycol Tetraacetic acid (EGTA), Sodium Ethylene Diamine Tetraacetic acid (EDTA), Sodium Fluoride, Sodium Orthovanadate, β-mercaptoethanol (βME), and Sodium Pyrophospate were from Sigma (Poole, UK).

Tris(hydroxymethyl)aminomethane (Tris) was from BDH (Lutterworth, UK).

i-Script Kit, Polymerase chain reaction plates (396- and 96-well), and Precision Plus protein markers were from Bio-Rad (Herts, UK).

InstantBlue® Protein Stain was from Expedeon (Cambridge, UK).

Bis-acrylamide (40% (w/v) 29:1) solution was from Flowgen Bioscience (Nottingham, UK).

Glutathione-sepharose, Nitrocellulose membrane, and Protein G-sepharose were from GE Healthcare Life Sciences (Buckinghamshire, UK).

25% Glutaraldehyde, Immobilon Western HRP Substrate, and Polyvinylidene difluoride (PVDF) were from Merck Millipore (Watford, UK).

HRP-conjugated secondary antibodies were from New England Biolabs (Herts, UK).

E.Z.N.A.® MicroElute Total RNA Kit was from Omega Bio-tek (GA, USA).

Skimmed milk powder (Marvel) was from Premier Beverages (Stafford, UK).

HALO-link resin was from Promega (Wisconsin, USA).

DNeasy Blood & Tissue Kit, HiSpeed Plasmid Maxiprep kits and HiSpeed Plasmid Midiprep kits were from Qiagen Ltd (Crawley, UK).

Protease Inhibitor Complete cocktail tablets were from Roche (Lewes, UK).

TB Green Premix Ex Taq II was from Takara Bio (St Germain en Laye, France).

ActinRed^{TM} 555 ReadyProbes® Reagent, AlexaFluor® secondary antibodies, NuPAGE® 10x Reducing agent, NuPAGE® 4x LDS sample buffer, NuPAGE® MES running buffer (20x), Pierce^{TM} BCA Protein Assay Kit, Precast NuPAGE® Novex 4-12% Bis-Tris gels, and SuperSignal West Femto chemiluminescent substrate were from Thermo-scientific (Essex, UK).

Acetone, ART Pipet Tips, DNAse Set RNAse free, Ethanol, Isopropanol, Methanol, and Microscope slides were from VWR (Leicestershire, UK).

3 mm Chromatography paper was from Whatmann International Ltd (Maidstone, UK).

2.1.2 Tissue Culture reagents

Cell culture plates/dishes and cryovials were from Corning Incorporated (NY, USA). Cell scrapers were from Costar (Cambridge, USA). Antibiotic/antimycotic solution, Dulbecco's Modified Eagle Medium (DMEM), KnockOut^{TM} Serum Replacement, L-glutamine solution, Non-essential amino acids, Opti-MEM reduced serum media, Penicillin/Streptomycin solution, Sodium pyruvate solution, Tissue culture grade Dulbecco's phosphate buffered saline (PBS), and Trypsin/EDTA solution were from GIBCO (Paisley, UK). Defined Foetal bovine serum (FBS), Glass circle coverslips 16

mm, and Lipofectamine LTX with Plus Reagent were from Thermo-scientific (Essex, UK).

2.1.3 In-house reagents

Bacterial culture media Luria Bertani (LB) broth and LB agar plates supplemented with antibiotics were provided by the media kitchen facility at the University of Dundee. The production team from MRC Reagents and Services and the Protein Production and Assay Development Team (PPAD), headed by James Hastie and Axel Knebel respectively, expressed and purified all proteins used in *in vitro* kinase and TUBE pulldown assays, as well as GST-LIF (DU1715) for mESC culture.

2.1.4 Buffers

EDTA and EGTA chelate divalent cations, which are proteolytic activity cofactors, so they are included in all lysis buffers. Complete Proteosome inhibitor cocktail contains benzamidine and PMSF. These inhibit serine proteases and metallo, aspartyl, cysteinyl, and seryl proteinases. Sodium fluoride, sodium pyrophosphate, and sodium β-glycerophosphate are used to inhibit serine/threonine protein phosphatases. Sodium orthovanadate (Na_3VO_4) inhibits protein tyrosine phosphatases, and is prepared through cycles of boiling and cooling until solution remains colourless at room temperature pH 10, as recommended by the manufacturer. This ensures that it is monomeric, the state which is effective for protein tyrosine phosphatase inhibition. The composition of commonly used buffers is noted in Table 2.1.

Table 2.1: Buffer Compositions.

BUFFER	COMPOSITION
IP-MS LYSIS BUFFER	20 mM Tris (pH 7.4), 150 mM NaCl, 1 mM EDTA, 1% NP-40 (v/v), 0.5% sodium deoxycholate (w/v), 10 mM β-glycerophosphate, 1 mM NaF, 2 mM Na_3VO_4, 10% glycerol, and Roche Complete Protease Inhibitor Cocktail tablets
HALO-LINK RESIN WASH BUFFER	50 mM Tris/HCl (pH 7.5), 0.5 M NaCl and 1% Triton-X100 (v/v)
HALO-LINK RESIN STORAGE BUFFER	50 mM Tris/HCl (pH 7.5), 150 mM NaCl, 0.1 mM EGTA, 270 mM sucrose, 0.07% βME (v/v)
LITHIUM DODECYL SULPHATE (LDS) SAMPLE BUFFER 4X (THERMO-SCIENTIFIC)	141 mM Tris base, 2% LDS (w/v), 10% glycerol (v/v), 0.51 mM EDTA, 0.22 mM SERVA Blue G, 0.175 mM Phenol Red (pH 8.5)
6-12% ACRYLAMIDE RESOLVING GELS	375 mM Tris/HCl (pH 8.6), 0.1% SDS (w/v) and 6-12% acrylamide (w/v). 0.1% ammonium persulphate (APS) (w/v) and 0.1% TEMED (v/v) to polymerise the gels
STACKING GEL	125 mM Tris/HCl (pH 6.8), 0.1% SDS (w/v) and 4% acrylamide (w/v). 0.1% ammonium persulphate (APS) (w/v) and 0.1% TEMED (v/v) to polymerise the gels
TRIS-GLYCINE SDS RUNNING BUFFER	25 mM Tris/HCl (pH 8.3), 192 mM glycine, 0.1% SDS (w/v)
TRIS-GLYCINE TRANSFER BUFFER	48 mM Tris/HCl (pH 8.3), 39 mM glycine, 20% methanol (v/v)
TBS PLUS TWEEN (TBS-T)	20 mM Tris/HCl (pH 7.5), 150 mM NaCl, 0.2% Tween-20 (v/v)
PVDF BLOCKING	TBS-T containing 3% non-fat milk (w/v)
PHOSPHATE BUFFERED SALINE (PBS)	2.7 mM potassium chloride, 1.5 mM potassium phosphate monobasic, 138 mM NaCl, 8.1 mM sodium phosphate dibasic

2.1.5 Compounds

Compounds were resuspended in DMSO (with the exception of Cycloheximide, which was resuspended in ethanol), aliquoted, and stored at -20 °C. All compounds used in this thesis can be found in Table 2.2.

Table 2.2: Compounds and Small Molecule Inhibitors.

COMPOUND	SOURCE	PRIMARY TARGET
AX15836	Tocris	ERK5
MG132	Sigma	Proteosome (Tsubuki et al., 1996)
CYCLOHEXIMIDE	Sigma	Translational elongation (Pestova and Hellen, 2003)
PD0325901	MRCPPU R&S	MEK1/2 (Barrett et al., 2008)
XMD8-92	N. Gray	ERK5

2.1.6 cDNA constructs

All mammalian expression constructs were cloned into pCAGGS vector plasmids with FLAG, 61-haemaglutinin (HA) or green fluorescent protein (GFP) tags, or no tag. The plasmids used in this thesis are detailed in Table 2.3. In each case, the position of the tag (N- or C-terminal) is noted. All constructs were generated by the DSTT cloning team and verified by DNA sequencing using Applied Biosystems Big-Dye Ver 3.1 chemistry on Applied Biosystems model 3730 automated capillary DNA sequencer (performed by DNA Sequencing & Services). For more information about the plasmids used in this thesis, the details can be found at http://mrcppureagents.dundee.ac.uk/reagents-cdna-clones and are publicly available for the worldwide research community.

Table 2.3: cDNA Constructs.

GENE	TAG	VECTOR	DU NUMBER	RESISTANCE MARKER
ERK5	No tag	pCAGGS	DU50514	Puromycin
ERK5 D200A	No tag	pCAGGS	DU50662	Puromycin
GFP-ERK5	N-terminal GFP	pCAGGS	DU50830	Puromycin
MEK5 S311D T315D	N-terminal 3xFLAG	pCAGGS	DU53252	Puromycin
KLF2	N-terminal 3xFLAG	pCAGGS	DU56075	Puromycin
KLF2 T171A S175A S243A T247A (4A)	N-terminal 3xFLAG	pCAGGS	DU53945	Puromycin
KLF2 T171A S175A	N-terminal 3xFLAG	pCAGGS	DU53826	Puromycin
KLF2 S243A T247A	N-terminal 3xFLAG	pCAGGS	DU53869	Puromycin
ZSCAN4	N-terminal HA	pCAGGS	DU61123	Puromycin
ZSCAN4	C-terminal HA	pCAGGS	DU61125	Puromycin
ZSCAN4	No tag	pCAGGS	DU61124	Puromycin
ANNEXIN A2	N-terminal HA	pCAGGS	DU61146	Puromycin
ANNEXIN A2	C-terminal HA	pCAGGS	DU61136	Puromycin
S100A10	N-terminal FLAG	pCAGGS	DU61138	Puromycin
S100A10	C-terminal FLAG	pCAGGS	DU61134	Puromycin
GFP		pCAGGS		Puromycin

2.1.7 qRT-PCR primers

Mouse qRT-PCR primers were either previously reported in the literature (references included where applicable) or designed using Primer3 (Koressaar & Remm, 2007) with a length of 20-24 bases and melting temperature between 58-62 °C. The melting curve and integrity were determined for each primer. All designed primers overlap the intron/exon boundary by seven bases, and produce a 100-300 base amplicon. Primers were supplied by Sigma-Aldrich. DNA oligonucleotides used for qRT-PCR of mRNA are listed in Table 2.5.

Table 2.4: qRT-PCR Primer Sequences.

TARGET	SEQUENCE (5'-3')	
	Forward	**Reverse**
KLF2	CTCAGCGAGCCTATCTTGCC	CACGTTGTTTAGGTCCTCATCC
GAPDH	CTCGTCCCGTAGACAAAA	TGAATTTGCCGTGAGTGG
ZSCAN4	CAGATGCCAGTAGACACCAC	GTAGATGTTCCTTGACTTGC
TDPOZ3	TCTCCAATGTCCAATGCTTTCTG	ACGGTTCCAACTATGCTCACC
ZFP352	AAGTCCCACATCTGAAGAAACAC	GGGTATGAGGATTCACCCACA
ANXA2	GAGGATCCATGTCTACTGTTCACGAA	GGACTAGTTCATCTCCACCACACA
S100A10	GACAAAGGAGGACCTGAGAGTG	CTCTGGAAGCCCACTTTGCCAT
NODAL	GGCCGTACATGTTGAGCCTCT	CGTGAAAGTCCAGTTCTGTCC
INHA	AGGAAGATGTCTCCCAGGCT	GGATGGCCGGAATACATAAG
INHBA	GATCATCACCTTTGCCGAGT	CACTTCTGCACGCTCCACTA
INHBB	CTAGAGTGTGATGGGCGGAC	GCGCAATGATCCAGTCGTTC
TGFB1	GCCCTGGATACCAACTATTGC	AAGTTGGCATGGTAGCCCTT
ACVR2A	ACACAGCCCACTTCAAATCC	AGGAGGGTAGGCCATCTTGT
ACVR2B	AGGGCCACAAGCCTTCTATT	CCAACCTGTCCATGGGTATC
TGFBR2	AACATGGAAGAGTGCAACGAT	CGTCACTTGGATAATGACCAACA

SMAD2	ATGTCGTCCATCTTGCCATTC	AACCGTCCTGTTTTCTTTAGCTT
CRIPTO	TTCTCAGCCCTGTACTGCCT	CTTGGGATGCTGCATTCTCT
LEFTY2	CAGCTGCAGCTCAGCCAGGCCC	AGCGGTCAGCGTCAGTTCCC
BRACHYURY	TCCCGAGACCCAGTTCATAG	TTCTTTGGCATCAAGGAAGG
MIXL	GCTGCTACCCGAGTCCAGGAT	GCCTTGAGGATAAGGGCTGAAA
DNMT1	CATGGTGCTGAAGCTCACACTGCG	CAGCCAAGATGATGGCCCTCCTTC
MUERVL	ATCTCCTGGCACCTGGTATG	AGAAGAAGGCATTTGCCAGA
TET2	GTCAACAGGACATGATCCAGGAG	CCTGTTCCATCAGGCTTGCT
XAF1	GAGCACCAGCAGGTTGGGTG	AATCATTTGGTTGCAATAAT
KCTD10	CTCGGAATTCCGATGGAAGAGATGTCAGGAGAC	CTGAGAATTCTCACTGGTGGAGGTGGGC
AP2	AAGGTGAAGAGCATCATAACCCT	TCACGCCTTTCATAACACATTCC
DPPA3	CCAATGAAGGACCCTGAAACT	AACAAAGTGCGGACCCTTCT
KLF4	CTGAACAGCAGGGACTGTCA	GTGTGGGTGGCTGTTCTTTT

2.1.8 Antibodies

The following commercial antibodies were used throughout this thesis (Table 2.6). In each case, the dilution factor of antibody to 3% milk in TBS-T is noted. PVDF membranes were incubated overnight at 4 °C with the antibody solution.

Table 2.5: Commercial Antibodies.

TARGET	SOURCE	CATALOGUE NO.	DILUTION	HOST
ZSCAN4	Millipore	AB4340	1:1000	Rabbit
KLF2	Merck Millipore	09-820	1:1000	Rabbit
ERK1	Santa Cruz Biotechnology	Sc-93	1:1000	Rabbit
ANNEXIN A2	BD	610068	1:1000	Mouse
S100A10	R&D Systems	AF2377	1:1000	Goat

DNMT1	Cell Signalling	5032	1:1000	Rabbit
UHRF1	Santa Cruz Biotechnology	Sc-373750	1:1000	Mouse
NANOG	Reprocell	RCAB001P	1:1000	Rabbit
SOX2	Cell Signalling	49005	1:1000	Mouse
KLF4	R&D Systems	AF3158	1:1000	Goat
EPHA2	Santa Cruz Biotechnology	Sc-924	1:1000	Rabbit
ID1				
OCT4	Santa Cruz Biotechnology	Sc-9081	1:1000	Rabbit
FLAG (HRP)	Sigma	A8592-2	1:1000	
HA (HRP)	Roche	12013819001	1:1000	
FLAG (M2)	Sigma	F3165	1:100 (for IF)	Mouse
HA	Abcam	Ab9110	1:200 (for IF)	Rabbit
SMAD2	Cell Signalling	5339P	1:1000	Rabbit
PSMAD2	Cell signalling	3101S	1:1000	Rabbit
GFP	Abcam	Ab13970	1:500	Chicken
HIF1A	R&D Systems	MAB1536	1:1000	Mouse
UBIQUITIN	Biolegend	646302	1:1000	Mouse

All in-house antibodies, generated by the antibody production group of the Division of Signal Transduction Therapy (DSTT), MRC PPU, University of Dundee, used in this thesis are found in Table 2.7. All were raised in sheep at Diagnostics Scotland (Carluke, Lanarkshire, UK), through two injections of adjuvant (either purified protein or short peptide) three weeks apart. One week after the second injection, a bleed was taken, and up to five bleeds were taken in total. Serum was then subjected to purification using 5-Carboxypentyl-sepharose coupled to the specific antigen. This was supervised by James Hastie, DSTT.

Table 2.6: In-house Antibodies.

TARGET	SHEEP NO.	BLEED NO.	DILUTION
ERK5	S420A	2	1:1000
KLF2 PS171/T175	SA386	3	1:1000
CULLIN2	S065D	3	1:1000

2.2 Methods

2.2.1 Competent *E. coli* transformation

Competent *E. coli* DH5α strains were generated by MRC Reagents and Services, University of Dundee. For transformation, an aliquot was thawed on ice. To 70 µl cells, roughly 5-20 ng DNA was added, and incubated on ice for 5 mins. To induce uptake of DNA by the cells, 42 °C heat shock was applied for 1 min, before being returned to ice for 2 mins. The bacteria were then transferred to a Luria-Bertani (LB) agar plate containing the antibiotic used to select for the plasmid (either 100 µg/ml ampicillin or 50 µg/ml kanamycin) and incubated for 16 hours at 37 °C.

2.2.2 DNA plasmid purification from *E. coli*

A single colony from a transformed DH5α LB plate was transferred to 150 ml liquid LB culture containing either 100 µg/ml ampicillin or 50 µg/ml kanamycin. This was incubated overnight at 37 °C shaking at 200 rpm. Cells were pelleted by centrifugation for 15 mins at 4 °C at 3000 rpm, prior to purification and isolation of plasmid DNA using DNA HiSpeed Maxi Kit (Qiagen) according to manufacturer's instructions. Approximate yield per maxiprep is 0.4-1 mg of plasmid DNA.

2.2.3 Nucleic acid concentration measurement

NanoDrop® spectrophotometer (Thermo Scientific) was used to measure DNA and RNA concentrations based on RNA/DNA absorption at 260 nm, as per manufacturer's instructions. 2 µl nuclease-free water was first used to calibrate the spectrophotometer, followed by 2 µl resuspension or elution buffer as a blank measurement. High nucleic acid purity is indicated by a 260/280 nm ratio greater than 1.8.

2.2.4 Cell culture

All mammalian cell culture procedures were carried out to biological safety standards, using aseptic technique. CCE mESCs were grown in a water-saturated incubator at 37 °C with 5% CO_2, in supplemented Dulbecco's modified eagle medium (DMEM) for mESC culture. DMEM was supplemented with 10% Defined FBS, 5% KnockOut Serum, 2 mM

L-glutamine, PenStrep, 1x non-essential amino acids and 1 mM sodium pyruvate, βME, 100 ng/ml GST-LIF (DU1715). For maintenance of lines, 0.1% (w/v) Porcine Gelatin in PBS was used to coat 10 cm^2 cell culture dishes prior to cell seeding. For experimental set ups, 0.1% Porcine Gelatin was used to coat any surface on which the cells would be seeded (eg 12-well or 6-well plates as well as 10 cm^2 dishes). Once grown to 70-80% confluency, cells were washed with PBS and dissociated from the plate with 1ml of Tryspin/0.05 % EDTA at 37 °C for 5 min. mESC culture media (as described above) was used to resuspend cells, prior to centrifugation at 1200 rpm for 5 min. The supernatant was then aspirated to remove the Trypsin, and cells were resuspended in 5 ml mESC culture media to a single cell suspension. mESCs were seeded at a 1:10 dilution, to be passaged every other day, with a media change on days when the cells were not passaged.

2.2.4.1 Freezing and thawing of cell lines

One confluent 10 cm^2 dish of mESCs were trypsinised and collected in culture media through centrifugation (1200 rpm, 5 mins). Media was aspirated, cells were resuspended in 4 ml freezing media (80% culture media, 10% DMSO, 10% Defined FBS), and transferred in 1ml aliquots into cryovials. These were stored in a Mr Frosty freezing container (Nalgene) at -80 °C for 24 hours before being transferred to liquid nitrogen for long term storage.

Cells were thawed at 37 °C for 2 mins, resuspended in 4 ml culture media, pelleted by centrifugation at 1200 rpm for 5 min, and media aspirated to remove cells from DMSO. Cells were then resuspended in 7 ml culture media and plated on a 10 cm^2 dish, and passaged twice prior to use for experiments to ensure full recovery from freezing.

2.2.4.2 Transfection

Lipofectamine LTX was used to transfect DNA into mESCs. Mammalian expression plasmids were mixed with OPTIMEM and Plus reagent before being incubated for 5 mins, after which LTX was added. This mixture was then vortexed for 10 secs and further incubated for 15 mins, during which cells were counted and plated into either 12-well, 6-well or 10 cm^2 dishes. The transfection mix was then added to the cells in a dropwise manner. mESC number, OPTIMEM, Plus reagent and LTX volumes used can be found

in Table 2.8. Selection was applied to cells 24 hours post-transfection using 2 µg/ml Puromycin cells to remove cells which had not be transfected.

Table 2.7: Transfection Mix Composition.

PLATE	MEDIA VOLUME	MESC NUMBER	PLUS	OPTIMEM	LTX
12-WELL	1ml	$0.2x10^6$	1µl	250µl	2.5µl
6-WELL	2ml	$0.4x10^6$	2µl	500µl	5µl
10CM²	5ml	$2x10^6$	4µl	1ml	10µl

2.2.4.3 Inhibitor treatment of mESCs

Compounds and small molecule inhibitors were added directly to the cell culture media and returned to a 37 °C incubator for the indicated times. Inhibitors were diluted in vehicle prior to treatment such that a 1:1000 dilution in culture media was required to achieve desired final concentration of inhibitor. The equivalent volume of vehicle (ethanol for cycloheximide, DMSO for all other inhibitors) was added as a negative control.

2.2.4.4 Cell lysis

Cells were washed with PBS to remove excess media, and IP-MS lysis buffer (composition found in Table 1) added. Plates were then scraped and lysates clarified through centrifugation (17000 g for 15 mins at 4 °C). The supernatant was removed to a clean tube, snap frozen in Liquid Nitrogen, and stored at -80 °C until use.

2.2.5 Telomere qPCR

The premise of this assay is to measure an average telomere length ratio by quantifying telomeric DNA with specially designed primer sequences and divide that amount by the quantity of a single-copy gene. The single copy gene that was used was the acidic ribosomal phosphoprotein PO (36B4) gene. Cells were seeded in 12-well plates. DNA was extracted from cells using DNeasy Blood and Tissue Kit (QIAGEN) using the

manufacturer's instructions. The primers used are noted in Table 2.9. Primers were supplied by Sigma-Aldrich.

Table 2.8: Telomere qPCR Primer Sequences.

PRIMER	SEQUENCE (5'-3')
TELOMERE FORWARD	CGG TTT GTT TGG GTT TGG GTT TGG GTT TGG GTT TGG GTT
TELOMERE REVERSE	GGC TTG CCT TAC CCT TAC CCT TAC CCT TAC CCT TAC CCT
36B4 FORWARD	ACT GGT CTA GGA CCC GAG AAG
36B4 REVERSE	TCA ATG GTG CCT CTG GAG ATT

Each reaction for the telomere portion of the assay included 12.5 µl SYBR Green PCR Master Mix (Takara), 300 nM each of the forward and reverse primers, 20 ng genomic DNA, and enough double-distilled H_2O to yield a 25 µl reaction. Three 20 ng samples of each DNA were placed in adjacent wells of a 96-well plate. An automated thermocycler (Prism 7000 Sequence Detection System, Applied Biosystems) was used with the following reaction conditions: 95 °C for 10 min followed by 30 cycles of data collection at 95 °C for 15 s and a 56 °C anneal–extend step for 1 min.

Each reaction for the 36B4 portion contained 12.5 µl SYBR Green PCR Master Mix (Takara), 300 nM forward primer, 500 nM reverse primer, 20 ng genomic DNA and enough double-distilled H_2O to yield a 25-µl reaction. Three 20 ng samples of each DNA were placed in adjacent wells of a 96-well plate. The thermocycler reaction conditions were: 95 °C for 10 min, followed by 35 cycles of data collection at 95 °C for 15 s, with 52 °C annealing for 20 s, followed by extension at 72 °C for 30 s.

Telomere and 36B4 reactions were performed on separate plates so to minimise variation due to location in plate, each sample was loaded into corresponding positions on each plate, such that the two plates had the same layout.

Analysis was performed by subtracting 36B4 Ct value from corresponding Telomere Ct value and normalising to the average of the control conditions. These log ratios were then plotted using GraphPad Prism software (version 7.03), which was used to perform

statistical tests. Original protocol for telomere qPCR protocol and subsequent data analysis reported by Callicott and Womack (2006).

2.2.6 qRT-PCR

Cells were seeded in 12-well plates. After 24-48 hours growth, the E.Z.N.A.® MicroElute Total RNA Kit was used, according to manufacturer's instructions, to extract RNA from cells. 1 µg of isolated RNA was used to generate cDNA using the i-Script cDNA kit (BioRad), following the manufacturer's protocol. Cycling conditions for qRT-PCR reactions are found in Table 2.10 and were performed in a CFX 384 Real time System qRT-PCR machine (BioRad). cDNA (2 µl), forward and reverse primers (400 nM each), SYBR Green Master Mix (5 µl; Takara) , and nuclease free water made up each 11 µl reaction. All primers were purchased from Sigma-Aldrich. The data was analysed using Pfaffl method (Pfaffl, 2001), normalising to *Gapdh*.

Table 2.9: qRT-PCR Programme Set-up.

TEMPERATURE	TIME	CYCLES
95 ℃	3:00	1
95 ℃	0:10	
60 ℃	0:30	45
RECORD		
65 ℃	0:05	1
RECORD		
95 ℃	0:50	1

2.2.7 Protein concentration measurement

Bicinchoninic acid (BCA; Pierce^{TM} BCA Protein Assay Kit) was used to determine protein concentration of cell lysates. In the assay, Cu^{2+} is reduced to Cu^{1+} by the presence of protein, in an alkaline medium, and colourmetric detection of Cu^{1+} is facilitated by bicinchoninic acid (Smith et al., 1985). A colour change from blue to purple is observed in the presence protein, and absorbance at 562 nm is measured to quantify this. A calibration curve is generated through serial dilutions of BSA from 2 mg/ml to 0.125

mg/ml. 3 µl lysate or BSA standard were added to a 96-well plate in technical triplicate, prior to addition of 150 µl BCA solution. The plate was then incubated at 37 °C for 15 mins, before absorbance at 562 nm was measured. Concentration of the sample was then calculated from the BSA calibration curve.

2.2.8 Immunoprecipitation

Following BCA protein concentration measurement, immunoprecipitation (IP) was used to enrich a protein of interest and associated proteins. Protein G-Sepharose, FLAG-agarose or HA-agarose beads were washed three times in IP-MS lysis buffer (Table 1). For IPs using Protein G-Sepharose, 10 µl washed packed beads were added to 2 mg clarified lysates and 5 µg antibody against protein of interest. For IPs using FLAG- or HA-agarose, 10 µl washed packed beads were added to 2 mg clarified lysates. In all cases, samples were then incubated for 3 hours at 4 °C shaking. The beads were centrifuged at 1000 g for 2 mins at 4 °C and washed three times in IP-MS lysis buffer. After washing, the supernatant was removed from the beads, the IP was denatured and reduced in 10 µl sample buffer containing 1x NuPAGE reducing agent.

2.2.9 HALO-TUBE pulldown assays

HALO-tagged UBQLN1 Tandem Ubiquitin Binding Element (TUBE) (MRC-PPU R&S DU23799) is a tetramer of the UBQLN1 UBA ubiquitin binding domain (aa536-589) provided by Dr. A. Knebel (MRC-PPU, Dundee). A mutant TUBE incapable of binding ubiquitin (M557K, L584K) was also used. HALO-TUBE beads were prepared by washing 1 ml packed HALO resin three times with HALO wash buffer (Table 1), resulting in a 1:4 slurry. The slurry was combined with 7 mg of HALO-TUBE or HALO-mutant TUBE and incubated on a rotating wheel at 4 °C overnight. After five washes first in 10 ml HALO wash buffer and then in 10 ml HALO storage buffer (Table 1), the beads were stored as a 20% slurry in HALO storage buffer at 4 °C, and washed three times in IP-MS lysis buffer immediately prior to usage.

To analyse ubiquitylation of a protein of interest, 10 µl washed packed beads were incubated with 1 mg clarified cell lysate for 3 hours at 4 °C shaking. After three washes

with IP-MS, then the pulldown was denatured and reduced in 10 µl sample buffer containing 1x NuPAGE reducing agent.

2.2.10 SDS-PAGE

15 µg of cell lysate was boiled for 2 mins with NuPAGE sample buffer (containing 4x LDS buffer and 10x Reducing agent). Either Commercial NuPAGE 4-12% Bis-Tris pre-cast gels or homemade SDS/PAGE gels were loaded with Precision Plus Protein™ All Blue Standards (Bio-Rad) and lysate samples. Homecast gels were made up of a resolving gel (pH 8.8, composition found in Table 1), and a stacking gel (pH 6.8, composition found in Table 1), and were run at a constant voltage of 150V in glycine running buffer for ~1.5 hours. Commercial NuPAGE 4-12% Bis-Tris pre-cast gels were run at 150V for ~1 hour in 1x MES buffer.

2.2.11 Immunoblotting

After separation of protein extracts by SDS-PAGE as described above, proteins were transferred onto polyvinylidene fluoride (PVDF) membranes (Millipore) which had been activated in methanol. Protein transfer was performed in 1x Glycine transfer buffer (Table 1), using either an XCell II™ Blot Module (Thermo Scientific) transfer system at 35 V for 1.5 hours for gels with up to 15 wells, or a Trans-Blot® Cell (Bio-Rad) transfer system at 100 V for 1 hour for gels containing 20 or 26 wells. Ponceau S was used to visualise the efficiency of protein transfer. Cutting the membranes using a scalpel allowed a single membrane to be used to perform multiple immunoblots. To prevent non-specific antibody binding, membranes were blocked in PVDF blocking buffer (Table 1) on a rocking platform for 15 mins at room temperature. Primary antibodies were diluted in PVDF blocking buffer, and the membranes incubated overnight at 4 °C on a rocking platform. The membranes were then washed in TBS-T three times, then incubated for 1 hour with secondary horseradish Peroxidase (HRP)-conjugated antibodies, diluted 1:10000 in PVDF blocking solution. After washing three times again with TBS-T, Immobilon Western HRP Substrate (for strong signal) or SuperSignal West Femto chemiluminescent substrate (for weak signal) was used to detect the immunoblot signal. The Chemidoc imaging system (Bio-Rad) was used to expose and develop membranes, and this also

allowed for subsequent quantification. Membrane images were processed using Adobe Illustrator CSC.

2.2.12 Quantitative proteomics

The quantitative proteomic procedures were carried out by Diana Rios-Szwed and Houjiang Zhou. Data analysis was performed in collaboration with Houjiang Zhou.

2.2.12.1 Protein Extraction and Digestion

The puromycin-selected transfected mESCs were washed in PBS and then lysed in 8.5 M urea, 50 mM ammonium bicarbonate (pH 8.0) supplemented with protease inhibitors. Lysate was sonicated using Biosonicator operated at 50% power for 30 sec on/off each on ice water bath for 5 min. The lysates were then centrifuged at 14,000 rpm for 10 mins at 4 °C. The supernatants were then collected. Protein concentration of the lysate was determined by BCA protein assay. Proteins were reduced with 5 mM DTT at 55 °C for 30 min and then cooled to room temperature. The reduced lysates were then alkylated with 10 mM iodoacetamide at room temperature for 30 min in the dark. The alkylation reaction was quenched by the addition of another 5 mM DTT. After 20 min of incubation at room temperature, the lysate was digested using Lys-C with the weight ratio of 1:200 (Enzyme/lysate) at 37 °C for 4 hours. The samples were further diluted to 1.5 M Urea with 50 mM ammonium bicarbonate (pH 8.0), and the sequencing-grade trypsin was added with the weight ratio of 1:50 (enzyme/lysate) and incubated overnight at 37 °C. The digest was acidified to pH 3 by addition of TFA to 0.2% and gently mixed at room temperature for 15 min; the resulting precipitates were removed by centrifugation at 7100 RCF for 15 min. The acidified lysate was then desalted using a C18 SPE cartridge (Waters) and the eluate was aliquoted into 100 µg and dried by vacuum centrifugation. To check the digests, 1 µg of each sample was analysed by mass spectrometry prior to TMT labelling.

2.2.12.2 TMT labelling and High pH Reverse Phase Fractionation

100 µg of peptide from each sample was re-suspended into 100 mM Triethylammonium bicarbonate buffer (pH 8.5). Then, 0.8 mg of TMT tag (Thermo) dissolved in 41 µl of anhydrous acetonitrile was transferred to the peptide sample and incubated for 60 min at

room temperature. The TMT labelling reaction was quenched with 5% hydroxylamine. 1 µg of each labelled sample was analysed by mass spectrometry to assess the labelling efficiency before pooling. After checking the labelling efficiency, the TMT-labelled peptides were mixed together and dried by vacuum centrifugation. After drying, the mixture of TMT-labelled peptides was dissolved into 0.2% TFA and then desalted using a C18 SPE cartridge. The desalted peptides were subjected to orthogonal basic pH reverse phase fractionation, collected in a 96-well plate and consolidated for a total of 20 fractions for vacuum dryness.

2.2.12.3 LC-MS/MS analysis

Each fraction was dissolved in 0.1% FA and quantified by Nanodrop. 1 µg of peptide was loaded on C18 trap column at a flow rate of 5 µl/min. Peptide separations were performed over EASY-Spray column (C18, 2 µm, 75 mm × 50 cm) with an integrated nano electrospray emitter at a flow rate of 300 nl/min. The LC separations were performed with a Thermo Dionex Ultimate 3000 RSLC Nano liquid chromatography instrument. Peptides were separated with a 180 min segmented gradient as follows: 7%~25% buffer B (80% ACN/0.1% FA) in 125 min, 25%~35% buffer B for 30 min, 35%~99% buffer B for 5 min, followed by a 5 min 99% wash and 15 min equilibration with buffer A (0.1% FA).

Data acquisition on the Orbitrap Fusion Tribrid platform with instrument control software version 3.0 was carried out using a data-dependent method with multinotch synchronous precursor selection MS3 scanning for TMT-9plex tags. The mass spectrometer was operated in data-dependent most intense precursors Top Speed mode with 3 seconds per cycle. The survey scan was acquired from m/z 375 to 1500 with a resolution of 120,000 resolving power with AGC target 400,000. The maximum injection time for full scan was set to 60 ms. For the MS/MS analysis, monoisotopic precursor selection was set to peptide. AGC target was set to 50,000 with the maximum injection time 120 msec. Charge states unknown and 1 or higher than 7 were excluded. The MS/MS analyses were performed by 1.2 m/z isolation with the quadrupole, normalised HCD collision energy of 37% and analysis of fragment ions in the Orbitrap using 15,000 resolving power with auto normal range scan starting from m/z 110. Dynamic exclusion was set to 60 seconds. For the MS3 scan, the MS3 precursor population from MS2 scan ranging from m/z 300-100

was isolated using the SPS waveform and then fragmented by HCD. The HCD normalized collision energy was set to 65. The MS3 scan were acquired from m/z 100 to 500 with a resolution of 50,000 and AGC target 50,000/ The maximum injection time for full scan was set to 86 ms.

2.2.12.4 Data Processing and Spectra Assignment

Data from the Orbitrap Fusion were processed using Proteome Discoverer Software (ver. 2.2). MS2 spectra were searched using Mascot against a UniProt Mouse database appended to a list of common contaminants (10 090 total sequences). The searching parameters were specified as trypsin enzyme, two missed cleavages allowed, minimum peptide length of 6, precursor mass tolerance of 20 ppm, and a fragment mass tolerance of 0.05Daltons. Oxidation of methionine and TMT at lysine and peptide N-termini were set as variable modifications. Carbamidomethylation of cysteine was set as a fixed modification. Peptide spectral match error rates were determined using the target-decoy strategy coupled to Percolator modeling of positive and false matches. Data were filtered at the peptide spectral match-level to control for false discoveries using a q-value cut off of 0.01, as determined by Percolator. For quantification, the signal-to-noise values higher than 10 for unique and razor peptides were summed within each TMT channel, and each channel was normalized with total peptide amount. Quantitation was further performed by adjusting the calculated p-values according to Benjamini-Hochberg (Benjamini & Hochberg, 1995). The significance regulated proteins with p-value less than 0.05 were further manually investigated with the standard deviations of biological replicates.

2.2.13 Preparation of coverslips for immunofluorescence

To prepare gelatin-coated coverslips, coverslips were first washed in 10% HCl overnight, then washed five times with water. Coverslips were then incubated with 2% (3-Aminopropyl)triethoxysilane (v/v) in acetone for 2 mins, then washed three times with water, and dried for 1 hour at 60 °C. Coverslips were then dipped in freshly boiled 0.66% porcine gelatin and left to dry, covered, overnight. Finally, coverslips were fixed with glutaraldehyde for 10 mins, washed five times with water and left to dry at room temperature.

2.2.14 Immunofluorescence microscopy

mESCs were seeded on gelatin-coated coverslips, and transfected as required as described above. After 24 hours growth, mESCs were fixed with 4% PFA (w/v) in PBS, before being permeabilised in 0.5% Triton X-100 in PBS (v/v) for 5 mins at room temperature. Coverslips were then blocked with 1% Fish gelatin in PBS (w/v), and then incubated with primary antibodies (dilutions in blocking buffer noted in Table 2.6) for 2 hours at room temperature in a humid chamber. After three washes with PBS, secondary antibodies conjugated to fluorophores were diluted 1:500 in blocking buffer and incubated on coverslips for 1 hour at room temperature in a humid chamber. Where cytoskeleton was being observed, Actin Red 555 reagent was added to the secondary antibody mix. After three washes with PBS, 0.1 μg/ml Hoescht was incubated with the coverslips for 5 mins at room temperature in a humid chamber to stain nuclei. After three more washes with PBS, coverslips were mounted onto cover slides using Fluorsave reagent (Millipore). Images were taken using a Leica SP8 confocal microscope, and processed using FIJI and Photoshop CSC software (Adobe).

2.2.15 Quantification of nuclear immunofluorescence signal

FIJI macro was written by Anna Segarra-Fas, nuclear quantification analysis was performed by myself. mESCs were prepared for immunofluorescence as described above, using 0.1 μg/ml Hoechst stain for nuclei and Alexafluor 488-conjugated secondary antibody for the protein of interest. Images were taken using a Leica SP8 confocal microscope and processed using FIJI software. A FIJI macro was written which subjects images to the following treatments:

- Split channels function
- On Blue Hoechst channel
    - Find edges function
    - Make binary conversion
    - Analyse particles function
        - Size micron^2=20-infinity
        - Circularity=0-1

        - Show=overlay and add to ROI manager
    - On Green Alexafluor 488 channel
        - Apply mask from ROI manager
        - Measure intensity of mask signal

This macro therefore identifies nuclei based on the blue Hoechst channel and calculated signal from the green Alexafluor 488 channel within those coordinates. Nuclear quantification data was generated from 10 coverslips across 3 biological replicates.

2.2.16 Statistical analysis

All data shown in this thesis have been replicated with at least two biological repeats that obtained similar results, with the exception of the quantitative proteomic screen. Furthermore, some assays, particularly qRT-PCR and telomere qPCR assays incorporate a number of technical repeats. In each case, the data shown represents each biological repeat as a single point (the average of any technical replicates), and all statistical analysis is performed on these biological data points. In this thesis, biological replicates are defined as experiments in which mESCs were plated on different days, and technical replicates are defined as multiple measurements made from a single sample. Error bars represent mean ± standard error of the mean, unless otherwise stated. Statistical significance of a single comparison is calculated using an unpaired Student T-test (for direct comparison of two conditions) or one-way ANOVA with multiple comparisons (for experiments with more than two conditions), and this and other statistical analysis was performed by GraphPad Prism. Power calculations for telomere qPCR assays were performed using an online tool (http://powerandsamplesize.com/Calculators/Compare-2-Means/2-Sample-Equality), with the following parameters: sample size nB = number of observed measurements for control group, Power = 0.80, p value = 0.05, Group A mean = mean of observed measurements for test group, Group B mean = mean of observed measurements for control group, Standard deviation = calculated standard deviation based on observed measurements for test group, Sampling ratio = 1. Total sample size was then read off the graph at Power = 0.80 and observed test group mean. Total sample size was divided by 2 to give number of samples required for each group, and replicates were randomly selected for each sample group.

3. Identification of ERK5-dependent Proteome Dynamics

3.1 ERK5 signalling in stem cells

ERK5 is a unique MAPK which possesses both a kinase domain and a putative transcriptional activation domain (Kasler et al., 2000). It has also been previously demonstrated to regulate the naïve-primed transition in mESCs (Williams et al., 2016). However, the mechanisms by which ERK5 regulates this transition are not known. Furthermore, the wider functions of ERK5 in mESCs have not been explored. Since many MAPKs regulate diverse biological processes through modulation of transcription factor expression (Boulton et al., 1991; Widmann et al., 1999), and there are several factors, such as MEF2 family members, known to be regulated in this way by ERK5 (Y. Kato, 1997), I performed an unbiased quantitative proteomic screen to identify novel proteins which are modulated by ERK5 signalling (Figure 3.1).

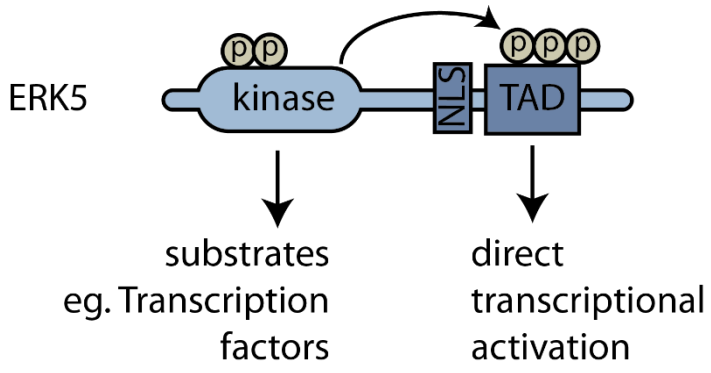

Figure 3.1: ERK5 can regulate proteome dynamics through kinase activity and transcriptional activation domain*. By phosphorylation of transcription factor substrates as well as through direct transcriptional regulation, ERK5 can regulate proteome dynamics by modulating the expression levels of ERK5-dependent proteins.*

3.2 Quantitative Proteomics to Investigate the ERK5-dependent Proteome

To investigate ERK5-dependent proteome dynamics, I designed an experimental approach which could be analysed by both immunoblotting and quantitative proteomics. ERK5 is specifically activated by upstream kinase MEK5. Therefore, I employed a constitutively active MEK5 mutant (S311D T315D) (hereafter MEK5DD) to specifically

activate the ERK5 pathway. To further demonstrate that any observed changes are attributable to ERK5 kinase activity, I included a condition in which MEK5DD was expressed, but mESCs were also treated with ERK5-specific inhibitor AX15836 (10 µM, 24 hr). mESCs were transfected with empty vector, MEK5DD, or MEK5DD with AX15836 treatment (10 µM, 24 hr), in triplicate. Previous validation of this transfection technique has found that between 60-75% cells are successfully transfected. Under conditions where ERK5 is active, ERK5 demonstrates retarded mobility on SDS-PAGE, as ERK5 C-terminal autophosphorylation retards its progression through the gel (Boulton et al., 1991) (Figure 3.2). Additionally, KLF2 is a known target of ERK5 (Morikawa et al., 2016; Sunadome et al., 2011). KLF2 levels increase when ERK5 is active and this is reversed when ERK5 is inhibited (Figure 3.2). MEK5DD is present in both pathway activated and ERK5 inhibited conditions. Interestingly, MEK5 levels are higher when ERK5 is inhibited, since active ERK5 results in MEK5 turnover through a negative feedback loop (Mody et al., 2003). These data demonstrate that ERK5-responsive proteins change expression upon transfection with MEK5DD, and this change is reversed with AX15836 treatment. This acts as a proof of principle for the quantitative proteomics approach.

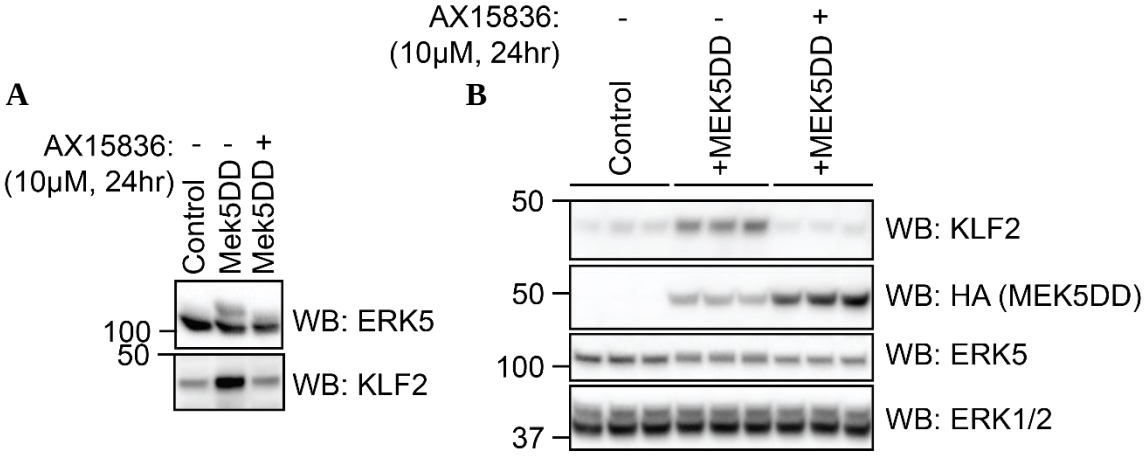

Figure 3.2: ERK5 activation with constitutively active MEK5 induces known ERK5 target KLF2. *A - mESCs were cultured under control (empty vector), pathway activated (+MEK5DD) and pathway inhibited (+MEK5DD +AX15836 (10 µM, 24 hr)) conditions. mESCs were lysed 48hr post transfection, with 24hr puromycin selection prior to lysis. KLF2 and ERK5 levels were determined by immunoblotting. KLF2 acts as a positive control as it is induced by ERK5 signalling, and returned to basal levels by ERK5 inhibition. Samples were run on a 6% agarose gel to highlight the retardation of ERK5 mobility upon autophosphorylation. Results are representative of 3 experiments. B - mESCs were cultured under the same conditions as A. KLF2, MEK5DD, and ERK5 levels were determined by immunoblotting. KLF2 was used as a positive control for ERK5 activation. ERK1/2 was used as a loading control. Results are representative of 3 experiments.*

To identify proteins which are regulated by ERK5, I used quantitative proteomics to detect proteins whose levels change with ERK5 signalling. Again, I transfected mESCs with either empty vector control or MEK5DD and treated with either DMSO control or AX15836 (10 μM, 24 hr) in biological triplicate. After 48 hours growth, I lysed the mESCs, digested proteins with trypsin, labelled with TMT and separated by liquid chromatography (Figure 3.3). I then subjected the samples to LC-MS/MS. As with the proof of principle experiment (Figure 3.2), I would hypothesise that proteins which respond to ERK5 signalling will be up- or down-regulated with MEK5DD, with this effect reversed with AX15836 treatment, as is seen with positive control KLF2.

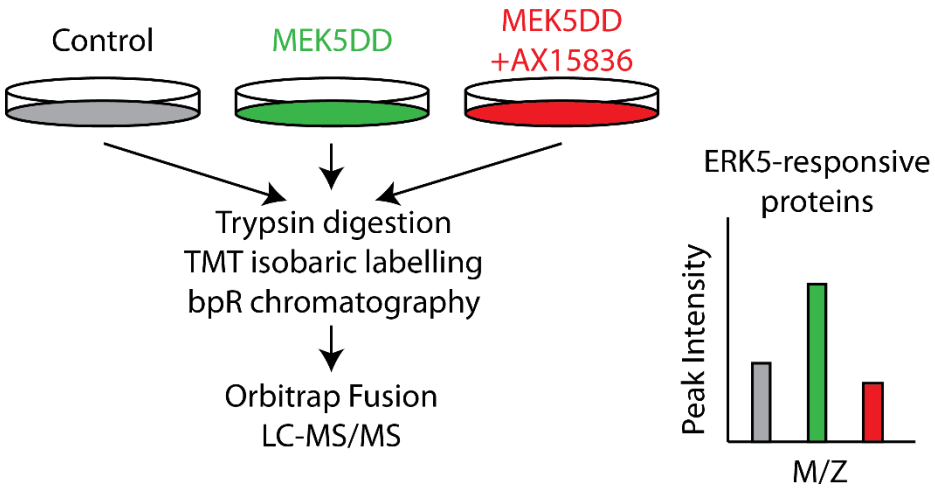

Figure 3.3: Workflow of quantitative proteomics pipeline to identify the ERK5-dependent proteome. *mESCs were transfected with either empty vector control or constitutively active MEK5 (MEK5DD) to activate ERK5 signalling and treated with either DMSO control or AX15836 (10 μM, 24 hr) to inhibit ERK5 signalling. After 48 hours of growth and 24 hours of puromycin selection, cells were lysed, proteins subjected to trypsin digestion, peptides labelled with Tandem Mass Tags (TMT), subjected to basic pH reverse phase (bpR) chromatography and submitted for mass spectrometry analysis. ERK5-responsive proteins are expected to exhibit a change in expression with MEK5DD which is reversed by MEK5DD with AX15836.*

3.3 ERK5 regulates a specific cohort of protein targets

I first investigated the coverage achieved by the mass spectrometry analysis. The quantitative proteomics detected 8732 proteins, of which 7639 proteins had at least 2 unique peptides assigned to them. All subsequent analysis has been performed on the

dataset of proteins with at least 2 unique peptides. This dataset has been uploaded to and is publicly available from Pride (www.ebi.ac.uk/pride/archive/projects/PXD024679).

Having generated a dataset of 7639 proteins, I investigated which proteins are responsive to ERK5 signalling. To do this, I calculated the fold change of each protein expressed in MEK5DD-expressing mESCs compared to mESCs transfected with empty vector, and calculated the significance of this fold change. This illustrated that ERK5 regulates a specific cohort of proteins, with only 53 out of 7639 proteins exhibiting $\log_2$(fold change) > 0.5 and a significance of $p < 0.05$ (Figure 3.4). The positive control KLF2 exhibited a larger fold change than all but one other protein.

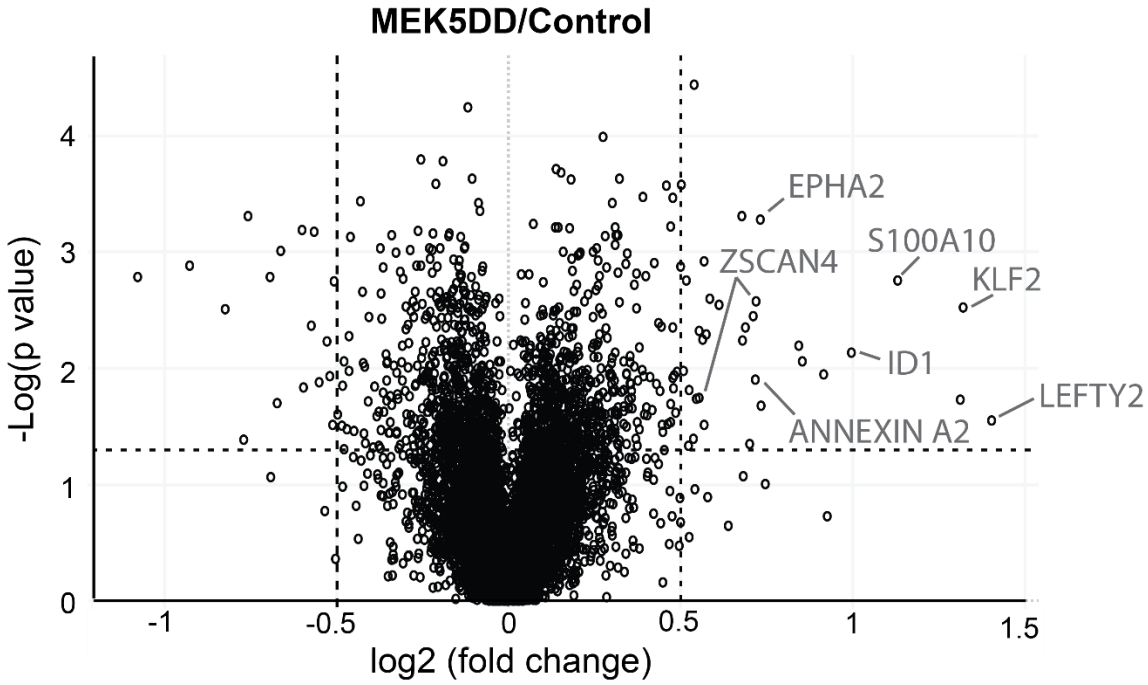

Figure 3.4: ERK5 regulates a specific cohort of proteins. *The plot shows log2(fold change) against significance (-log(p value)) for all proteins detected by quantitative proteomics, comparing MEK5DD-expressing mESCs with control mESCs transfected with empty vector. Each data point represents the mean fold change (n=3). Fold change thresholds were set at log2(fold change)<-0.5 and >0.5. Significance threshold was set at p<0.05. Positive control KLF2 and other proteins of interest are highlighted.*

To confirm whether the 53 identified proteins were ERK5-specific targets, I verified whether AX15836 treatment reversed the effect by overlaying a bar graph of MEK5DD/control (green) with a bar graph of MEK5DD+AX15836/control (red). This illustrates that AX15836 inhibits the expression of all these proteins to some extent

(Figure 3.5). This data confirms that the 53 proteins identified in the MEK5DD condition are ERK5-specific.

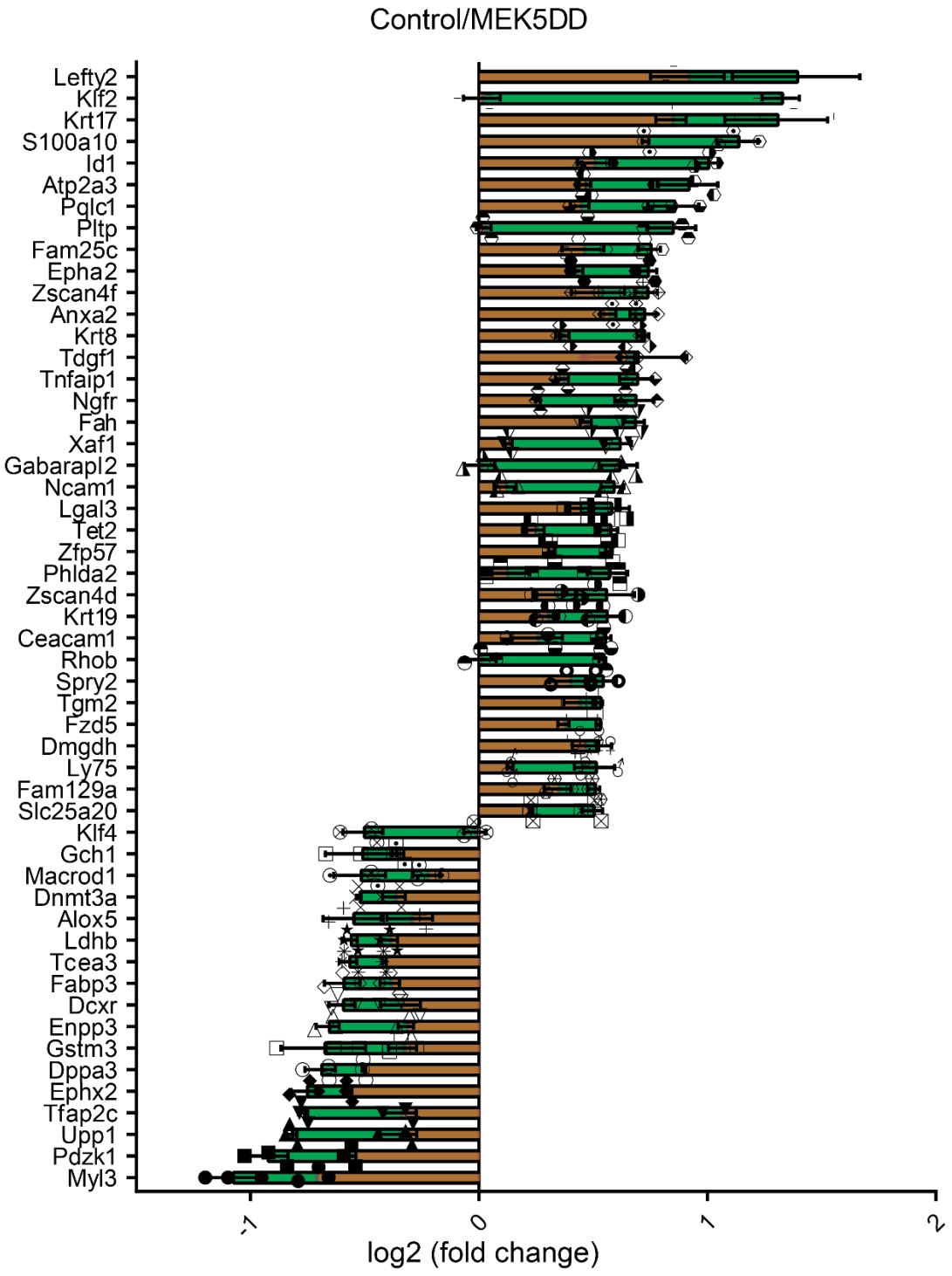

Figure 3.5: Summary of significantly-regulated ERK5-dependent proteins. *The plot shows log2(fold change), comparing pathway activated and control conditions (in green) and pathway inhibited and control (in red) for the 53 proteins which exhibit a significant fold change by proteomics. Each data point represents a biological replicate compared to the mean of control conditions. Error bars indicate SD.*

I next investigated if other pluripotency factors are regulated by ERK5 signalling by generating a volcano plot comparing control and MEK5DD conditions and highlighting proteins with known roles in pluripotency and stem cell maintenance (list from Maguire et al., 2013). The majority of these proteins lie within the no significant fold change regions (Figure 3.6); however nine including KLF2, the positive control for this experiment, are significantly upregulated by ERK5 signalling. Other stem cell factors which are regulated by ERK5 include LEFTY2 (a TGFβ pathway inhibitor), ID1 (an inhibitor of differentiation), ZSCAN4 (a regulator of stem cell rejuvenation), TDGF1 (a NODAL co-receptor), and NCAM1 (a neural cell adhesion protein). Additionally, DPPA3 (protects DNA methylation during zygotic genome activation) and KLF4 (transcription factor which prevents differentiation) are downregulated in response to ERK5 signalling.

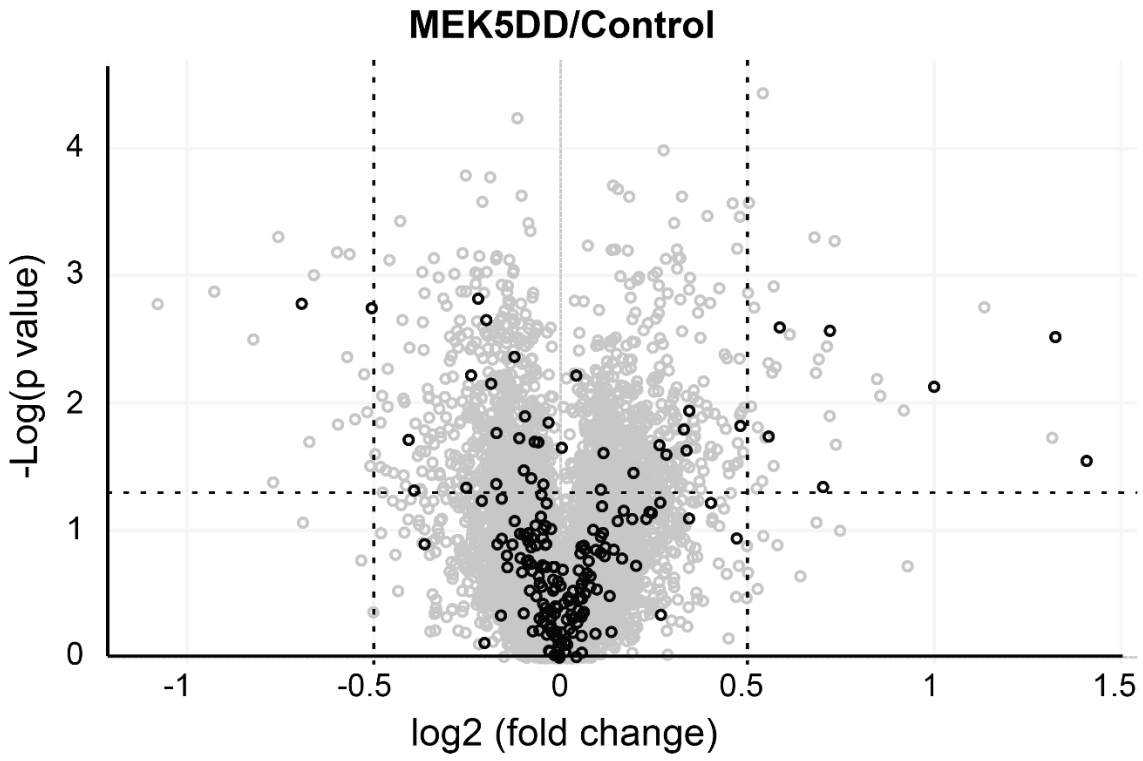

Figure 3.6: Pluripotency factors are not generally upregulated by ERK5 signalling. *The plot shows log2(fold change) against significance (-log(p value)) for the proteomic data, comparing pathway activated (+MEK5DD) and control conditions. Fold change and significance thresholds are indicated by dotted lines ($p<0.05$). Pluripotency factors are highlighted in black.*

Given that pluripotency markers were not generally upregulated, I asked which classes of proteins were responsive to ERK5 signalling. To do this, I performed GO term analysis on the 53 putative targets. First, I performed a Statistical Overrepresentation Test, which calculates how many times a given GO term is likely to appear in a dataset of a particular size. Four GO terms were significantly overrepresented – namely response to growth factor, epithelial cell differentiation, cellular response to chemical stimulus, and regulation of protein metabolic process (Table 3.1). This confirms what is already known about ERK5, in that ERK5 responds to external stimuli including growth factors and chemicals, and regulates differentiation to particular cell fate lineages.

Table 3.1: Statistical Overrepresentation Test on Biological Process GO terms.

GO BIOLOGICAL PROCESS	#	EXPECTED	FOLD ENRICHMENT	RAW P VALUE	FDR
RESPONSE TO GROWTH FACTOR	5	0.31	16.19	1.05E-05	4.16E-02
EPITHELIAL CELL DIFFERENTIATION	6	0.38	15.83	1.28E-06	2.02E-02
CELLULAR RESPONSE TO CHEMICAL STIMULUS	10	1.78	5.61	1.59E-06	1.25E-02
REGULATION OF PROTEIN METABOLIC PROCESS	10	2.07	4.82	6.37E-06	3.35E-02

I then performed a functional classification analysis of ERK5-dependent proteins on biological process GO terms. This highlights the role of ERK5 signalling in regulating processes such as cellular response to stimulus, signal transduction, development, cell cycle, and cell survival (Gírio et al., 2007; Iñesta-Vaquera et al., 2010; Kato et al., 1998; Roberts et al., 2009), as well as introducing potentially novel ERK5 functions in cellular

component organisation, which is defined as “a process that results in the biosynthesis of constituent macromolecules, assembly, arrangement of constituent parts, or disassembly of a cellular component” (Figure 3.7). GO term analysis has limitations when applied to a small list of genes such as the ERK5-dependent proteins identified by proteomics. This may have been improved by comparing the ERK5-dependent proteins against the genes identified in the proteomics rather than against the complete genome.

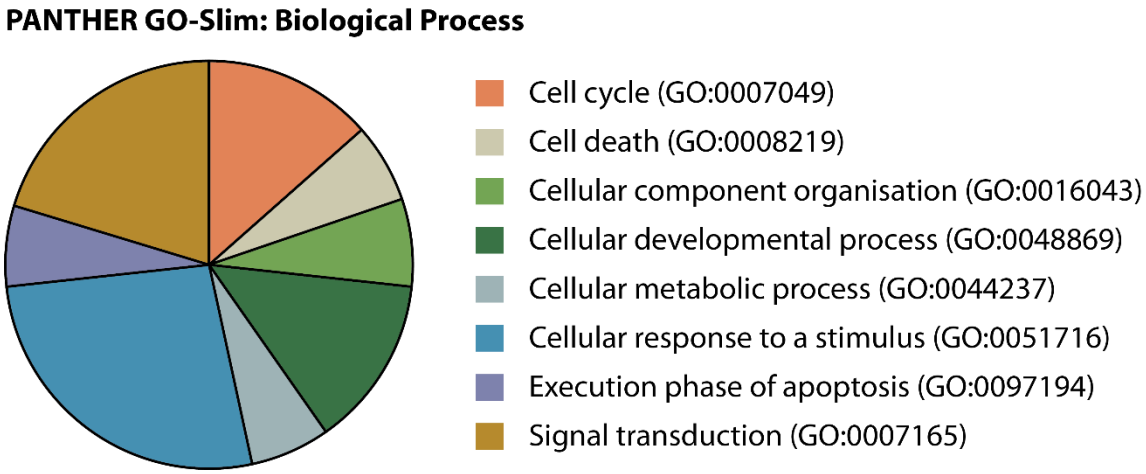

Figure 3.7: GO term analysis indicates roles for ERK5 in biological processes. *Analysis was performed by PANTHER online tool, on the 53 proteins which exhibited a significant fold change with MEK5DD compared to control conditions in the proteomics.*

Having ascertained general themes of ERK5-dependent biological processes, I next investigated the individual hits from the proteomic screen (Figure 3.8). These proteins were prioritised for validation and further investigation either because they play a well-characterised role in stem cell processes or development, or because they have previously not been investigated in stem cells, but have been implicated in a process relevant to stem cell biology. In particular, I prioritised six proteins with clear hypotheses for functions in mESCs which displayed the most significant fold changes between control and MEK5DD conditions (Table 3.2).

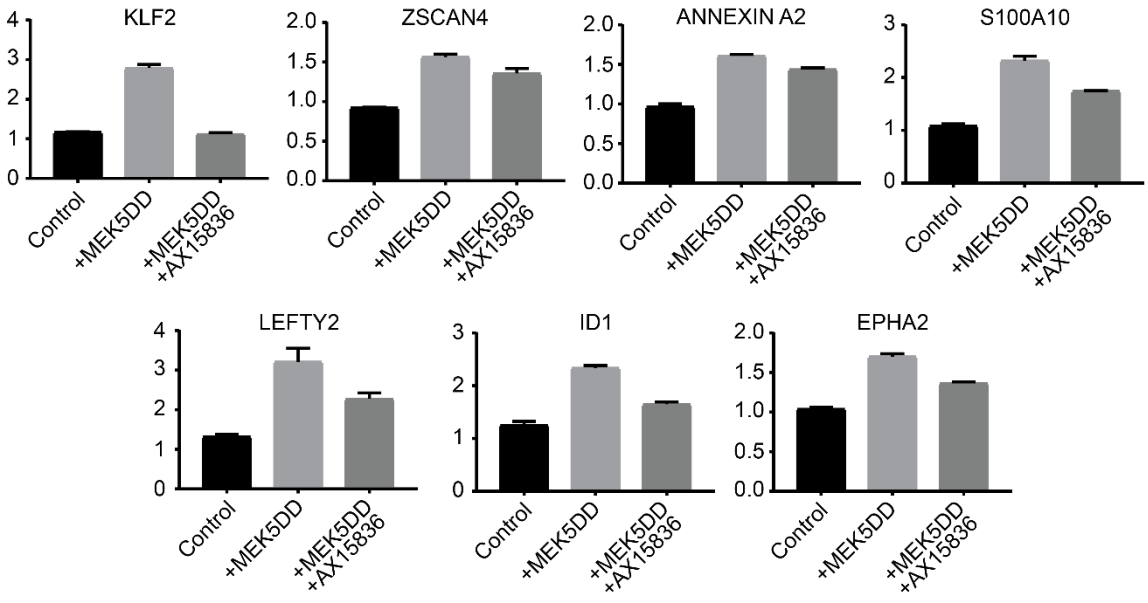

Figure 3.8: Potential ERK5-dependent proteins identified by proteomic analysis. *Bars indicate mean fold change with MEK5DD compared to control condition from the proteomic data. Error bars indicate SD (n=3). KLF2 is a known target of ERK5 and has been included as a positive control.*

Table 3.2: Proteomic screen hits prioritised for validation.

PROTEIN	FUNCTION	REFERENCE
ZSCAN4	A key regulator of stem cell rejuvenation, an essential process which allows cultured stem cells to maintain their genomic stability during indefinite passaging	(Zalzman et al., 2010)
ANNEXIN A2 AND S100A10	Form a heterotetrameric complex which has been implicated in a number of membrane-bound processes including migration, epithelial-mesenchymal transition, and vesicle trafficking	(D. B. N. Lee, 2004)
LEFTY2	An inhibitor of the TGFβ pathway, required for left-right asymmetry determination	(Ulloa & Tabibzadeh, 2001)
ID1	A transcriptional regulator implicated in several cellular processes including cell growth, senescence, differentiation, apoptosis, angiogenesis and neoplastic transformation	(Ruzinova & Benezra, 2003)
EPHA2	A receptor tyrosine kinase which, in response to its ligand EFNA1, regulates migration, adhesion, proliferation and differentiation	(Miao et al., 2015)

3.4 Validation of four novel ERK5-responsive proteins

In order to confirm that these proteins are regulated by ERK5, I next validated the proteins identified by the proteomic screen through western blot analysis. To do this, I transfected mESCs with either empty vector or MEK5DD, and treated with either DMSO or AX15836, as before. I first investigated proteins with known roles in pluripotency. ZSCAN4, a key regulator of stem cell rejuvenation, is upregulated by ERK5 signalling, validating the results from the proteomics (Figure 3.9). Consistent with the quantitative proteomics analysis, ERK5 does not regulate protein levels of other pluripotency factors, such as NANOG and SOX2.

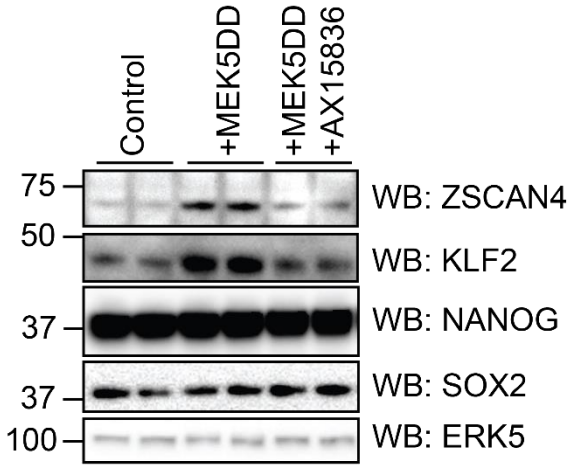

Figure 3.9: ZSCAN4 is induced by ERK5 signalling. *mESCs were cultured under control (empty vector), pathway activated (+MEK5DD) and pathway inhibited (+MEK5DD +AX15836 (10 μM, 24 hr)) conditions. mESCs were lysed 48hr post transfection, with 24hr puromycin selection prior to lysis. ZSCAN4, KLF2, NANOG and SOX2 levels were determined by immunoblotting. KLF2 was used as a positive control, ERK5 was used as a loading control. Results are representative of 3 experiments.*

I next investigated two other hits, ANNEXIN A2 and S100A10, which form a complex that regulates diverse membrane processes (Bharadwaj et al., 2013). ANNEXIN A2 and S100A10 are both upregulated by ERK5 signalling, validating the results from the proteomics (Figure 3.10).

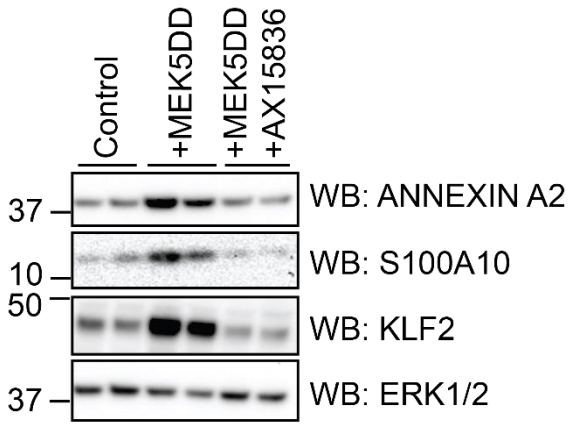

Figure 3.10: ANNEXIN A2 and S100A10 are induced by ERK5 signalling. *mESCs were cultured under control (empty vector), pathway activated (+MEK5DD) and pathway inhibited (+MEK5DD +AX15836 (10 μM, 24 hr)) conditions. mESCs were lysed 48hr post transfection, with 24hr puromycin selection prior to lysis. ANNEXIN A2, S100A10, and KLF2 levels were determined by immunoblotting. KLF2 was used as a positive control, ERK1/2 was used as a loading control. Results are representative of 3 experiments.*

I finally investigated two more hits, ID1 and EPHA2, which had been of previous interest to the lab as regulators of differentiation and early embryonic compartmentalisation respectively (Fernandez-Alonso et al., 2020; Yokota, 2001). ID1 and EPHA2 show conflicting results between the proteomic and immunoblot approaches, in that no induction by MEK5DD was observed through western blot analysis, and as such were not prioritised for further study (Figure 3.11).

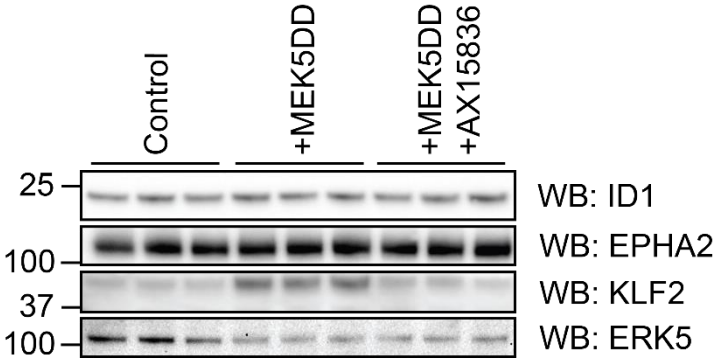

Figure 3.11: ID1 and EPHA2 do not show induction with ERK5 signalling by immunoblotting. *mESCs were cultured under control (empty vector), pathway activated (+MEK5DD) and pathway inhibited (+MEK5DD +AX15836 (10 μM, 24 hr)) conditions. mESCs were lysed 48hr post transfection, with 24hr puromycin selection prior to lysis. ID1, EPHA2 and KLF2 levels were determined by immunoblotting. KLF2 was used as a positive control, ERK5 was used as a loading control. Results are representative of 3 experiments.*

3.4.1 ERK5 signalling does not modulate TGFβ signalling

LEFTY2 is one of the most dynamically regulated proteins identified in the proteomic screen, but, as a secreted protein (Westmoreland et al., 2007), poses challenges for immunoblotting. LEFTY2 protein is rapidly secreted upon induction of expression, so although some LEFTY2 may be detectable by immunoblot in cell lysates, it is likely that changes in LEFTY2 levels would be difficult to detect, or could be detected in the growth media instead. However, as ERK5 regulates gene transcription through multiple mechanisms, I tested whether *Lefty2* mRNA is regulated by ERK5 signalling. These data confirm that *Lefty2* is dynamically regulated by ERK5 signalling (Figure 3.12).

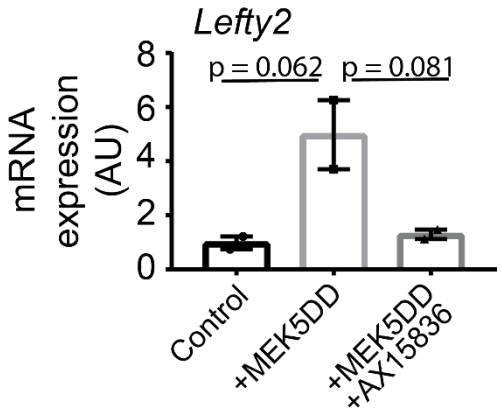

Figure 3.12: Lefty2 is transcriptionally regulated by ERK5 signalling. *mESCs were cultured under control (empty vector), pathway activated (+MEK5DD) and pathway inhibited (+MEK5DD +AX15836 (10 μM, 24 hr)) conditions. mESCs were lysed 48hr post transfection, with 24hr puromycin selection prior to lysis. RNA was extracted and subjected to qRT-PCR. Error bars indicate SEM (n=2). Significance calculated by one-way ANOVA with multiple comparisons.*

TGFβ signalling is induced by ligand binding to a TGFβ receptor. This leads to receptor dimerisation and activation of the receptor kinase activity. The receptor then phosphorylates SMAD proteins, which translocate to the nucleus, leading to the regulation of TGFβ target genes (Choi et al., 1996; Wrana et al., 1992; Wrana et al., 1994; Younai et al., 1994). LEFTY2 regulates the TGFβ pathway by inhibiting SMAD2 phosphorylation after TGFβ receptor activation (Ulloa & Tabibzadeh, 2001). I therefore hypothesised that ERK5 signalling modulates TGFβ signalling through LEFTY2. To test

this, I transfected mESCs with either empty vector or MEK5DD, and treated with either DMSO or AX15836 as before, as well as inducing TGFβ signalling with Activin (a ligand which stimulates TGFβ signalling), and inhibiting TGFβ signalling using SB505124 (a small molecule inhibitor of the TGFβ receptor).

These data show that although SMAD2 phosphorylation increases with Activin and decreases with SB505124 as expected, no change is seen with either MEK5DD or AX15836 (Figure 3.13). This suggests that ERK5 does not impact on TGFβ signalling as measured by canonical SMAD2 phosphorylation. This experimental design allows the investigation of whether ERK5 signalling modulates TGFβ signalling relative to basal or a positive and negative control. However, it would also have been informative to combine MEK5DD or AX15836 treatment with activation of TGFβ signalling to understand whether, for example, ERK5 signalling can reduce maximal TGFβ signalling.

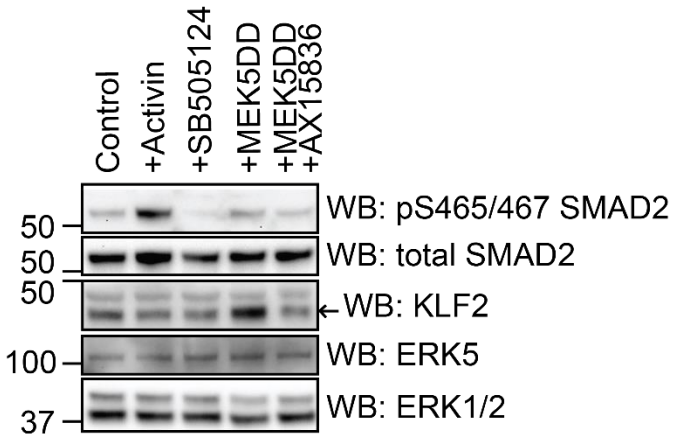

Figure 3.13: ERK5 signalling does not regulate TGFβ signalling through SMAD phosphorylation. *mESCs were cultured under control (empty vector), TGFβ pathway activated (+Activin) and inhibited (+SB505124 (10 μM, 24 hr)), ERK5 pathway activated (+MEK5DD) and pathway inhibited (+MEK5DD +AX15836 (10 μM, 24 hr)) conditions. mESCs were lysed 48hr post transfection, with 24hr puromycin selection prior to lysis. pS465/467 SMAD2, total SMAD2, KLF2 and ERK5 levels were determined by immunoblotting. KLF2 was used as a positive control for ERK5 signalling, ERK1/2 was used as a loading control. Results are representative of 3 experiments.*

To test whether ERK5 regulates the mRNA of other TGFβ pathway members, I performed qRT-PCR analysis on genes representing different hierarchical levels of the TGFβ pathway. TGFβ1 and NODAL are TGFβ family ligands, whereas LEFTY2 and INHBB are TGFβ signalling inhibitors from different inhibitor families. Other than *Lefty2*, these genes do not show an effect with MEK5DD which is reversed by AX15836, suggesting ERK5 signalling does not regulate TGFβ signalling activation or inhibition, other than via LEFTY2 (Figure 3.14).

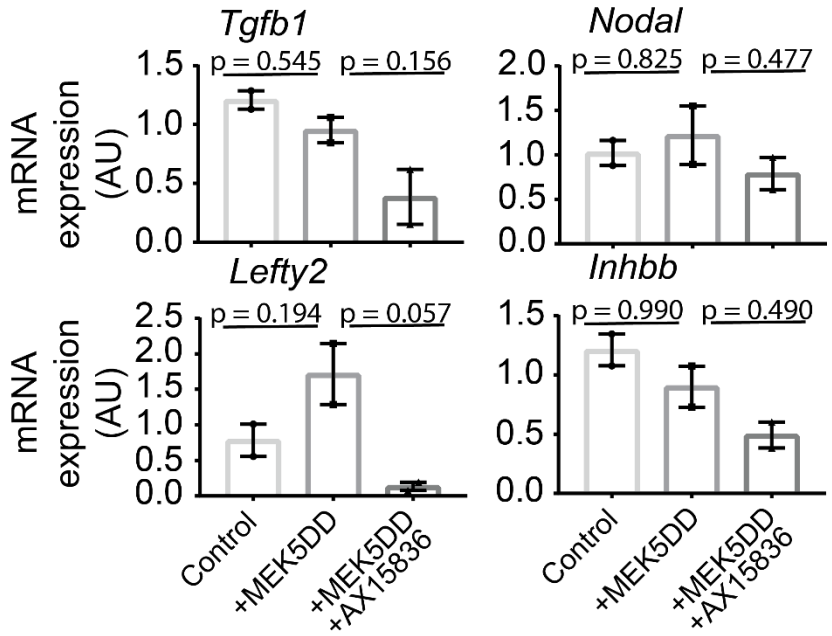

Figure 3.14: ERK5 signalling does not regulate TGFβ family ligands or inhibitors other than LEFTY2. *mESCs were cultured under control (empty vector), pathway activated (+MEK5DD) and pathway inhibited (+MEK5DD +AX15836 (10 μM, 24 hr)) conditions. mESCs were lysed 48hr post transfection, with 24hr puromycin selection prior to lysis. RNA was extracted and subjected to qRT-PCR. TGFβ1 and NODAL are examples of TGFβ pathway activators. Lefty2 and Inhbb belong to different families of TGFβ pathway inhibitors. Error bars indicate SEM (n=2). Significance calculated by one-way ANOVA with multiple comparisons.*

Activin receptors and TGFβ receptors respond to Activin and TGFβ ligand binding by phosphorylating intracellular pathway components. These genes do not show a significant effect upon MEK5DD expression which is reversed by AX15836, although *Acvr2a* shows a trend of downregulation with MEK5DD which is partially reversed with AX15836 treatment (Figure 3.15).

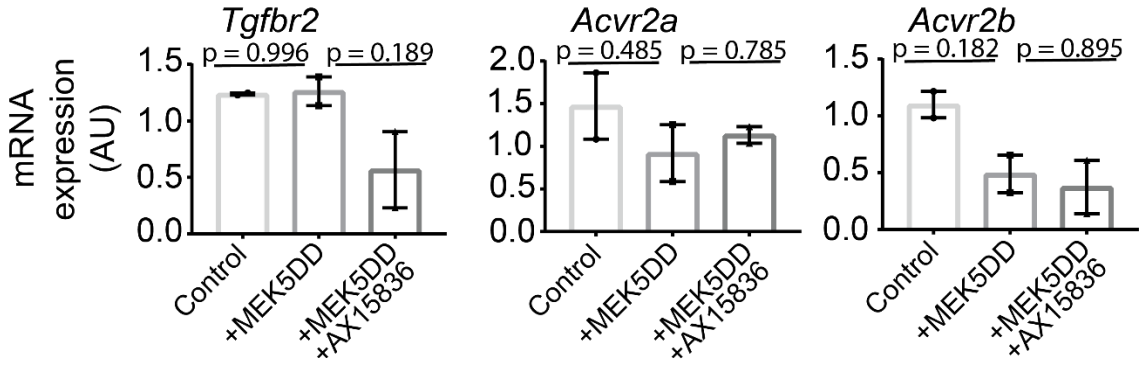

Figure 3.15: ERK5 signalling does not consistently regulate TGFβ receptor expression. *mESCs were cultured under control (empty vector), pathway activated (+MEK5DD) and pathway inhibited (+MEK5DD +AX15836 (10 μM, 24 hr)) conditions. mESCs were lysed 48hr post transfection, with 24hr puromycin selection prior to lysis. RNA was extracted and subjected to qRT-PCR. TGFβR2, ACVR2A and ACVR2B are examples of TGFβ family receptors. Error bars indicate SEM (n=2). Significance calculated by one-way ANOVA with multiple comparisons.*

Downstream of TGFβ signalling, target genes such as *Brachyury* and *Mixl* are induced. Neither exhibits a significant fold change in response to ERK5 signalling (Figure 3.16). In summary, ERK5 signalling dynamically regulates *Lefty2* mRNA, but this does not appear to affect TGFβ pathway regulation or functions.

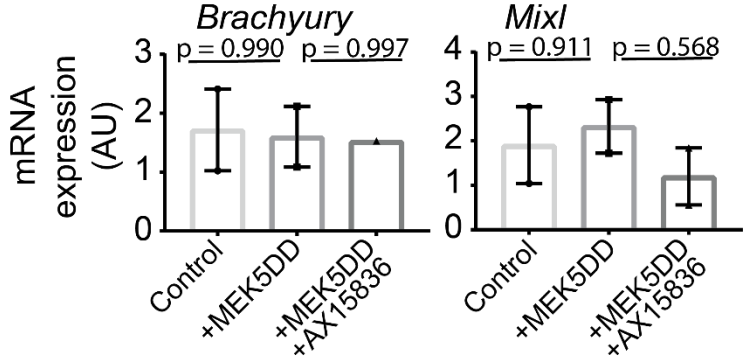

Figure 3.16: TGFβ signalling target genes are not regulated by ERK5 signalling. *mESCs were cultured under control (empty vector), pathway activated (+MEK5DD) and pathway inhibited (+MEK5DD +AX15836 (10 μM, 24 hr)) conditions. mESCs were lysed 48hr post transfection, with 24hr puromycin selection prior to lysis. RNA was extracted and subjected to qRT-PCR. Brachyury and Mixl are target genes of TGFβ signalling. Error bars indicate SEM (n=2). Significance calculated by one-way ANOVA with multiple comparisons.*

3.5 Discussion

The objectives for this chapter were to use a proteomic screen to identify proteins regulated by ERK5. I used GO term analysis to identify ERK5-dependent biological processes based on the results from the proteomic screen. I next performed preliminary validation which confirmed four novel ERK5-dependent targets, namely ZSCAN4, ANNEXIN A2, S100A10 and *Lefty2*. Although *Lefty2* was initially a promising hit, subsequent TGFβ pathway analysis revealed that ERK5 signalling does not significantly regulate this pathway.

The quantitative proteomics assigned peptides to 8732 proteins. A previous total proteomic approach conducted by the Findlay lab identified 9183 proteins, suggesting that the majority of the proteins detectable in mESCs were detected in this screen, and therefore it is likely that most ERK5-dependent proteins were captured by this screen (Fernandez-Alonso et al., 2017). However, as mass spectrometry may not detect every protein in the cell, some ERK5-dependent proteins may have been missed.

As stimuli that specifically and selectively activate ERK5 signalling have not yet been identified in mESCs, I transfected mESCs with MEK5DD. However, there are a number of limitations associated with transfection approaches. Firstly, the transfection efficiency may be less than 100%. Unless a single-cell analysis is used, the data will therefore be an average over cells in which ERK5 is active and those in which ERK5 is not active. This may lead to protein level fold changes being underrepresented. Additionally, the transfection efficiency may vary between biological replicates. This could give a high degree of variation in the data.

Despite ERK5 being identified as a critical regulator of stem cell pluripotency (Williams et al., 2016), the proteomic data suggests ERK5 regulates a very specific cohort of proteins, with the majority of the proteome, and particularly stem cell and pluripotency factors, unchanged by ERK5 signalling. This suggests that ERK5 regulates specific processes rather than large scale transcriptional and gene expression changes, as large-scale transcriptional changes would likely be associated with large numbers of ERK5-dependent proteins. This is unusual for signalling pathways regulating pluripotency as

many modulate the expression of pioneer factors such as OCT4, which then regulate a hierarchy of pluripotency factors (Lanner & Rossant, 2010; Onishi & Zandstra, 2015). However, ERK5 plays a critical role in the maintenance of naïve pluripotency (Williams et al., 2016). It may be, therefore, that ERK5 fine-tunes pluripotency within the wider context of the pluripotency signalling network through ERK5's own specific transcriptional programme, for example through KLFs. Previous studies have shown that ERK5 can regulate pluripotency factors such as OCT4 and NANOG over longer timescales and thereby support naïve pluripotency more generally (Williams et al., 2016). As such, this proteomic approach provides a snapshot view of early events in ERK5 signalling. Therefore, it may be that KLF2 is a primary target of ERK5 signalling, which then facilitates the longer-term effects of the pathway. This is consistent with the concept of pluripotency factors regulating each other to support and maintain pluripotency (Boyer et al., 2005).

Additionally, the small cohort of ERK5-dependent proteins and low fold change values may indicate that this approach and timeframe are not fully optimised. For example, if these proteins are transcriptionally regulated, a transcriptomic approach at an earlier time point might capture more statistically significant ERK5-dependent responses, which may have ceased by 48 hours when the proteomic samples were taken. Furthermore, as many ERK5 functions are regulated by KLF2 (Sunadome et al., 2011), it may be that determining the optimal conditions for primary and secondary targets of ERK5 signalling will be crucial for future work.

Since ERK5 is a MAPK, and MAPKs propagate signalling downstream of external factors including growth factors and chemical stimuli (Boulton et al., 1991; Widmann et al., 1999), the GO term analysis data showing that ERK5 regulates proteins associated with cellular response to a stimulus and signal transduction are not surprising. Similarly, MAPK signalling often leads to metabolic changes (Qi & Elion, 2005; Yang et al., 2003), so that GO term is also consistent with previous literature. However, an overrepresentation of proteins involved in epithelial cell differentiation is unexpected, as ERK5 prevents differentiation and maintains pluripotency in stem cells (Williams et al., 2016). Conversely, ERK5 has been shown in many systems to be required for

differentiation, such as osteoclast, macrophage, and myogenic differentiation (Amano et al., 2015; Chen et al., 2017; Luiz et al., 2020). Therefore, ERK5 is likely to prevent differentiation in some contexts, such as mESCs, and promote differentiation in other contexts, such as later in development.

I have validated several targets identified by the proteomic screen as ERK5-responsive. These data show that ERK5 regulates ZSCAN4, ANNEXIN A2/S100A10 and *Lefty2*. This has interesting implications for the role of ERK5 in stem cells. *Lefty2* is dynamically responsive to ERK5 signalling. Despite this, TGFβ signalling is unaffected by ERK5 signalling. This may be due to the diverse set of TGFβ signalling activators and inhibitors, meaning that LEFTY2 may not be the dominant inhibitory ligand in this context. Instead, another inhibitory ligand, such as LEFTY1, may be more highly expressed, such that even a 5-fold increase in *Lefty2* does not significantly increase the complement of inhibitory species relative to the activating species. To investigate this hypothesis, I interrogated a proteomic dataset previously generated by the Findlay lab which quantifies the average copy number for each protein in mESCs. However, only one peptide was identified for the LEFTY proteins and was assigned as both LEFTY1 and LEFTY2, and as such I was unable to determine the relative levels at which LEFTY1 and LEFTY2 are expressed. Additionally, it should be noted that performing qPCR analysis with small n numbers (for example n=2) is likely to give low statistical significance, so these experiments may require further replicates to determine conclusively whether these data are of biological importance. Interestingly, in lung and renal systems, ERK5 and TGFβ signalling may regulate each other. However, it has been suggested that this is a positive regulation, with inhibition of ERK5 signalling blocking TGFβ functions, and TGFβ activating ERK5 signalling (Browne et al., 2008; Kadoya et al., 2019). As ERK5 signalling does not have a clear role in TGFβ signalling in mESCs, I chose to further investigate stem cell rejuvenation through ZSCAN4 and membrane dynamics through the ANNEXIN A2/S100A10 heterotetramer.

ZSCAN4 is a key regulator of stem cell rejuvenation, a process through which stem cells must cycle to maintain the genomic stability required for indefinite culture (Zalzman et al., 2010). The rejuvenative state shares features with the 2-cell (2C) stage of embryo

development (Eckersley-Maslin et al., 2016). Since stem cells cultured in LIF/Serum exist in a dynamic equilibrium lying along the developmental timeline (from 2C to naïve pluripotency to primed pluripotency), reprogramming cells back to the 2C stage through expression of ZSCAN4 may provide a mechanism by which ERK5 maintains naïve pluripotency.

Interestingly, ZSCAN4 is associated with a specific transcriptional programme typical of the 2C stage of embryonic development, so it may be that ERK5 regulates this programme (Hirata et al., 2012). Furthermore, the 2C transcriptional programme is complemented by global DNA demethylation. DPPA3, observed to be downregulated by MEK5DD in the proteomic dataset, protects DNA methylation during zygotic genome activation (Dan et al., 2017; Ficz et al., 2011). Downregulation of DPPA3 by ERK5 is therefore consistent with ERK5 regulating the 2C state. By reverting cells to a more developmentally early state, ERK5 could prevent differentiation and maintain mESCs in a more naïve state as previously described (Williams et al., 2016).

ERK5 has not previously been shown to regulate membrane dynamics. Furthermore, although the ANNEXIN A2/S100A10 complex has been well studied in different systems, its role in stem cells has not been investigated. Whilst the ANNEXIN A2/S100A10 complex has been implicated in a wide variety of membrane-associated processes including vesicular trafficking and lysosome formation (Morel & Gruenberg, 2007; Zobiack et al., 2003), it is particularly exciting to note that it has been implicated in cell-cell contacts and interaction with the extracellular matrix (Madureira et al., 2011). This presents a clear hypothesis of how ANNEXIN A2 and S100A10 influence stem cell behaviour, as cell motility and responding to changing extracellular environments is key for organism development. Furthermore, as these roles have largely been identified in cancer systems, this could implicate ERK5 in cancer progression (Feighery et al., 2008; Grindheim et al., 2017; Lee, 2004). Additionally, I identified TDGF1 and NCAM1 as ERK5-responsive proteins in the proteomic dataset. TDGF1 and NCAM1 are associated with cell-cell contacts (as a NODAL co-receptor and adhesion protein respectively). Therefore, induction of these proteins by ERK5 could indicate that ERK5 regulates the interactions between mESCs and their environment, including the extracellular matrix and

other neighbouring cells (Julio et al., 2011; Lanier et al., 1991). This would be consistent with previously described roles of ERK5 in vascularisation and cancer progression (Pereira et al., 2019; Ramsay et al., 2011; Roberts et al., 2010).

4. ANNEXIN A2/S100A10 complex is regulated by ERK5 signalling

4.1 Introduction to ANNEXIN and S100 proteins

The annexin protein family bind through basic residues to negatively charged phospholipid membranes in a calcium-dependent manner to aggregate or organise ("annex") membranes (Creutz et al., 1978). They are conserved across vertebrates, invertebrates, fungi and protozoa, plants, and protists, although the structures of the annexins are highly divergent between and within these groups, resulting in the subclassification of annexins into A, B, C, D and E, where A type annexins are expressed in vertebrates (Human Gene Nomenclature Committee).

Annexins are characterised by their structural domains, namely a variable N-terminal head domain, responsible for protein interaction specificity and post-translational modification, and a conserved C-terminal core domain, which embeds into phospholipid membranes (Gerke & Moss, 2002). Although integral to membranes, annexins are not transmembrane proteins, however they can be found on either the inner or outer leaflet of the membrane (Bharadwaj et al., 2013). The C-terminal domain typically contains four homologous domains, made up of five α-helices. At least one of these domains will house the characteristic endonexin fold, containing a calcium-binding motif (KGXGT-38 residues-D/E) (Gerke & Moss, 2002).

The annexins typically form dimers or heterotetramers with an S100 protein (Rintala-Dempsey et al., 2008). Each annexin forms a specific interaction with a given S100 family member, as determined by the interaction motifs in the variable N-terminal head domain, although some annexins and S100s may bind multiple partners due to a more permissive interaction sequence (Rintala-Dempsey et al., 2008). S100 family members are small calcium-binding proteins containing two EF-hand motifs. They are structurally similar to calmodulin; however, while calmodulin is expressed at all times and in many cell types, S100 family members are expressed in a cell type-specific manner, often in response to a particular stimulus (Heizmann et al., 2002; Marenholz et al., 2004).

ANNEXIN A2 (also referred to as ANNEXIN II or Calpactin I Heavy Chain) binds to S100A10 (also known as p11) to form a highly specific heterotetramer (Réty et al., 1999). This complex differs from other ANNEXIN/S100 complexes in that its calcium dependence is reduced, due to mutations in the calcium binding sites in S100A10 (Glenney, 1986). While ANNEXIN A2 can exist as a monomer, S100A10 cannot, as ANNEXIN A2 binding of S100A10 protects S100A10 from rapid ubiquitylation and degradation (He et al., 2008).

The ANNEXIN A2/S100A10 tetramer is implicated in many cellular processes. As a high affinity F-actin binding protein, ANNEXIN A2/S100A10 regulates the growth of newly formed actin filaments (Hayes et al., 2006; Ikebuchi & Waisman, 1990). Additionally, through actin remodelling, ANNEXIN A2/S100A10 regulates exo- and endocytosis, and is found at actin-rich cell-cell contacts (Creutz & Snyder, 2005; Hansen et al., 2002).

On the extracellular portion of the plasma membrane, ANNEXIN A2/S100A10 regulates the cell surface generation of plasmin by colocalising with the plasminogen activator and receptor complex, leading to fibrin breakdown (Madureira et al., 2011). As such, ANNEXIN A2/S100A10 facilitates tumour progression, by enabling tumour-associated cells to digest the extracellular matrix and other tissue barriers organised by fibrin (Madureira et al., 2012), empowering tumour-associated cells to become increasingly invasive and metastatic. Furthermore, ANNEXIN A2 expression dysregulation is strongly correlated with cancer progression, particularly by modulating key events such as invasion, metastasis and drug resistance (Bharadwaj et al., 2013). In cancer cells, ANNEXIN A2 is transcriptionally regulated in response to insulin, fibroblast growth factor (FGF) and epidermal growth factor (EGF) (Keutzer & Hirschhorn, 1990). ANNEXIN A2 upregulation is also observed in cells transformed by v-*src*, v-H-*ras*, v-*mos*, or SV40, through the vascular endothelial growth factor (VEGF) and PKCβ pathway, and in osteoblastic cells under hypoxic conditions through a VEGFR1/Neuropilin pathway and SRC and MEK kinase pathway (Genetos et al., 2010; Ozaki & Sakiyama, 1993; Zhao et al., 2009). Additionally, as formation of the ANNEXIN A2/S100A10 complex can be upregulated in response to oncogenes, ANNEXIN A2 and S100A10 are frequently co-overexpressed to protect S100A10 from degradation.

Whilst ANNEXIN A2/S100A10 have not been studied extensively in mESCs, the weight of evidence suggesting ANNEXIN A2/S100A10 promotes motility and invasion could have interesting implications for a role of the complex in epithelial-mesenchymal transition, and as such, in changes in behaviour, morphology, and motility in mESCs.

4.2 Results

4.2.1 Orthogonal validation of ANNEXIN A2 and S100A10 induction by ERK5 signalling

In Chapter 3, I showed that activation of the ERK5 pathway by MEK5DD induces both ANNEXIN A2 and S100A10. To validate the induction of ANNEXIN A2 and S100A10 by ERK5 signalling, I used an orthogonal approach in which I test the same hypothesis but from a different experimental direction. I reconstituted ERK5 signalling in *Mapk7/Erk5*$^{-/-}$ (hereafter *Erk5*$^{-/-}$) mESCs by transfecting *Erk5*$^{-/-}$ mESCs with either empty vector control, wildtype ERK5 or a kinase-dead (D200A) mutant ERK5, in the presence of MEK5DD to activate the ERK5 pathway. Since ERK5 kinase activity is required for transcriptional activation and nuclear localisation signal revelation (Kondoh et al., 2006), kinase-dead ERK5 is unable to transcriptionally induce its target genes. Both ANNEXIN A2 and S100A10 are induced by wildtype but not kinase-dead ERK5, confirming the results of Chapter 3 (Figure 3.10) which suggest that ERK5 signalling induces these proteins (Figure 4.1). Although ERK5 and MEK5 have not been immunoblotted in this figure, ERK5 activity is suggested by both the modest induction of KLF2 and the strong induction of ANNEXIN A2 and S100A10 which recapitulates the results of Chapter 3 (Figure 3.11).

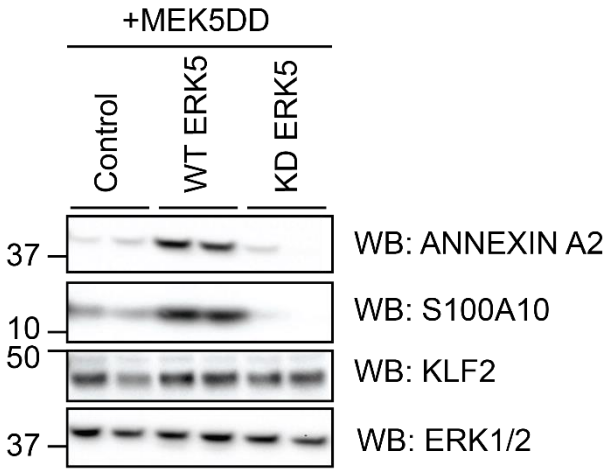

Figure 4.1: ANNEXIN A2 and S100A10 are induced by ERK5 signalling in Erk5$^{-/-}$ mESCs. *Erk5$^{-/-}$ mESCs were transfected with MEK5DD co-expressed with either control (empty vector), wildtype ERK5 or kinase dead (D200A) ERK5. mESCs were lysed 48hr post transfection, with no puromycin selection prior to lysis. ANNEXIN A2, S100A10, and KLF2 levels were determined by immunoblotting. KLF2 was used as a positive control for ERK5 signalling, ERK1/2 was used as a loading control. Experiment performed with Ludivine Guillet. Results are representative of 3 experiments.*

4.2.2 ERK5-dependent expression and regulation of ANNEXIN and S100 family members in mESCs

ANNEXIN A2 and S100A10 are members of protein families which are expressed widely across different cell types. Therefore, I investigated which other ANNEXIN and S100 family members are expressed in mESCs. To do this, I interrogated a total proteomic dataset previously generated within the Findlay lab which gives average protein copy number estimation for 9184 proteins (Fernandez-Alonso et al., 2017). Copy number estimations are calculated using the "histone ruler" approach, which assumes that every cell has the same number of histones (Wiśniewski et al., 2014). Therefore, average copy numbers of other proteins can be calculated based on relative MS signal intensities. ANNEXIN A2 is the most highly expressed of the nine ANNEXIN proteins present in mESCs, with 1.92×10^6 copies, although ANNEXIN A6 is also highly expressed with 1.82×10^6 copies (Figure 4.2). All other ANNEXINs are expressed at lower levels, all below 0.6×10^6 copies. In comparison, three S100 proteins are detected in mESCs, of which S100A10 exhibits the lowest expression (0.71×10^5 copies). However, it is important to note that although other S100 family members have not been detected, such

as S100A13 which was detected in the ERK5-dependent proteomic approach described in Chapter 3, this does not necessarily mean they are not expressed.

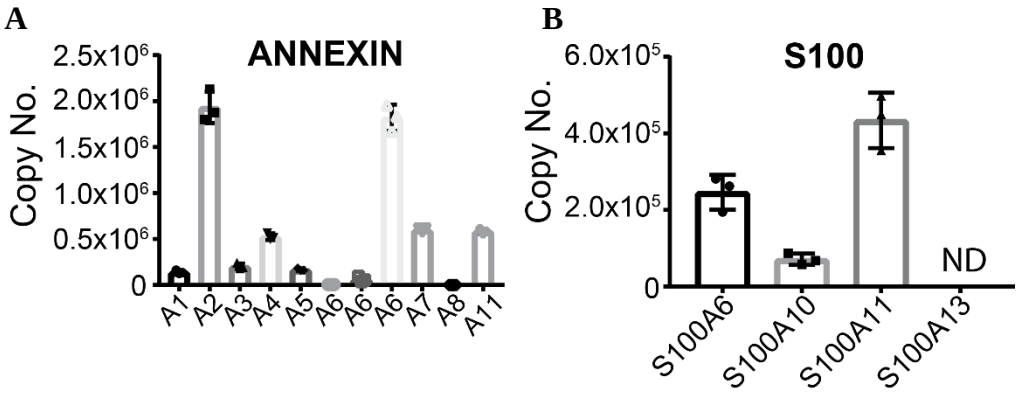

Figure 4.2: ANNEXIN and S100 family expression in mESCs. *The average copy number of each member of the ANNEXIN (A) and S100 (B) families was identified by total proteomics using the histone ruler method* (Fernandez-Alonso et al., 2017; Wiśniewski et al., 2014).

I then asked whether any of these ANNEXIN and S100 family members are regulated by ERK5 signalling. ANNEXIN A2 is the only ANNEXIN family member which is dynamically upregulated by ERK5 signalling (Figure 4.3A). Similarly, S100A10 is the only S100 family member which is dynamically regulated by ERK5 signalling (Figure 4.3B). This indicates that ERK5 specifically regulates the ANNEXIN A2/S100A10 complex, rather than ANNEXIN-S100 complexes more generally.

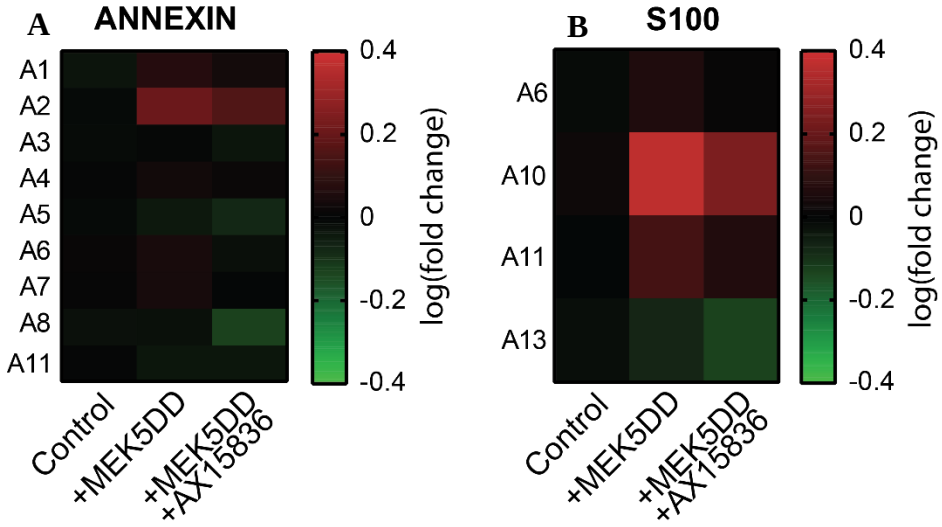

Figure 4.3: ERK5 specifically regulates ANNEXIN A2 and S100A10. *The average log(fold change) between control, pathway activation with MEK5DD and pathway inhibition with MEK5DD and AX15836 (24 hr, 10 μM) was calculated from quantitative proteomics for each member of the ANNEXIN (A) and S100 (B) families and displayed as a heat map. Red represents upregulation, green represents downregulation.*

4.2.3 ERK5 signalling does not significantly regulate *Anxa2* and *S100a10* mRNA

As ERK5 possesses a transcriptional activation domain and has been shown to regulate target genes such as *Klf2* (Sunadome et al., 2011), I next asked whether ERK5 can regulate the expression of *Anxa2* and *S100a10* mRNA. For this, I generated RNA extracts from wildtype mESCs in which ERK5 signalling was induced. To do this, I transfected wildtype mESCs with either empty vector control or MEK5DD to activate ERK5 signalling (as I showed in Figure 3.2), and treated with DMSO control or AX15836 to inhibit ERK5 signalling. These data suggest the *Anxa2* and *S100a10* mRNA may be regulated by ERK5 signalling, although this is not statistically significant (Figure 4.4). This timepoint of 48hrs of transfection was chosen based on optimisation experiments (Appendix B).

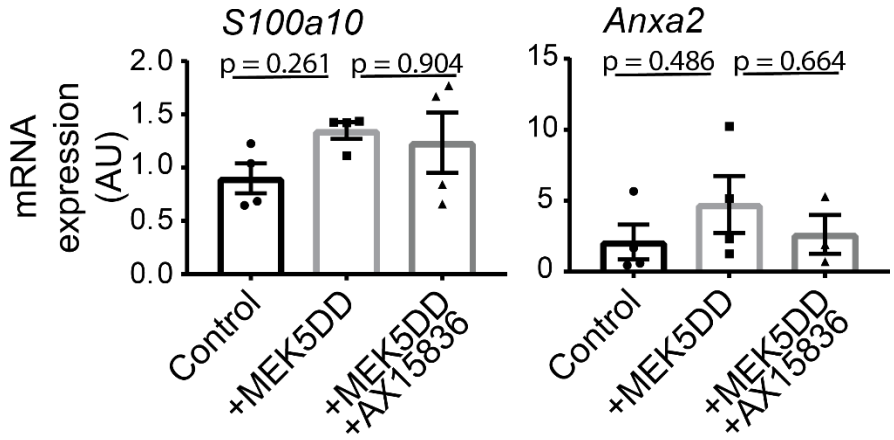

Figure 4.4: ERK5 signalling does not significantly regulate Anxa2 and S100a10 mRNA. *mESCs were cultured under control (empty vector), pathway activated (+MEK5DD) and pathway inhibited (+MEK5DD +AX15836 (10 μM, 24 hr)) conditions. mESCs were lysed 48hr post transfection, with 24hr puromycin selection prior to lysis. RNA was extracted and subjected to qRT-PCR. Error bars indicate SEM (n=4). Significance calculated by one-way ANOVA with multiple comparisons.*

I further validated this using *Erk5*$^{-/-}$ mESCs expressing MEK5DD and reconstituted with either empty vector, wildtype ERK5 or kinase-dead ERK5, subjecting RNA samples to qRT-PCR analysis. Again, these data exhibit a trend suggesting *Anxa2* and *S100a10* may be induced by wildtype but not kinase-dead ERK5, however this is not statistically significant (Figure 4.5). Induction of *Klf2*, which is transcriptionally regulated by ERK5

(Morikawa et al., 2016; Sunadome et al., 2011), is also not statistically significant, which may indicate that the assay is not optimised.

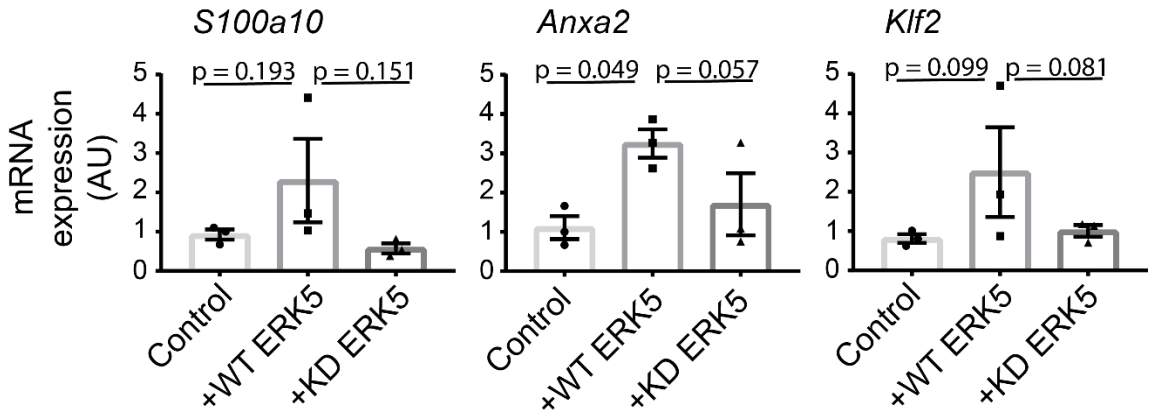

Figure 4.5: ERK5 signalling does not significantly regulate Anxa2 and S100a10 mRNA in Erk5$^{-/-}$ mESCs. *Erk5$^{-/-}$ mESCs were transfected with MEK5DD co-expressed with either control (empty vector), wildtype ERK5 or kinase dead (D200A) ERK5. mESCs were lysed 48hr post transfection, with no puromycin selection prior to lysis. RNA was extracted and subjected to qRT-PCR. Klf2 was used as a positive control. Error bars indicate SEM (n=3). Significance calculated by one-way ANOVA with multiple comparisons. These results have been replicated in 3 independent Erk5$^{-/-}$ mESCs clones (UD3, SD2, SD3).*

4.2.4 ANNEXIN A2 and S100A10 are induced in a KLF2-dependent manner

As it is unclear from my data whether ERK5 regulates *Anxa2* and *S100a10* mRNA (Figures 4.4-4.5), I used an alternative approach to confirm whether the ERK5-KLF2 signalling axis regulates *Anxa2* and *S100a10*. ERK5 transcriptionally induces *Klf2* (Morikawa et al., 2016; Sunadome et al., 2011) which is itself a transcription factor (Atkins & Jain, 2007), and many ERK5-dependent transcriptional effects occur through KLF2 acting as an intermediate transcription factor (Sunadome et al., 2011). I therefore investigated whether KLF2 expression induces *Anxa2* and *S100a10* mRNA.

First, I investigated whether KLF2 or other KLF family members bind promoter sequences in any ANNEXIN or S100 family genes by mining the CODEX ChIP database, which reports the genomic binding sites for transcription factors in ESCs (http://codex.stemcells.cam.ac.uk/). KLFs bind multiple sites on many ANNEXIN and S100 family gene promoters, suggesting that they could transcriptionally regulate them (Figure 4.6). Interestingly, there is little discrimination in numbers of binding sites

between family members. However, the position of KLF2 binding sites proximal to the transcriptional start site suggests that KLF2 may be an important regulator of these genes.

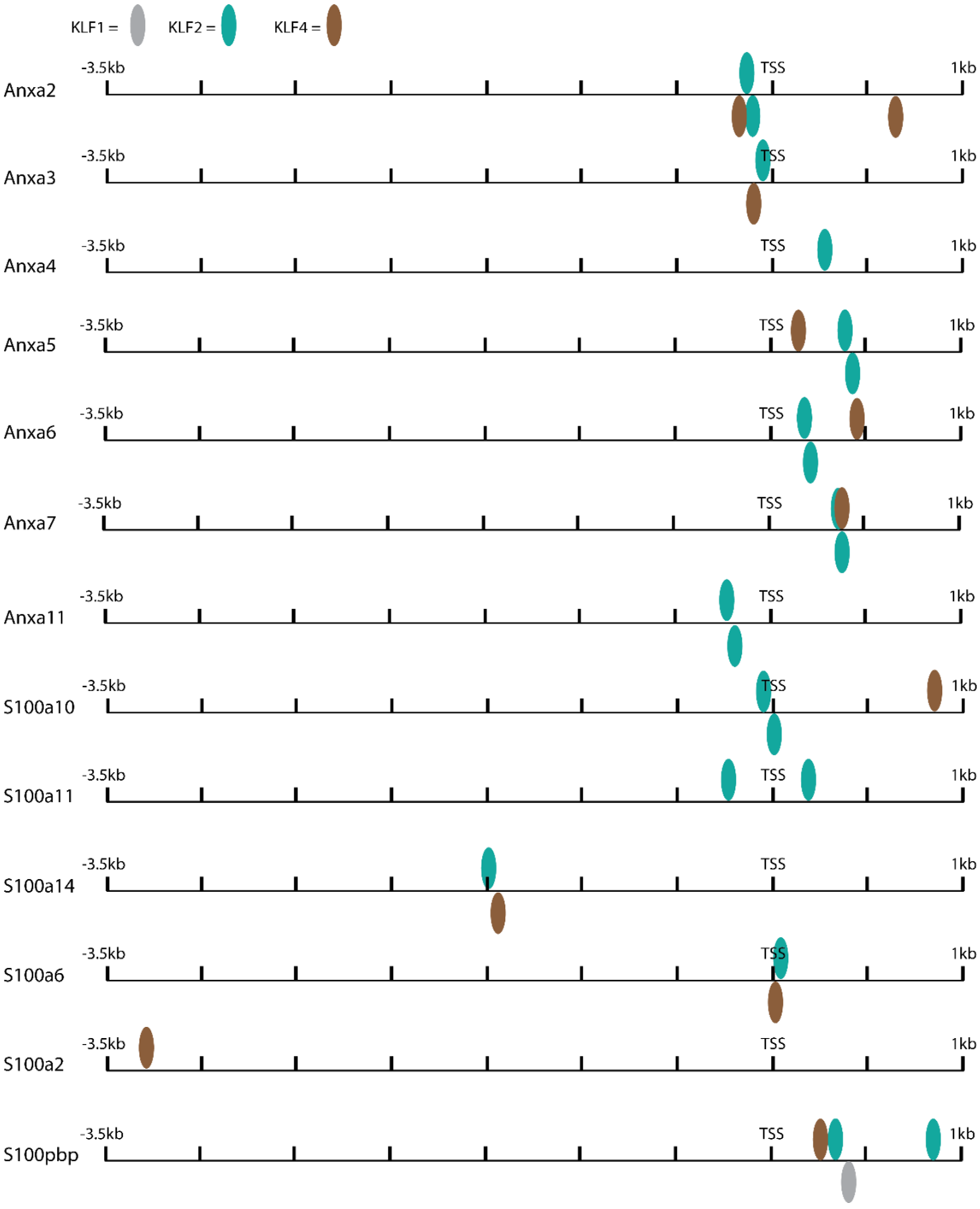

Figure 4.6: KLFs engage Annexin and S100 family member gene promoters. *Data extracted from CODEX database (http://codex.stemcells.cam.ac.uk/). KLFs 1, 2 and 4 were only KLFs found in database.*

In order to test whether perturbation of KLF2 disrupts ANNEXIN A2 and S100A10 induction, I next compared wildtype (*Klf2*$^{+/+}$) mESCs to mESCs in which the *Klf2* gene locus has been disrupted using CRISPR/Cas9 (*Klf2*$^{\Delta/\Delta}$). As a critical regulator of pluripotency, there is a significant selection pressure for expression of KLF2 (Yeo et al., 2014). As such, disruption of KLF2 expression in *Klf2*$^{\Delta/\Delta}$ cells does not represent a true knockout as residual levels of a low molecular weight species remains, which may be a truncated form of KLF2. This hypothesis is supported by the low level ERK5-dependent induction of this low molecular weight species. I transfected *Klf2*$^{+/+}$ and *Klf2*$^{\Delta/\Delta}$ with empty vector or MEK5DD and treated with DMSO or AX15836 as before. When *Klf2* gene expression is disrupted, ANNEXIN A2 and S100A10 are not efficiently induced, suggesting KLF2 acts as an intermediate between ERK5 signalling and ANNEXIN A2 and S100A10 induction (Figure 4.7). There is however a low level induction of ANNEXIN A2, which may be explained by the presence of the low molecular weight species in the KLF2 blot.

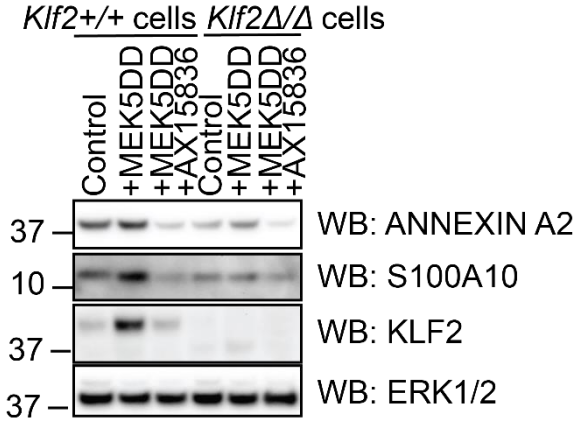

Figure 4.7: ERK5-dependent induction of ANNEXIN A2 and S100A10 requires KLF2. *mESCs (Klf2*$^{+/+}$ *or Klf2*$^{\Delta/\Delta}$*) were cultured under control (empty vector), pathway activated (+MEK5DD) and pathway inhibited (+MEK5DD +AX15836 (10 μM, 24 hr)) conditions. mESCs were lysed 48hr post transfection, with no puromycin selection prior to lysis. ANNEXIN A2, S100A10, and KLF2 levels were determined by immunoblotting. ERK1/2 was used as a loading control. Experiment performed with Ludivine Guillet . Results are representative of 3 experiments.*

To test this more directly, I titrated KLF2 into *Klf2*$^{\Delta/\Delta}$ mESCs, and analysed *Anxa2* and *S100a10* mRNA levels by qRT-PCR. As KLF2 levels increase, *Anxa2* and *S100a10* mRNA levels also increase (Figure 4.8). This reiterates that KLF2 transcriptionally induces expression ANNEXIN A2 and S100A10. These data suggest that the ERK5 pathway via KLF2 does indeed control expression of these genes (Figure 4.9). This

confirms the trend seen with ERK5 signalling, although this was not statistically significant (Figures 4.4 and 4.5).

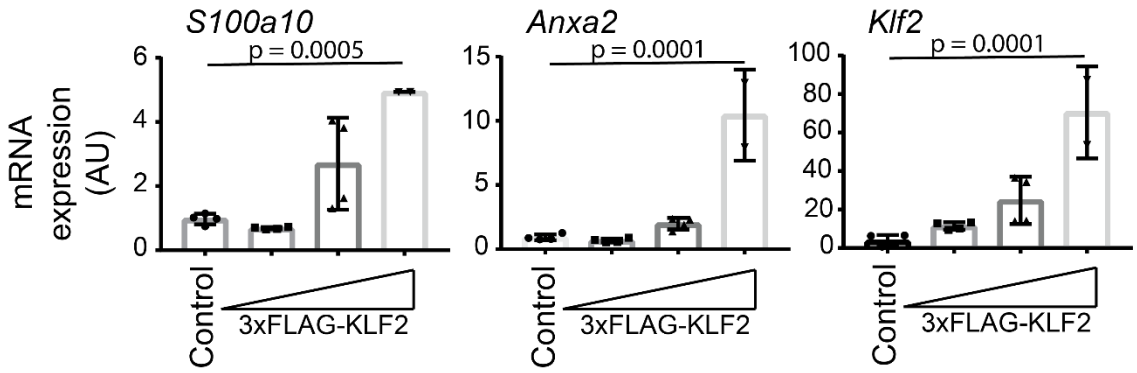

Figure 4.8: Titration of KLF2 into Klf2$^{\Delta/\Delta}$ mESCs induces Anxa2 and S100a10 mRNA expression. *Increasing concentrations of 3xFLAG-KLF2 were transfected into Klf2$^{\Delta/\Delta}$ mESCs to simulate induction of KLF2 expression by ERK5 signalling. mESCs were lysed 48hr post transfection, with 24hr puromycin selection prior to lysis. RNA was extracted and subjected to qRT-PCR. Experiment performed with Ludivine Guillet. Error bars indicate SEM (n=4, 0.5µg KLF2 n=2). Significance calculated by one-way ANOVA with multiple comparisons. These results have been replicated in 3 independent Klf2$^{\Delta/\Delta}$ mESCs clones (K2, K9, K13).*

4.2.5 ANNEXIN A2/S100A10 complex forms in mESCs

I then asked what effect ERK5/KLF2 regulation of *Anxa2* and *S100a10* expression has on ANNEXIN A2/S100A10-dependent processes. In other cellular systems, ANNEXIN A2 and S100A10 form a heterotetrameric complex (Réty et al., 1999). To confirm whether such a higher order multimer exists in mESCs, I employed gel filtration. ANNEXIN A2 is eluted in fractions which are expected to contain complexes ranging in size from approximately 150kDa to 40kDa (Figure 4.9). As a 40kDa protein, this is the range in which monomeric or dimeric ANNEXIN A2, or the previously described heterotetramer with S100A10, is predicted to elute. Furthermore, S100A10 is seen at low levels in the same fractions as ANNEXIN A2, suggesting that the heterotetrameric complex could form in mESCs.

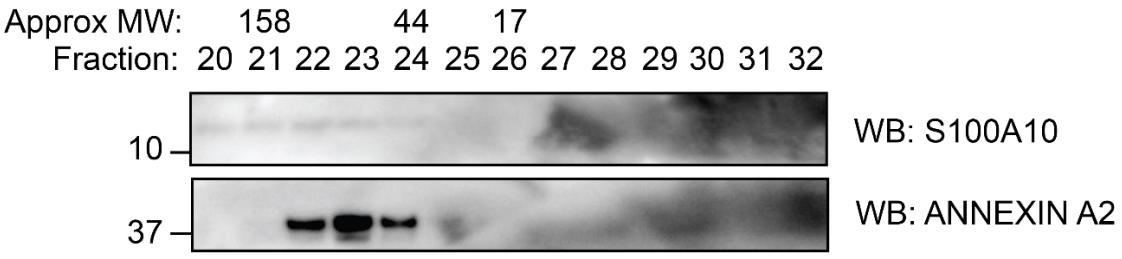

Figure 4.9: ANNEXIN A2 and S100A10 may form a higher order complex in mESCs. *Gel filtration separates complexes by size. S100A10 and ANNEXIN A2 levels were determined by immunoblotting. Preliminary data (n=1). Gel filtration performed by Anna Segarra-Fas.*

To confirm whether the ANNEXIN A2/S100A10 complex does form in mESCs, I expressed tagged constructs of ANNEXIN A2 (HA) and S100A10 (3xFLAG) and performed an immunoprecipitation with FLAG-binding resin to pull down S100A10 and any interacting partners. S100A10 is pulled down in both samples in which it is expressed as expected, whilst ANNEXIN A2 is only pulled down when S100A10 is present, indicating that a specific ANNEXIN A2/S100A10 complex forms in mESCs (Figure 4.10). Interestingly, S100A10 is immunoprecipitated to a greater extent when coexpressed with ANNEXIN A2. This is likely to be explained by the higher levels of S100A10 in the lysates of mESCs coexpressing ANNEXIN A2 and S100A10 and may be due to the protection from degradation afforded to S100A10 by forming a complex with ANNEXIN A2 (He et al., 2008).

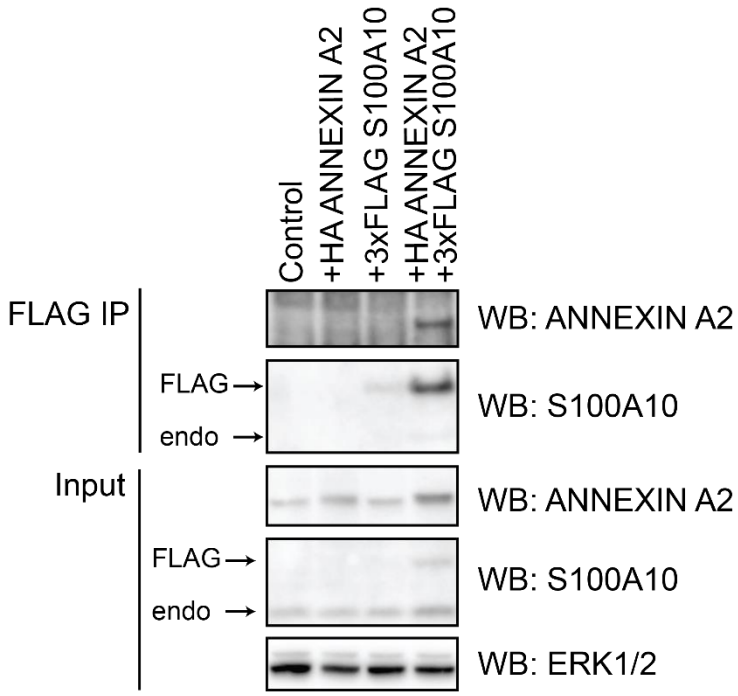

Figure 4.10: ANNEXIN A2 and S100A10 co-immunoprecipitate in mESCs.*3xFLAG-S100A10 and HA ANNEXIN A2 were expressed either alone or together, with mESCs lysed 48hr post transfection, with no puromycin selection prior to lysis. FLAG IP was used to pulldown S100A10 and interactors. ANNEXIN A2 and S100A10 levels were determined by immunoblotting. ERK1/2 was used as a loading control for input samples. Results are representative of 3 experiments.*

4.2.6 ERK5 signalling to ANNEXIN A2/S100A10 drives an mESC morphology change

The ANNEXIN A2/S100A10 heterotetrameric complex has been implicated in membrane processes, including membrane dynamics at the cell surface (Bharadwaj et al., 2013; Creutz & Snyder, 2005; Hansen et al., 2002; Madureira et al., 2011). Therefore, I investigated cell morphology associated with ANNEXIN A2/S100A10 induction by transfecting either 3xFLAG-S100A10 alone or 3xFLAG-S100A10 with HA-ANNEXIN A2 to simulate overexpression due to induction by ERK5 signalling. Both S100A10 and ANNEXIN A2 exhibit cytoplasmic and nuclear localisation, with the majority localised to the cytoplasm (Figure 4.11). This is consistent with what has been described previously, and indicates that the tags are not causing mislocalisation of ANNEXIN A2 and S100A10 (Morel & Gruenberg, 2007). S100A10 expression alone does not result in a morphology change compared to GFP control. However, co-expression of S100A10 and ANNEXIN A2 leads to a flattened, spread cell morphology with a large number of protrusions,

characteristic of filopodia. As protrusions such as filopodia are associated with cells migrating from a leading edge, this morphology is consistent with previous studies showing a role for ANNEXIN A2/S100A10 in cell motility and invasiveness (Heizmann et al., 2002).

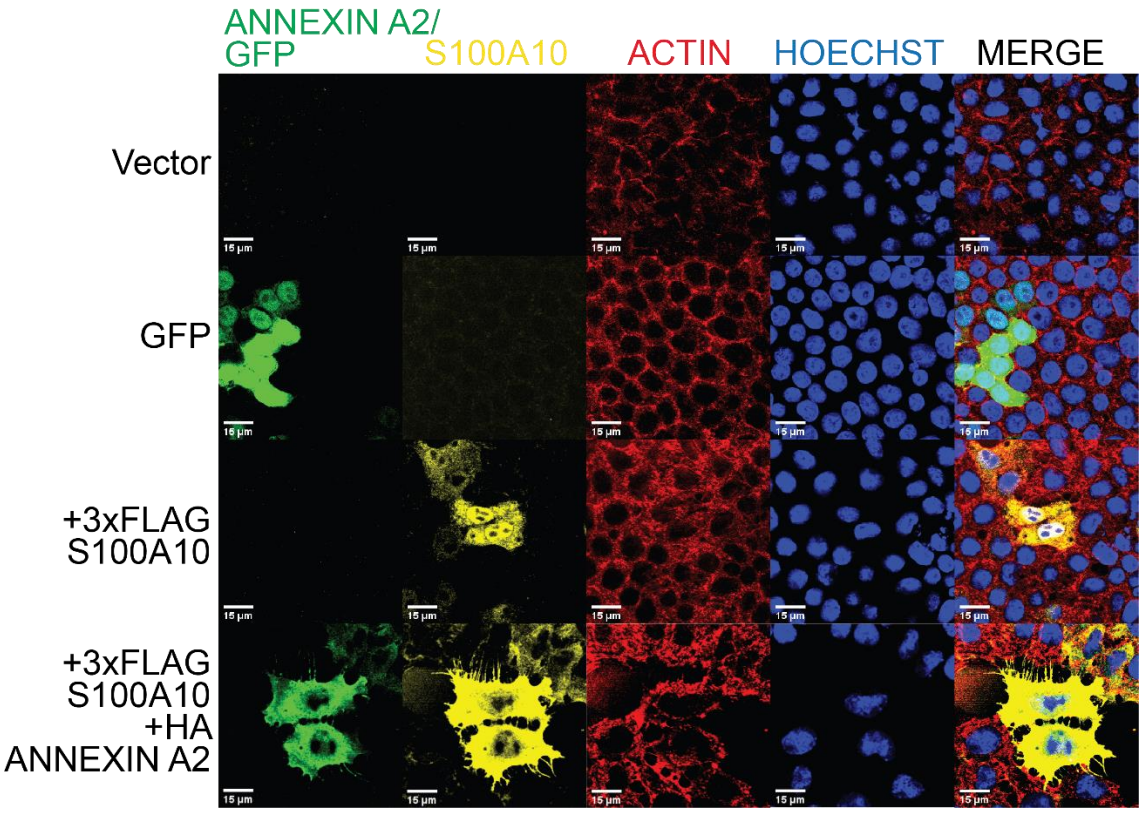

Figure 4.11: ANNEXIN A2/S100A10 expression results in morphology change characterised by protrusions. *mESCs were transfected with either empty vector, GFP, 3xFLAG-S100A10, or 3xFLAG-S100A10 with HA-ANNEXIN A2 for 24 hr with no puromycin selection prior to fixing with 4% PFA. ANNEXIN A2 was visualised using an Alexafluor 488-conjugated secondary antibody. S100A10 was visualised in both cases using an Alexafluor 647-conjugated secondary antibody. ActinRed stain (555nm) was used to show plasma membranes, and Hoechst stain was used to show nuclei. GFP transfection control was used to confirm whether transfection was responsible for any morphology change unrelated to ANNEXIN A2/S100A10. Experiment performed with Hayley Shaw (representative images, n=2).*

As ANNEXIN A2/S100A10 are induced by ERK5 signalling, this result predicts that ERK5 signalling may induce a similar change in morphology. To test this, I transfected mESCs with either GFP-ERK5 alone or GFP-ERK5 with MEK5DD. Although I have not tested the efficiency of cotransfection of GFP-ERK5 and MEK5DD, previous experiments involving cotransfection have shown a very high correlation of transfection between constructs. This is expected from this method of transfection, where constructs are transfected via lipid droplets which will either take up the combination of constructs

or neither construct. Without MEK5DD, ERK5 localises predominantly to the cytoplasm, whereas upon ERK5 activation with MEK5DD, ERK5 translocated to the nucleus (Figure 4.12).

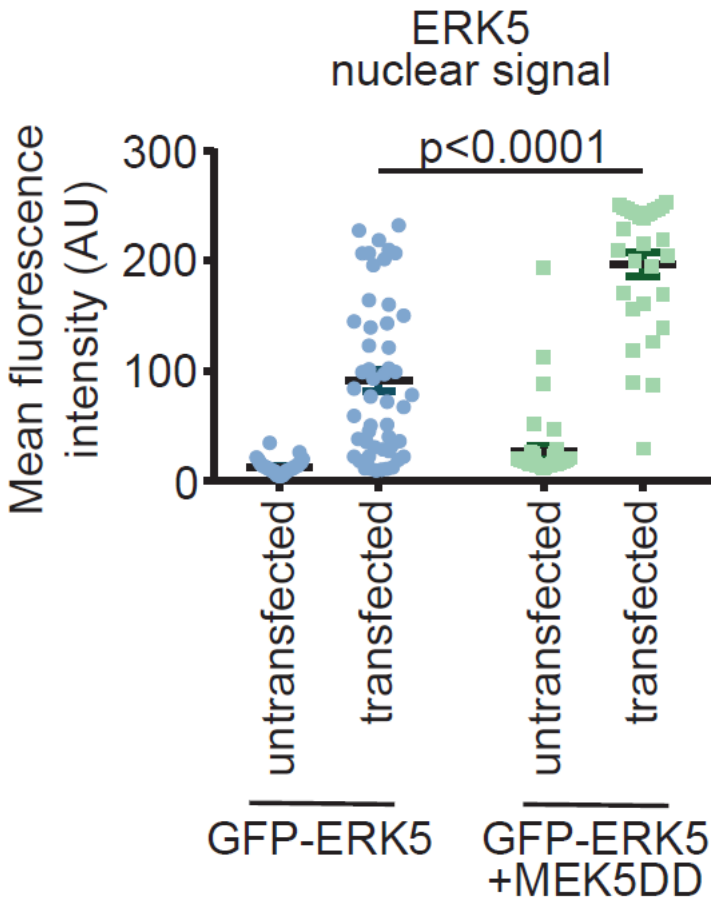

Figure 4.12: ERK5 translocated to the nucleus upon activation of ERK5 signalling with MEK5DD. *mESCs were transfected with either empty vector, GFP ERK5 or GFP ERK5 with MEK5DD for 24hr with no puromycin selection prior to fixing in 4% PFA. GFP (ERK5) was visualised using an Alexafluor 488-conjugated secondary antibody. Hoechst stain was used to show nuclei. Nuclear GFP-ERK5 signal was quantified by a FIJI mask. Each data point represents GFP-ERK5 signal in one nucleus, with cells imaged from 3 biological replicates.*

This change in cellular localisation is associated with a morphology change, where mESCs expressing MEK5DD appear flatter, with protrusions (Figure 4.13). This is similar to the morphology seen with ANNEXIN A2 and S100A10 overexpression (Figure 4.11). A caveat of these images is that the signal from the actin stain is weak, so it is difficult to assess whether GFP-ERK5 signal extends to the plasma membrane of the cell and the morphology of cells not expressing GFP-ERK5. This indicates that ERK5 signalling may induce a morphology change through ANNEXIN A2/S100A10

upregulation (Figure 4.14), which could implicate ERK5 signalling in processes such as epithelial-mesenchymal transition, cell motility or cell-cell adhesion.

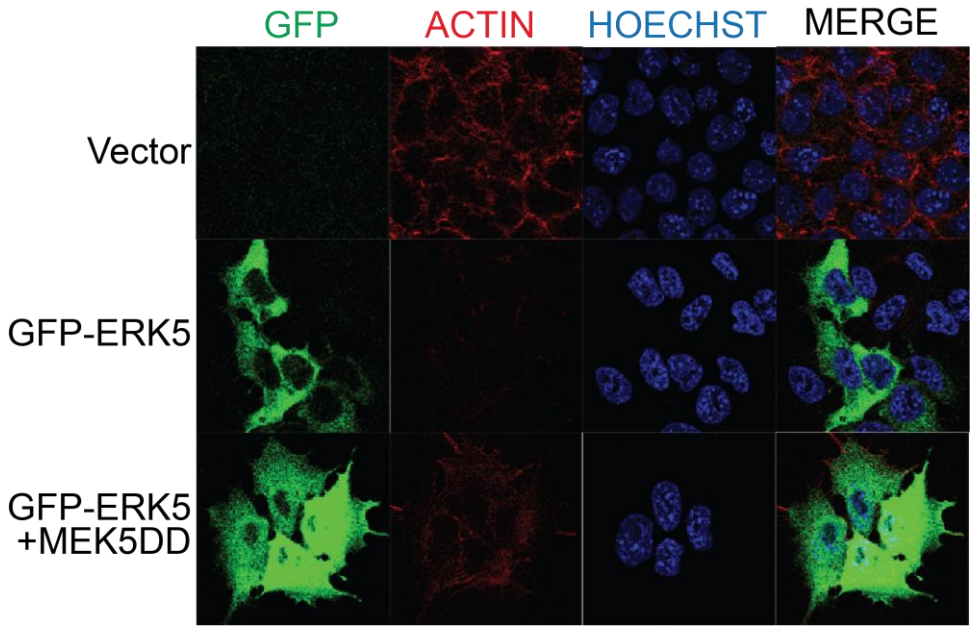

Figure 4.13: ERK5 signalling induces morphology change characterised by protrusions. *mESCs were transfected with either empty vector, GFP ERK5 or GFP ERK5 with MEK5DD for 24hr with no puromycin selection prior to fixing in 4% PFA. GFP (ERK5) was visualised using an Alexafluor 488-conjugated secondary antibody. ActinRed stain (555nm) was used to show plasma membranes, and Hoechst stain was used to show nuclei (representative images, n=3).*

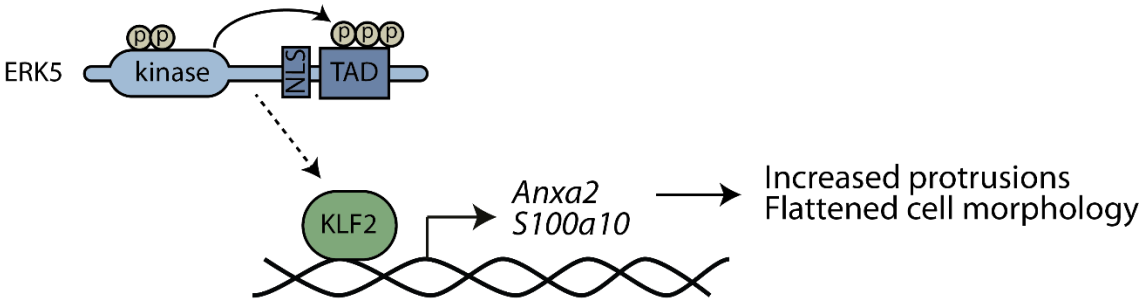

Figure 4.14: Model showing that ERK5 induction of Anxa2 and S100a10 through KLF2 induces a change in cell morphology characterised by increased protrusions.

4.3 Discussion

In this chapter, I have shown ERK5 signalling regulates expression of ANNEXIN A2 and S100A10 protein and mRNA, through intermediate transcription factor, KLF2. I have also demonstrated that they form a complex in mESCs. Furthermore, I have shown ERK5 signalling regulates known ANNEXIN A2/S100A10 biology, specifically that when ANNEXIN A2/S100A10 is expressed (either through transfection or through induction by ERK5 signalling), cells undergo a dramatic morphology change characterised by large numbers of protrusions.

Whilst it is clear that ERK5 signalling induces ANNEXIN A2 and S100A10 protein expression, the mechanism of regulation is less clear. As ChIP-Seq analysis of mESCs identifies binding sites for KLF2 immediately upstream of *Anxa2* and *S100a10* promoters, this suggests that KLF2 may directly regulate *Anxa2* and *S100a10* transcription. This is further supported by data demonstrating induction of *Anxa2* and *S100a10* upon titration of KLF2 in mESCs. However, *Anxa2* and *S100a10* mRNA are not significantly upregulated in response to ERK5 signalling, either with MEK5DD treatment or in *Erk5*$^{-/-}$ mESCs. This may be due to limitations of the transfection approach which has a variable transfection efficiency which is less than 100%, as discussed in Chapter 3. As ERK5 is known to induce KLF2, and KLF2 regulates *Anxa2* and *S100a10* mRNA, it is likely that ERK5 signalling does induce *Anxa2* and *S100a10* mRNA, although further optimisation of the experimental system, such as looking at different time points after transfection, may be required to conclusively observe this effect. However, as ANNEXIN A2 and S100A10 protein are induced by ERK5 signalling and both ANNEXIN A2/S100A10 protein and *Anxa2* and *S100a10* mRNA are regulated by KLF2, it is likely that *Anxa2* and *S100a10* are regulated transcriptionally by ERK5 rather than by an alternative mechanism.

I have shown that ANNEXIN A2 and S100A10 form a complex in mESCs, consistent with previous studies. I have also shown that ERK5 signalling induces expression of ANNEXIN A2 and S100A10. As S100A10 and ANNEXIN A2 are coexpressed to protect S100A10 from degradation, I hypothesise that induction of S100A10 and ANNEXIN A2 by ERK5 signalling drives the formation of ANNEXIN A2/S10010 heterotetramer

(Madureira et al., 2012), although I have yet to demonstrate this. As the ANNEXIN A2/S100A10 complex has been implicated in many membrane processes, this suggests that ERK5 could regulate processes as diverse as endo- and exocytosis, motility and cell-cell contacts (Y. Liu et al., 2014), which could be investigated using live cell imaging.

Here I have used tagged constructs of ANNEXIN A2 (HA) and S100A10 (FLAG) to assess the impact of ANNEXIN A2 and S100A10 expression, as overexpression by transfection mimics ANNEXIN A2 and S100A10 induction by ERK5 signalling. The data show that ANNEXIN A2 and S100A10 localise across the cells, primarily in the cytoplasm with some nuclear expression. This is consistent with previous literature describing the subcellular localisation of ANNEXIN A2 and S100A10 (Morel & Gruenberg, 2007). However, these data should be caveated that tagging these proteins may cause mislocalisation, or inhibit complex formation and membrane association. As such, the generation of *Anxa2*$^{-/-}$ and *S100a10*$^{-/-}$ mESC lines would be required to draw definitive conclusions.

The morphology change characterised by increased protrusions is indicative of processes in which ANNEXIN A2/S100A10 are implicated, including motility, invasion, metastasis, and epithelial-mesenchymal transition (Bharadwaj et al., 2013; Creutz & Snyder, 2005; Hansen et al., 2002; Madureira et al., 2011). This is particularly interesting as cultured mESCs behave as an epithelial-like layer, and induction of epithelial-mesenchymal transition could be interesting to study further. The observed protrusions may represent filopodia, which are slender cytoplasmic projections from the leading edge of migrating cells (Mattila & Lappalainen, 2008). This would be consistent with ANNEXIN A2/S100A10 facilitating increased cell motility and could be investigated by studying markers of filopodia such as talin, syndapin and Abl interactors (DePasquale & Izzard, 1991; Qualmann & Kelly, 2000; Stradal et al., 2001). However, as these projections are observed from all sides of cells rather than a leading edge, this may indicate a flattening and spreading phenotype rather than a migratory one. Alternatively, it may suggest an increase in migratory capacity poised for a signal to determine the direction of migration.

Filopodia formation is regulated through signalling pathways including those involving small GTPases such as CDC42 (Krugmann et al., 2001). In this way, cells respond to signals from the plasma membrane and respond by altering membrane dynamics. Another stimulus which could be received by the plasma membrane is mechanical stress. How stem cells respond to mechanical signals is an emerging area in stem cell research, and mechanical signalling and matrix stiffness have recently been shown to regulate cell fate decisions (Verstreken et al., 2019). Furthermore, ERK5 has been shown to be activated by shear stress, suggesting it could be involved in this process (Clark et al., 2011). As such, ANNEXIN A2 and S100A10 could function to alter matrix stiffness in response to mechanical signalling, and indeed it has been shown that they interact with and manipulate the extracellular matrix (Madureira et al., 2012). This could therefore implicate ERK5 in the regulation of the extracellular matrix, which then facilitates cell spreading.

The implications for the role of ANNEXIN A2 and S100A10 in ERK5-overexpressing cancers are significant. Often during tumour progression, tumour cells re-express stem cell genes including pluripotency factors, leading to cancer stem cell generation (Liu et al., 2013). OCT4, NANOG and SOX2 in particular drive cancer stem cell generation by providing cells with the capacity for unlimited proliferation, and coexpression of these three pluripotency factors is associated with tumour metastasis and treatment resistance (Ben-Porath et al., 2008; Feske, 2007). Additionally, although OCT4, NANOG and SOX2 inhibit the epithelial-mesenchymal transition programme required for cancer cell motility (R. Li et al., 2010; Redmer et al., 2011; Samavarchi-Tehrani et al., 2010), it has been shown in breast cancer that a sequential transition occurs, where epithelial-mesenchymal transition is first induced to allow motility and invasiveness, followed by mesenchymal-epithelial transition to regain self-renewal (S. Liu et al., 2014). As ANNEXIN A2 and S100A10 are known effectors of epithelial-mesenchymal transition, it could be speculated that ERK5 signalling may drive this process in cancer stem cells. As a result, the cancer cells would exhibit increased cell spreading and motility, critical properties for metastasis.

Furthermore, ERK5 may be involved in the generation of cancer stem cells. ERK5 has been suggested to drive cancer stem cell generation in a number of systems including

colon cancer, breast cancer, and leukaemia, through the induction of downstream target genes (Pereira et al., 2019; Tusa et al., 2018; Ucar et al., 2019). Additionally, ERK5-overexpressing prostate cancer cells are more motile and invasive, and ERK5 activation by oncogenic SRC in fibroblasts results in invasive adhesions, similar to the phenotypes of ANNEXIN A2/S100A10-expressing cancers (Barros & Marshall, 2005; McCracken et al., 2008; Schramp et al., 2008).

5. ERK5-KLF2 axis regulates stem cell rejuvenation

5.1 Introduction to ZSCAN4 and stem cell rejuvenation

ZSCAN4 is a developmentally regulated protein which is highly expressed at the 2-cell stage of early embryonic development (Falco et al., 2007). The gene locus consists of a family of 6 genes (ZSCAN4A-F) and 3 pseudogenes (Falco et al., 2007). ZSCAN4D is the predominant isoform that is expressed during the 2-cell (2C) stage of development, whereas ZSCAN4C is the predominant isoform expressed in mESCs (Falco et al., 2007). These genes and proteins are highly similar, with at least 94.66% sequence identity between isoforms (NCBI Blast), and are therefore difficult to distinguish by immunoblot or qRT-PCR.

In mESCs, ZSCAN4 is expressed in a transient population of cells, estimated to be around 5% (Zalzman et al., 2010) (Figure 5.1). Cells expressing ZSCAN4 appear to have reverted to a 2C-like state, as they also express other 2C genes including *Tdpoz3*, *Zfp352* and endogenous retroviral elements such as *Muervl* (Eckersley-Maslin et al., 2016). mESCs must cycle through this transient 2C-like ZSCAN4^{+} state every nine passages to maintain pluripotency and continuous self-renewal (Zalzman et al., 2010).

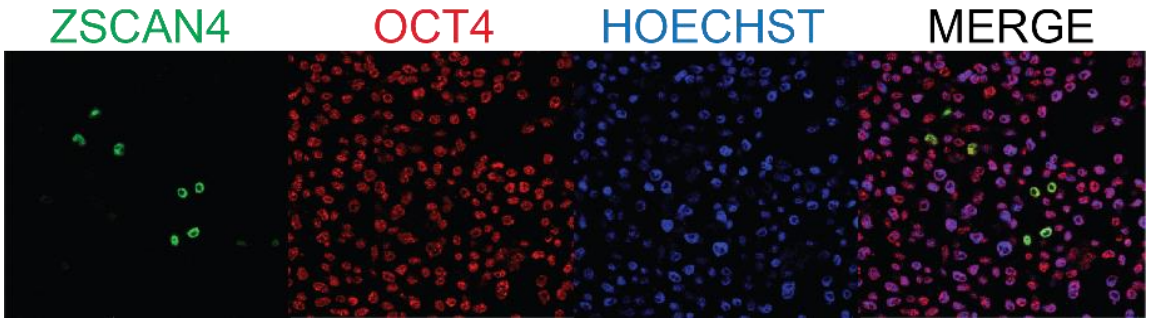

Figure 5.1: ZSCAN4 is expressed in a small subpopulation of mESCs at any given time. *mESCs were grown for 24hr prior to fixing with 4% PFA. ZSCAN4 was visualised using an Alexafluor 488-conjugated secondary antibody. OCT4 (Alexafluor 546) was used to show pluripotent cells, and Hoechst stain was used to show nuclei (representative images, n=3).*

Transition to a ZSCAN4^{+} state promotes global DNA hypomethylation and rapid telomere extension in a telomerase-independent manner (Zalzman et al., 2010), a key process underpinning mESC rejuvenation. ZSCAN4 coordinates DNA demethylation and

telomere extension by recruiting UHRF1, an E3 ubiquitin ligase, to ubiquitylate and degrade DNMT1, the DNMT responsible for maintenance DNA methylation (Dan et al., 2017). This drives genomic hypomethylation and facilitates telomere sister chromatid exchange (T-SCE), resulting in telomere extension which maintains genomic stability during cell division (Zalzman et al., 2010).

While the downstream effects of ZSCAN4 and the biological consequences for mESCs entering the ZSCAN4 2C-like state are known, the upstream pathways regulating the expression of these genes are relatively uncharacterised. PI3K signalling was identified to upregulate ZSCAN4 expression when cells are exposed to DNA damaging agents (Storm et al., 2009, 2014). ZSCAN4 induction by PI3K signalling causes an accumulation of cells in G2/M phase, suggesting ZSCAN4 regulates progression through the cell cycle, particularly in the S/G2 transition (Storm et al., 2014). Therefore, ZSCAN4 levels are regulated by signalling, although the pathways and mechanisms have not been comprehensively explored.

5.2 Results

5.2.1 Validation of the role of ERK5 activity in ZSCAN4 induction

In Chapter 3, I showed using quantitative proteomics that activation of ERK5 signalling induces an increase in ZSCAN4 protein levels. To validate the role of ERK5 kinase activity in ZSCAN4 induction using an orthogonal approach, I expressed constitutively-active MEK5DD in *Erk5*$^{-/-}$ mESCs and co-expressed either empty vector control, wildtype ERK5 or a kinase-inactive ERK5 D200A mutant. ZSCAN4 is induced by wildtype but not kinase-inactive ERK5 (Figure 5.2), confirming that ZSCAN4 is indeed regulated by ERK5 signalling.

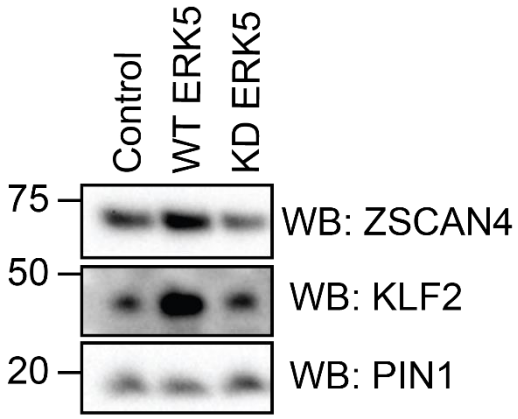

Figure 5.2: ZSCAN4 is induced by ERK5 in Erk5$^{-/-}$ mESCs. *Erk5$^{-/-}$ mESCs were transfected with MEK5DD and either empty vector, wildtype ERK5 or kinase-dead ERK5. mESCs were lysed 48hr post transfection, with no puromycin selection prior to lysis. ZSCAN4 and KLF2 levels were determined by immunoblot. KLF2 was used as a positive control for ERK5 signalling. PIN1 was used as a loading control. Results are representative of 3 experiments.*

As these experiments were performed by ectopically activating ERK5 using constitutively active MEK5DD, I next tested whether ZSCAN4 protein levels are sensitive to inhibition of endogenous ERK5 signalling using the selective ERK5 inhibitor AX15836. Indeed, ZSCAN4 levels are reduced by AX15836 treatment compared to DMSO control (Figure 5.3), suggesting that endogenously activated ERK5 signalling promotes ZSCAN4 expression in mESCs.

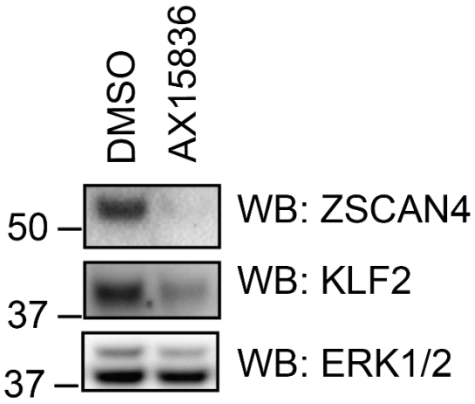

Figure 5.3: Inhibition of endogenous ERK5 reduces ZSCAN4 levels. *mESCs were cultured for 48hr and treated with either DMSO or 10 μM AX15836 for 24 hr prior to lysis. ZSCAN4 and KLF2 levels were determined by immunoblot. KLF2 was used as a positive control for ERK5 signalling, ERK1/2 was used as a loading control. Results are representative of 3 experiments.*

ERK5 kinase activity is required for activation of the transcriptional activation domain and exposure of the nuclear localisation signal, as well as the phosphorylation of transcription factor substrates (Kondoh et al., 2006). This again raised the possibility that ZSCAN4 protein levels are regulated by ERK5 signalling at the level of gene expression. I therefore tested whether *Zscan4* mRNA, and mRNA levels of two further genes which are co-expressed in the 2C-like state (*Tdpoz3* and *Zfp352*) (Macfarlan et al., 2012; Speakman et al., 2014), are regulated by ERK5. To do this, I transfected mESCs with either empty vector control or MEK5DD. Analysis of *Zscan4*, *Tdpoz3* and *Zfp352* mRNA levels suggests that expression of these genes is induced by ERK5 activation (Figure 5.4).

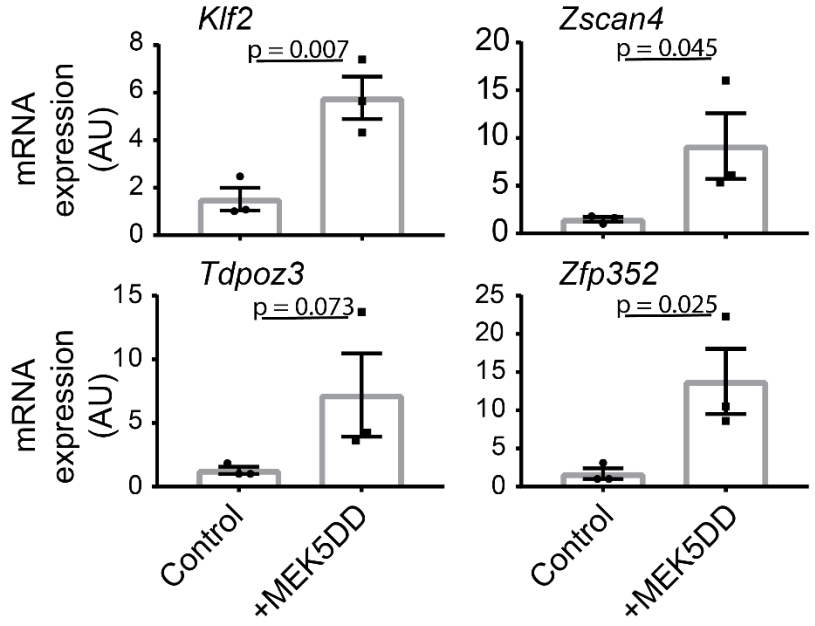

Figure 5.4: Zscan4 and other 2C gene mRNA is induced by ERK5 signalling. *mESCs were transfected with either empty vector or MEK5DD. mESCs were lysed 48hr post transfection, with 24hr puromycin selection prior to lysis. RNA was extracted and subjected to qRT-PCR. Error bars indicate SEM (n=3). Significance calculated by unpaired student t-test.*

To confirm this using an orthogonal approach, I generated RNA samples from *Erk5*$^{-/-}$ mESCs reconstituted with either empty vector, wildtype ERK5 or kinase dead (D200A) ERK5, and subjected these to qRT-PCR analysis. These data indicate that *Zscan4*, and *Tdpoz3*, but not *Zfp352* mRNA levels are significantly regulated by ERK5 signalling (Figure 5.5). *Zfp352* demonstrates a trend with wildtype ERK5 which could suggest that *Zfp352* mRNA is induced in response to ERK5 signalling, although this is not reversed with kinase dead ERK5. Taken together, these data suggest that ERK5 may control expression of 2C genes.

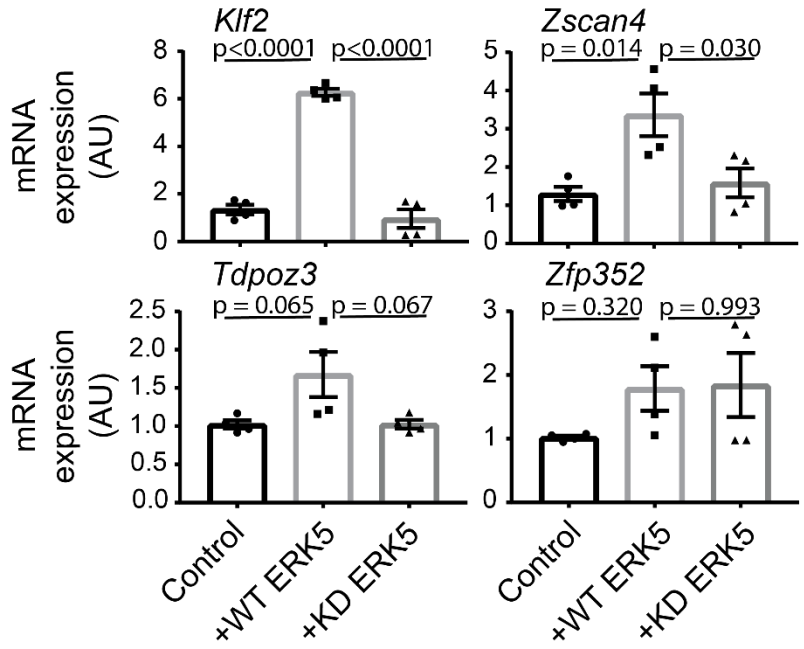

Figure 5.5: Zscan4 and other 2C gene mRNA is regulated by ERK5 signalling in Erk5$^{-/-}$ mESCs. *Erk5$^{-/-}$ mESCs were transfected with MEK5DD and either empty vector, wildtype ERK5 or kinase-dead ERK5. mESCs were lysed 48hr post transfection, with no puromycin selection prior to lysis. RNA was extracted and subjected to qRT-PCR. Klf2 was used as a positive control for ERK5 signalling. Error bars indicate SEM (n=4). Significance calculated by one-way ANOVA with multiple comparisons. These results have been replicated in 3 independent Erk5$^{-/-}$ mESCs clones (UD3, SD2, SD3).*

5.2.2 ZSCAN4 and 2C genes are induced by ERK5 in a KLF2-dependent manner

I next asked by what mechanism ERK5 regulates ZSCAN4. Although ERK5 itself has a transcriptional activation domain and phosphorylates transcription factor substrates, the transcription factor KLF2 has been identified as a direct target of ERK5 that mediates many of the downstream functions of the ERK5 pathway in development (Atkins & Jain, 2007; Morikawa et al., 2016; Sunadome et al., 2011; Williams et al., 2016). Therefore, I hypothesised that, similar to ANNEXIN A2 and S100A10, ERK5 induces ZSCAN4 through KLF2 as an intermediate transcription factor. To test this, I first compared ZSCAN4 protein induction by MEK5DD in *Klf2*$^{+/+}$ mESCs with mESCs in which the *Klf2* has been disrupted (*Klf2*$^{\Delta/\Delta}$). ZSCAN4 is more strongly induced by MEK5DD in *Klf2*$^{+/+}$ mESCs, although there is some residual induction in *Klf2*$^{\Delta/\Delta}$ mESCs (Figure 5.6). This may be explained by the lower molecular weight species in the KLF2 blot, which

appears to be residual expression of truncated KLF2 expressed as a result of the CRISPR editing in the *Klf2*$^{\Delta/\Delta}$ mESCs, as previously described in Chapter 4.

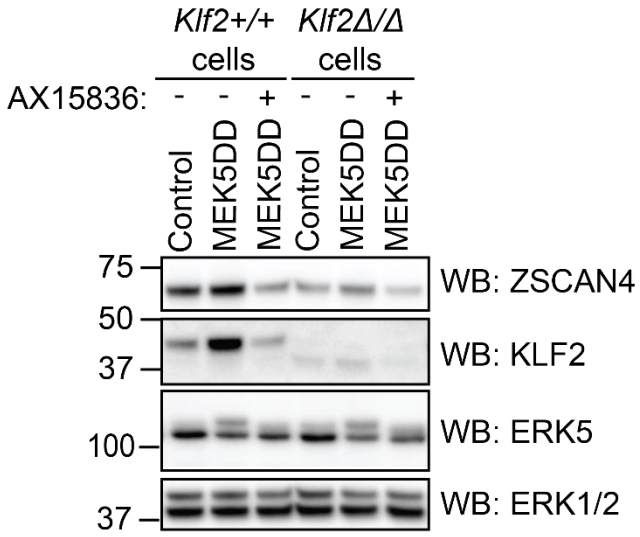

Figure 5.6: ERK5-dependent induction of ZSCAN4 requires KLF2. *mESCs (Klf2*$^{+/+}$ *or Klf2*$^{\Delta/\Delta}$*) were transfected with MEK5DD to activate ERK5 signalling and AX15836 (10 μM, 24 hr) was used to inhibit the pathway. mESCs were lysed 48hr post transfection, with no puromycin selection prior to lysis. ZSCAN4, KLF2, and ERK5 levels were determined by immunoblotting. ERK5 mobility retardation was used as a positive control for ERK5 signalling, ERK1/2 was used as a loading control. Results are representative of 3 experiments.*

To confirm whether disruption of the *Klf2* gene results in a reduction of ZSCAN4 basal levels, ZSCAN4 induction by MEK5DD or both, I quantified the immunoblot data. This showed that ZSCAN4 displays a modest reduction in both basal levels and induction with MEK5DD (Figure 5.7). This suggests that ERK5 may regulate ZSCAN4 expression via KLF2.

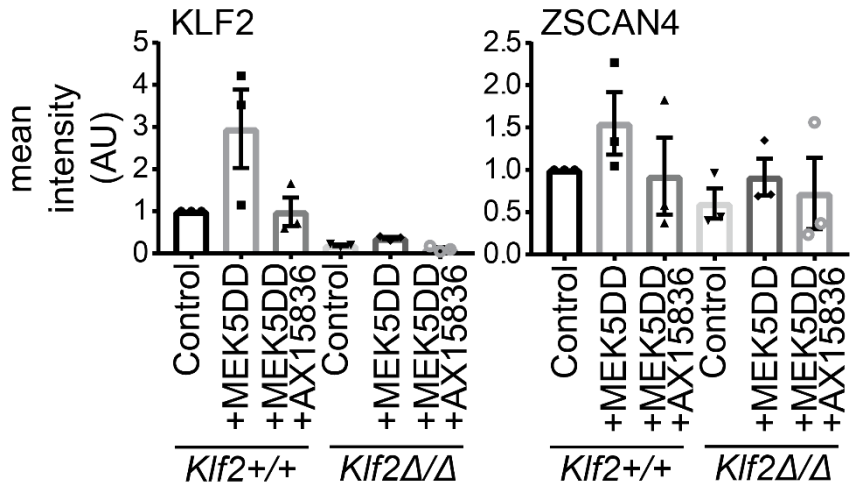

Figure 5.7: ERK5-dependent induction of ZSCAN4 requires KLF2. *mESCs ($Klf2^{+/+}$ or $Klf2^{\Delta/\Delta}$) were transfected with MEK5DD to activate ERK5 signalling and AX15836 (10 μM, 24 hr) was used to inhibit the pathway. mESCs were lysed 48hr post transfection, with no puromycin selection prior to lysis. ZSCAN4, KLF2, and ERK1/2 levels were determined by immunoblotting. ZSCAN4 and KLF2 immunoblot bands were quantified and normalised to ERK1/2 loading control (n=3).*

To directly test whether ZSCAN4 protein levels are induced by KLF2, I titrated KLF2 into *Klf2*$^{+/+}$ mESCs to simulate KLF2 induction by ERK5 signalling. ZSCAN4 expression increases as KLF2 levels increase, suggesting KLF2 induces ZSCAN4 expression (Figure 5.8).

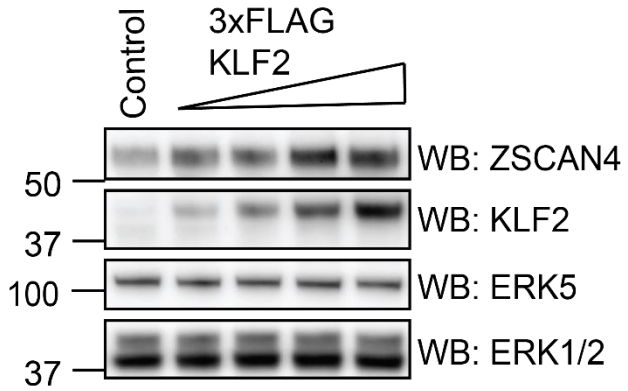

Figure 5.8: KLF2 titration induces ZSCAN4 expression. *KLF2 was titrated into wildtype mESCs. mESCs were lysed 48hr post transfection, with no puromycin selection prior to lysis. ZSCAN4, KLF2 and ERK5 levels were determined by immunblotting. ERK1/2 was used as a loading control. Results are representative of 3 experiments.*

To determine whether KLF2 induction of ZSCAN4 protein is accounted for by increased *Zscan4* mRNA levels as would be expected if *Zscan4* is transcriptionally regulated by the ERK5-KLF2 axis, I subjected parallel RNA samples generated alongside the protein lysates (Figure 5.8) to qRT-PCR analysis. These data show that *Zscan4, Tdpoz3* and *Zfp352* mRNA expression increases as *Klf2* levels increase (Figure 5.9). This suggests that KLF2 regulates the expression of *Zscan4* and other markers of stem cell rejuvenation (Figure 5.10).

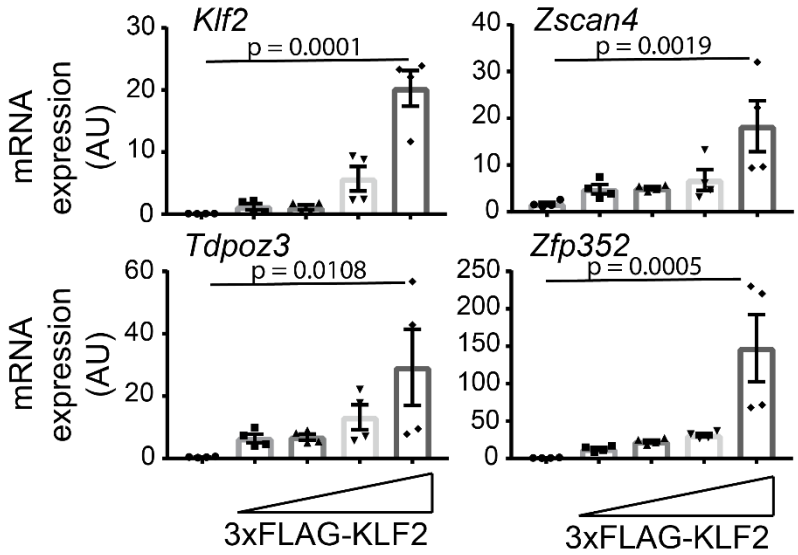

Figure 5.9: KLF2 titration induces Zscan4 and other 2C gene mRNA. *Increasing concentrations of 3xFLAG-KLF2 were transfected into Klf2$^{+/+}$ mESCs to simulate induction of KLF2 expression by ERK5 signalling. mESCs were lysed 48hr post transfection, with no puromycin selection prior to lysis. RNA was extracted and subjected to qRT-PCR. Error bars indicate SEM (n=4). Significance calculated by one-way ANOVA with multiple comparisons. These results have been replicated in 3 independent Klf2$^{\Delta/\Delta}$ mESCs clones (K2, K9, K13).*

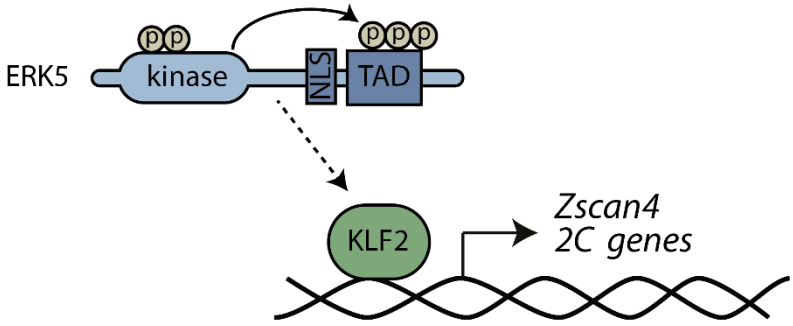

Figure 5.10: Model showing Zscan4 induction by ERK5 through intermediate transcription factor KLF2.

5.2.3 ERK5 does not significantly regulate *Muervl* or *Dux*

The embryonic 2C-like state is associated with a large transcriptional network (Eckersley-Maslin et al., 2016). Therefore, I sought to investigate the mechanisms by which KLF2 transcriptionally induces 2C genes. KLF2 ChIP-Seq databases have not shown direct binding to ZSCAN4 promoters. However, previous studies have described a role for transposable elements (DNA sequences that can change their position within the genome (Boeke et al., 1985)) acting with KLFs in the regulation of transcriptional programmes (Pontis et al., 2019). As *Muervl*, a transposable element which is usually restricted to preimplantation embryos, is expressed in the 2C-like state (Eckersley-Maslin et al., 2016), I tested whether *Muervl* expression is induced by ERK5 signalling. I did this by transfecting mESCs with either empty vector or MEK5DD, and treating with either DMSO or AX15836. These data indicate that *Muervl* may be induced by ERK5 signalling, although this is not statistically significant, and this is not reversed by treatment with AX15836 (Figure 5.11A). Therefore, the role for ERK5 in regulating *Muervl* remains uncertain.

The DUX family of transcription factors have also been implicated in zygotic genome activation through the regulation of 2C transcriptional network dynamics (De Iaco et al., 2017), and have been shown to activate *Muervl* as part of this process (Hendrickson et al., 2017). Therefore, I tested whether expression of *Dux*, the only mouse DUX family member, is induced by ERK5 signalling. Again, some induction of *Dux* is seen in mESCs transfected with MEK5DD and treated with either DMSO or AX15836 (Figure 5.11B).

However, this is not statistically significant so a definitive conclusion about the role of ERK5 in the regulation of retrotransposons or *Dux* cannot be drawn from these data.

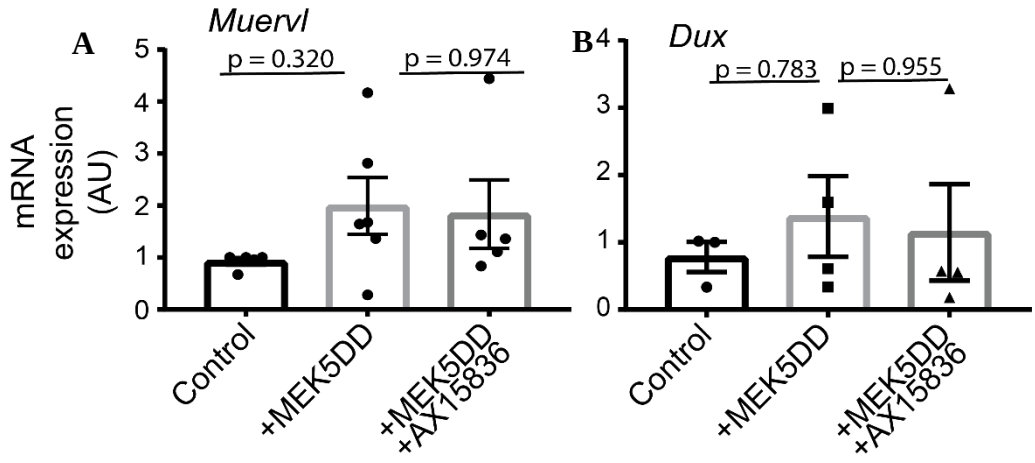

Figure 5.11: ERK5 signalling does not significantly regulate Muervl or Dux. *A - Wildtype mESCs were transfected with either empty vector or MEK5DD, and AX15836 (10 μM, 24 hr) was used to inhibit the ERK5 pathway. mESCs were lysed 48hr post transfection, with 24hr puromycin selection prior to lysis. Error bars indicate SEM (n=6). Significance calculated by one-way ANOVA with multiple comparisons. B - Wildtype mESCs were transfected with either empty vector control or MEK5DD, and AX15836 (10 μM, 24 hr) was used to inhibit the ERK5 pathway. mESCs were lysed 48hr post transfection, with 24hr puromycin selection prior to lysis. RNA was extracted and subjected to qRT-PCR. Error bars indicate SEM (n=4). Significance calculated by one-way ANOVA with multiple comparisons.*

5.2.4 ERK5 signalling regulates telomere length

ZSCAN4-mediated DNMT1 degradation leads to global DNA demethylation, which facilitates T-SCE, resulting in an increase in telomere length, a key process in stem cell rejuvenation (Dan et al., 2017). I therefore determined whether ERK5 regulation of ZSCAN4 results in changes in telomere length, as this is an important function of ZSCAN4. To verify if ZSCAN4 induction by ERK5 signalling increases telomere length, I used a qPCR approach to measure the average number of telomeric repeats compared to a standard non-telomere genomic locus (T/S ratio) (Callicott & Womack, 2006). To confirm that this assay correctly and sensitively measures changes in telomere length in mESCs, I first compared telomere length of mESCs grown in LIF/Serum compared to those grown in 2i media, as mESCs grown in 2i media have shorter telomeres than those grown in LIF/Serum (Guo et al., 2018). Average telomere length measured by T/S ratio confirms shorter telomeres in mESCs cultured in 2i media compared to those in LIF/Serum, as previously shown (Guo et al., 2018) (Figure 5.12). As this assay gives high

biological variation, I employed a statistical power test for all subsequent experiments to calculate the appropriate number of biological replicates required to observe a significant effect. However, it should be noted that by calculating the statistical power from the observed data, this calculation will always give a number of replicates for a statistically significant effect, irrespective of the biological relevance of the magnitude of this effect.

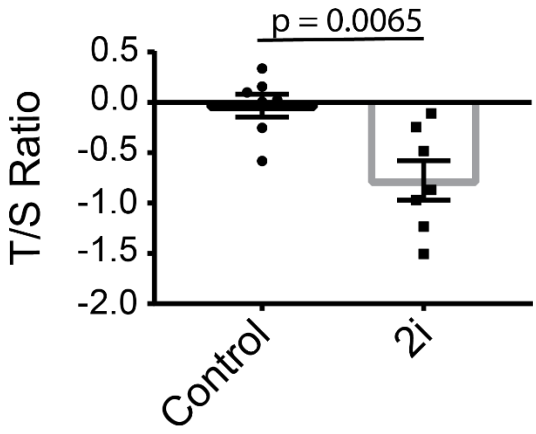

Figure 5.12: Telomere length is shorter in cells grown in 2i compared to LIF/Serum. *DNA was extracted from mESCs maintained in either LIF/Serum or 2i media and analysed by telomere qPCR. T/S ratio represents the log transformed ratio of telomeric repeat signal to that of a single copy locus and indicates relative telomere length. Error bars indicate SEM. Statistical power test was used to calculate the appropriate number of biological replicates required to observe a significant effect (n=7). Significance calculated by unpaired student t-test.*

As ZSCAN4 is implicated in the regulation of telomere length in mESCs, I hypothesised that ZSCAN4 overexpression would increase telomere length, which would further confirm assay sensitivity to changes in telomere length. These data show that ZSCAN4 overexpression increases telomere length compared to empty vector control (Figure 5.13).

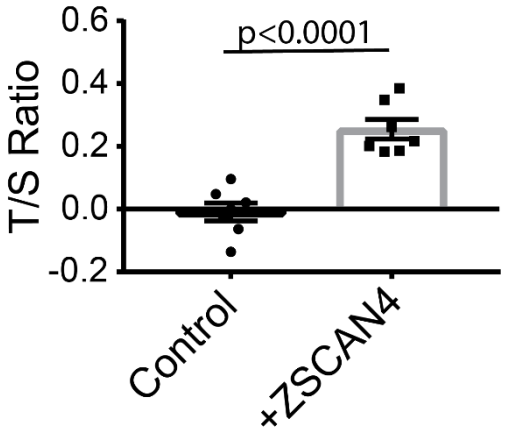

Figure 5.13: Telomere length increases upon ZSCAN4 overexpression. *mESCs were transfected with either empty vector control or ZSCAN4. mESCs were lysed 48hr post transfection, with no puromycin selection prior to lysis. DNA was extracted and subjected to telomere qPCR. T/S ratio represents the log transformed ratio of telomeric repeat signal to that of a single copy locus and indicates relative telomere length. Error bars indicate SEM. Statistical power test was used to calculate the appropriate number of biological replicates required to observe a significant effect (n=7). Significance calculated by unpaired student t-test.*

As ERK5 drives ZSCAN4 induction, I hypothesised that ERK5 activation will increase telomere length. These data show that upon ERK5 activation with MEK5DD, telomere length as indicated by T/S ratio increases, and this is partially reversed with AX15836 (Figure 5.14). This indicates that telomere length is regulated by ERK5 signalling.

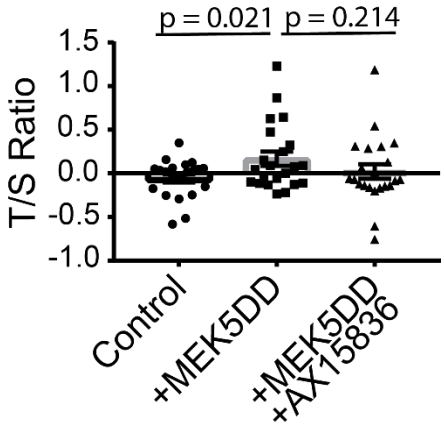

Figure 5.14: Telomere length increases upon ERK5 activation with MEK5DD. *mESCs were grown with MEK5DD to activate ERK5 signalling and treated with AX15836 (10 μM, 24 hr) to inhibit ERK5 signalling. mESCs were lysed 48hr post transfection, with 24hr puromycin selection prior to lysis. DNA from these mESCs was then subjected to telomere qPCR. T/S ratio represents the log transformed ratio of telomeric repeat signal to that of a single copy locus and indicates relative telomere length. Error bars indicate SEM. Statistical power test was used to calculate the appropriate number of biological replicates required to observe a significant effect (n=22). Significance calculated by one-way ANOVA with multiple comparisons.*

I then tested whether endogenous ERK5 signalling was sufficient for telomere elongation. To do this, I treated mESCs with either DMSO control or AX15836 to inhibit ERK5 signalling in the absence of MEK5DD. These data indicate that endogenous ERK5 signalling is sufficient for telomere elongation (Figure 5.15). Taken together, these data indicate that ERK5-dependent induction of ZSCAN4 increases telomere length (Figure 5.16), suggesting that ERK5 signalling regulates a key process that is required for stem cell rejuvenation.

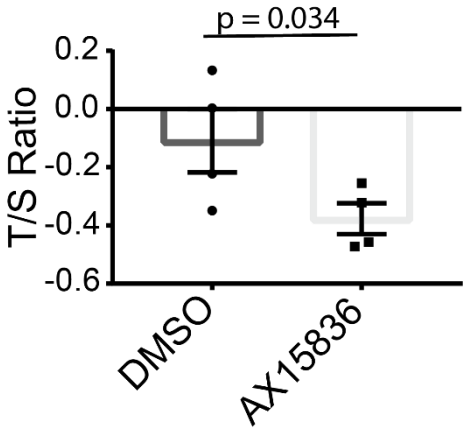

Figure 5.15: Endogenous ERK5 signalling is sufficient for telomere elongation. *mESCs were grown for 48hr with either DMSO or AX15836 (10 μM) treatment 24hr prior to lysis. DNA was extracted and subjected to telomere qPCR. T/S ratio represents the log transformed ratio of telomeric repeat signal to that of a single copy locus and indicates relative telomere length. Error bars indicate SEM. Statistical power test was used to calculate the appropriate number of biological replicates required to observe a significant effect (n=4). Significance calculated by unpaired student t-test.*

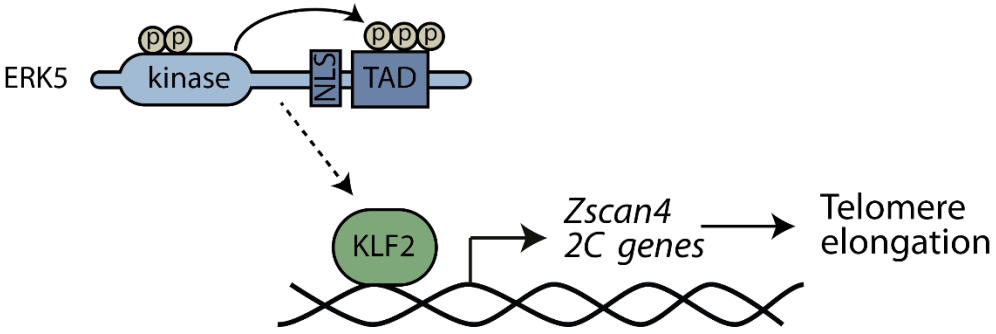

Figure 5.16: Model showing ERK5 induction of Zscan4 leads to telomere elongation.

5.3 KLF2 is a novel ERK5 substrate

Having confirmed ZSCAN4 as a novel target of ERK5, I next investigated the role of ERK5 kinase activity in ZSCAN4 regulation. ERK5 kinase activity can also regulate ERK5 target gene expression through phosphorylation of transcription factor substrates, such as the MEF2 family members (Kato, 1997; Yan et al., 2001). Therefore, a phosphoproteomic screen was performed by Charles Williams in the Findlay lab to identify novel ERK5 substrates. This screen identified KLF2 as an ERK5 substrate, and this was subsequently validated through *in vitro* kinase assay techniques. ERK5 phosphorylates two proline rich motifs (TPPXSP) in KLF2, each of which contains 2 potential phosphorylation sites (T/S). Previous work in the lab has identified that at least three of these four possible residues are phosphorylated by ERK5 *in vitro* (Figure 5.17). However, the role of KLF2 phosphorylation by ERK5 in mESCs is yet to be ascertained. Firstly, it has not been demonstrated whether ERK5 can phosphorylate KLF2 in mESCs. Additionally, the impact of KLF2 phosphorylation on ERK5/KLF2-dependent processes, such as ZSCAN4 regulation, has not been studied.

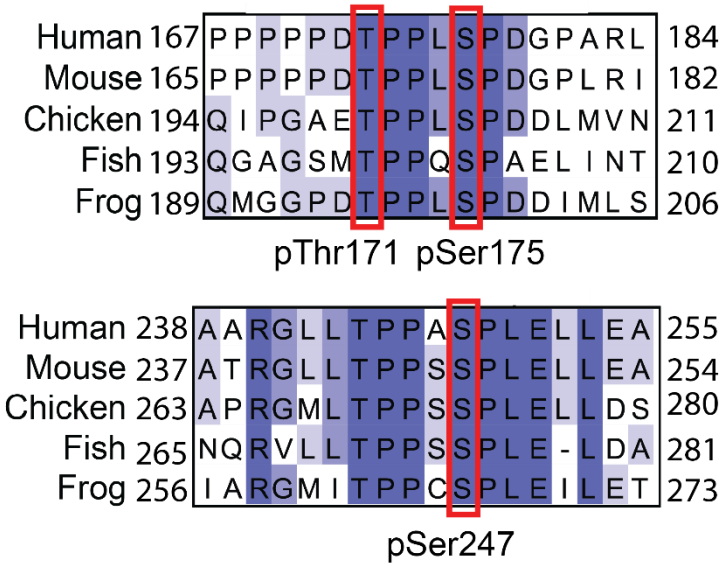

Figure 5.17: ERK5 phosphorylates KLF2 on at least 3 sites within 2 conserved motifs. *Three ERK5-dependent phosphorylation sites on KLF2 have been identified through in vitro kinase assays and mass spectrometry. These fall within two conserved TPPXSP motifs, and represent three out of four potential MAPK consensus phosphorylation sites (Williams, Thesis 2017).*

5.3.1 KLF2 is phosphorylated by ERK5 in mESCs

To study KLF2 phosphorylation in mESCs, an antibody against pT171/pS175 KLF2 (representing the major ERK5 phosphorylation motif) was generated by MRC Reagents and Services. To validate the specificity of this antibody, I expressed KLF2 constructs with either the first phospho-motif (T171/S175) , the second phospho-motif (T243/S247) or both mutated to alanine (termed 2AN, 2AC and 4A respectively), and assessed phospho-KLF2 signal by immunoblot analysis. When the T171/S175 pair is mutated (2AN), phospho-KLF2 signal is abolished, whereas phospho-KLF2 signal is observed for constructs in which the T171/S175 pair is intact (i.e. wildtype and 2AC mutant), indicating that the antibody specifically recognises phosphorylation at these sites (Figure 5.18). Given that these are major ERK5 phosphorylation sites, this is a useful tool for studying ERK5 phosphorylation of KLF2. Interestingly, the phosphorylation signal is lower for the 2AC mutant compared to wildtype. This may be due to lower expression levels of KLF2 in these samples.

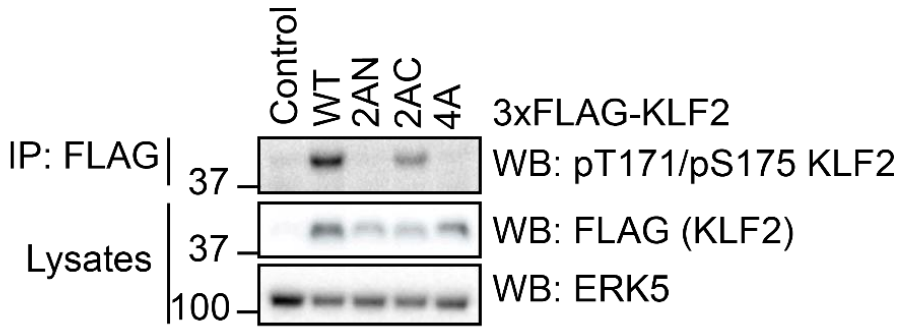

Figure 5.18: phospho-KLF2 antibody detects KLF2 phosphorylation at T171/S175. *mESCs were transfected with 3xFLAG KLF2 constructs (WT = wildtype, 2AN = T171A S175A, 2AC = T243A S247A, 4A = T171A S175A T243A S247A). mESCs were lysed 48hr post transfection, with no puromycin selection prior to lysis. FLAG IP was performed to remove contribution of endogenous KLF2. pT171/pS175 KLF2 and total KLF2 (FLAG) levels were determined by immunoblotting. ERK5 was used as a loading control. Results are representative of 3 experiments.*

In order to assess whether ERK5 phosphorylates KLF2 in mESCs, I next transfected KLF2 into *Erk5*$^{-/-}$ mESCs which had been reconstituted with either empty vector control, wildtype ERK5 or kinase-dead ERK5. KLF2 phosphorylation is induced by active ERK5 but not kinase inactive, demonstrating ERK5 phosphorylates KLF2 in mESCs (Figure 5.19).

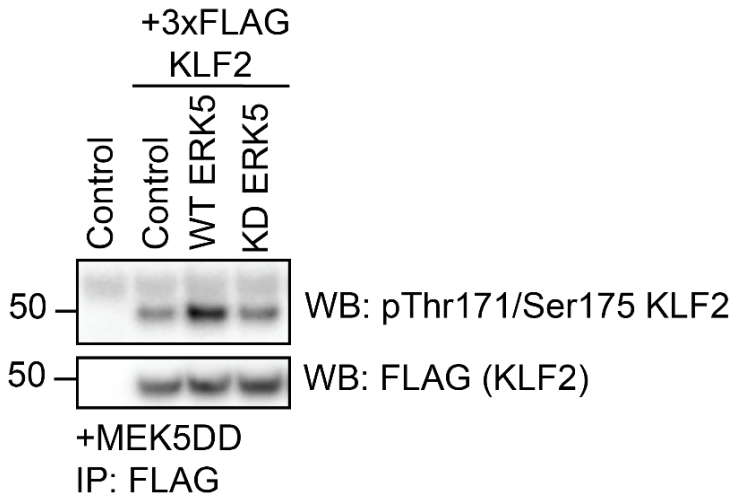

Figure 5.19: KLF2 is phosphorylated in response to ERK5 signalling in Erk5$^{-/-}$ mESCs. *Erk5$^{-/-}$ mESCs were reconstituted with empty vector control, wildtype ERK5 or kinase dead (D200A) ERK5, as well as MEK5DD to activate the pathway and 3xFLAG KLF2. mESCs were lysed 48hr post transfection, with 24hr puromycin selection prior to lysis. FLAG IP was performed to remove contribution of endogenous KLF2. pT171/pS175 KLF2 and total KLF2 (FLAG) levels were determined by immunoblotting. Experiment performed with Charles Williams. Results are representative of 3 experiments.*

5.3.2 KLF2 phosphorylation recruits FBXW7/CUL1 leading to ubiquitylation

Previous work in the lab illustrated that KLF2 phosphorylation at these ERK5-dependent phosphosites drives KLF2 ubiquitylation. Furthermore, mutation of these sites to alanine (T171A S175A T243A S247A, hereafter 4A KLF2) reduces KLF2 ubiquitylation. To confirm this, and to include an additional control of TUBE mutant (M557K L584K) beads which are unable to bind ubiquitin, I transfected both wildtype and 4A KLF2 into mESCs and performed a TUBE pulldown. These data confirm data previously generated by Charles Williams that KLF2 is ubiquitylated to a lesser extent when ERK5 phosphorylation sites are mutated (Figure 5.20). Data from Charles Williams also shows that 4A KLF2 is more stable than wildtype KLF2, as the degradative ubiquitin signal is lower.

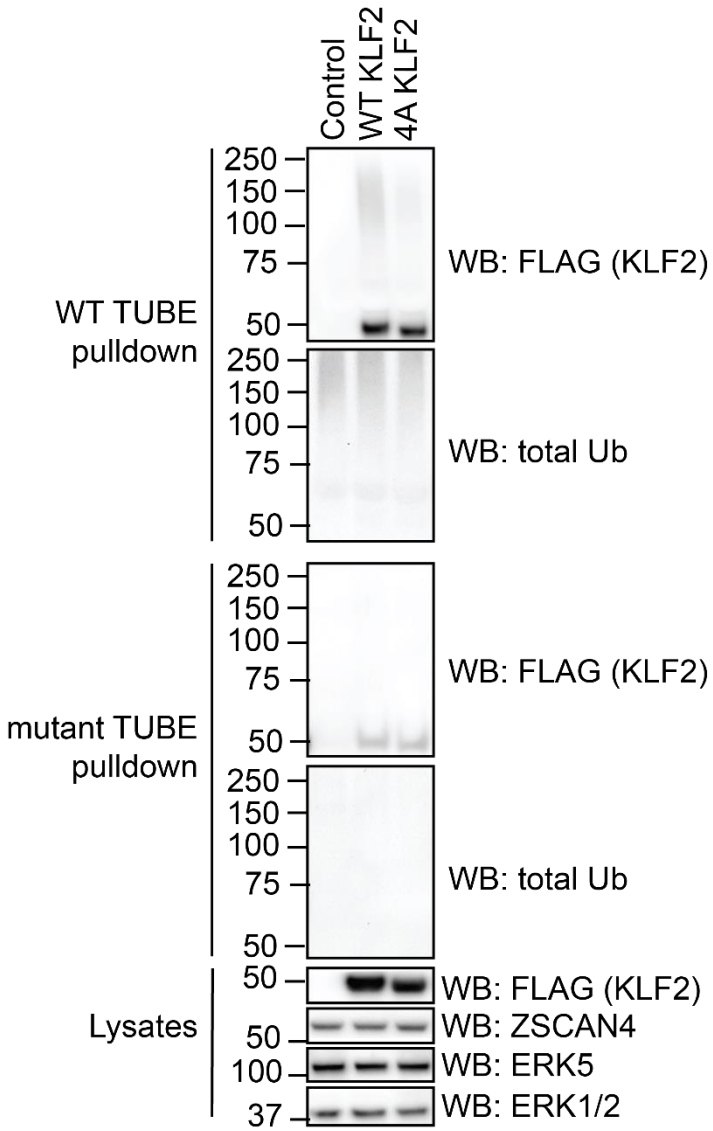

Figure 5.20: KLF2 is ubiquitylated in a phosphorylation-dependent manner. *Empty vector, wildtype KLF2 or 4A (T171A S175A T243A S247A) KLF2 were transfected into mESCs. mESCs were lysed 48hr post transfection, with no puromycin selection prior to lysis. Extracts were subjected to TUBE pulldown (to bind ubiquitin). Mutant TUBE beads were used to confirm that smears seen in wildtype TUBE pulldown were due to presence of ubiquitin. Total ubiquitin blot was used to assess ubiquitin pulldown efficiency. KLF2, ZSCAN4 and ERK5 levels were determined by immunoblotting. ERK1/2 blot was used as a loading control. Results are representative of 3 experiments. WT TUBE pulldown and mutant TUBE pulldown were run on the same gel and visualised on the same membrane. However, these samples were not run in adjacent lanes, with additional samples run between them. Therefore, in the interests of clarity, these blots have been separated for this figure, despite being directly comparable.*

Having established that KLF2 is ubiquitylated in response to phosphorylation by ERK5, I identified a candidate for the E3 ubiquitin ligase responsible for this ubiquitylation. FBW7 is a Cullin substrate adaptor that is recruited to phosphorylated substrates (Welcker & Clurman, 2008). Previous studies have identified FBW7 as a candidate E3 ubiquitin

ligase for KLF2 (R. Wang et al., 2013). I therefore hypothesised that the FBW7/Cullin complex ubiquitylates KLF2 upon phosphorylation by ERK5.

To assess whether FBW7 interacts with KLF2 in cells, I transfected HA-FBW7 and 3xFLAG-KLF2 mutants into mESCs, and immunoprecipitated KLF2 using anti-FLAG resin. FBW7 co-immunoprecipitates efficiently with wildtype KLF2, with the 2AN mutant to a lesser extent, and does not co-immunoprecipitate with 2AC or 4A KLF2 (Figure 5.21). This suggests that FBW7 interacts specifically with phosphorylated KLF2, supporting the hypothesis that FBW7 is the E3 ubiquitin ligase responsible for KLF2 ubiquitylation upon phosphorylation by ERK5. It would have been useful to further confirm this by testing whether HA-FBXW7 interaction with wildtype KLF2 is disrupted by ERK5 inhibition with AX15836.

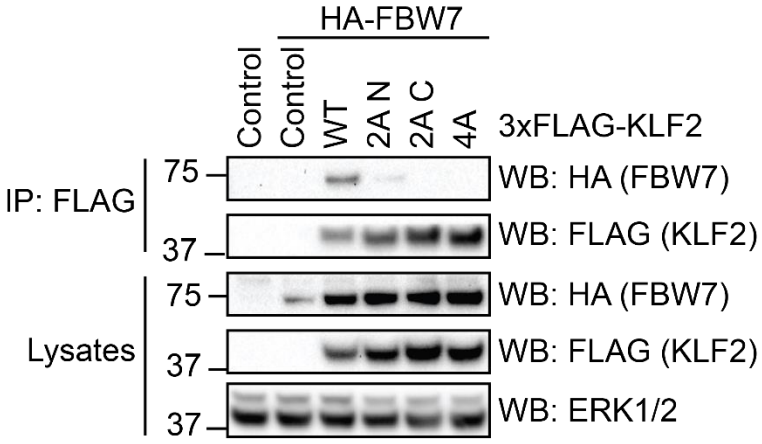

Figure 5.21: FBW7 interacts with KLF2 in a phosphorylation-dependent manner. *HA-FBW7 was transfected into mESCs with KLF2 phosphorylation mutants (WT = wildtype, 2AN = T171A S175A, 2AC = T243A S247A, 4A = T171A S175A T243A S247A). mESCs were lysed 48hr post transfection, with no puromycin selection prior to lysis. FLAG IP was used to pull down KLF2 with interaction partners such as FBW7. FBW7 (HA) and KLF2 (FLAG) levels were determined by immunoblotting. ERK1/2 was used as a loading control. Experiment performed with Saria Mansoor. Results are representative of 3 experiments.*

KLF2 usually localises to the nucleus. However, as phosphorylation can regulate many cellular functions including cellular localisation, I performed immunofluorescence microscopy as a control to assess whether unphosphorylatable KLF2 is localised correctly and is therefore functional. These images show wildtype KLF2 localising to the nucleus as expected, but unphosphorylatable 4A KLF2 localising at high levels in the nucleus with low signal detected in the cytoplasm (Figure 5.22).

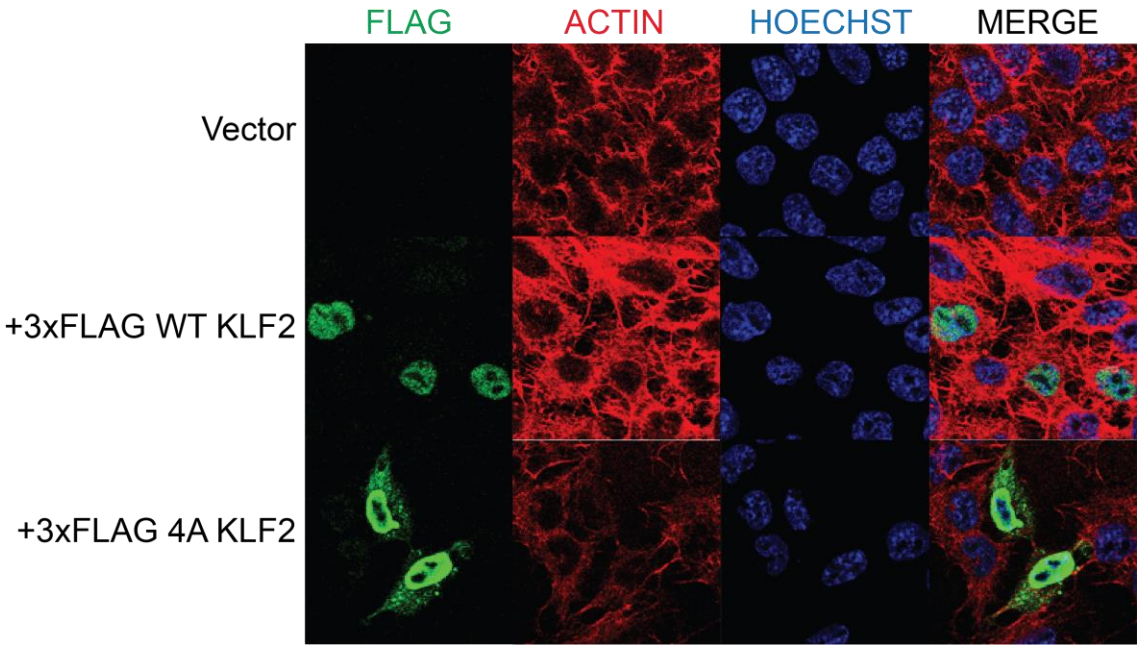

Figure 5.22: KLF2 phosphorylation modulates subcellular localisation. *mESCs were transfected with either empty vector control, wildtype KLF2 or 4A (T171A S175A T243A S247A) KLF2 for 24hr with no puromycin selection prior to fixing with 4% PFA. FLAG (KLF2) was visualised using an Alexafluor 488-conjugated secondary antibody. ActinRed stain (555nm) was used to show cytoskeleton, and Hoechst stain was used to show nuclei (representative images, n=3).*

Quantification of the nuclear KLF2 signal confirms that 4A KLF2 is expressed at higher levels in mESC nuclei (Figure 5.23).

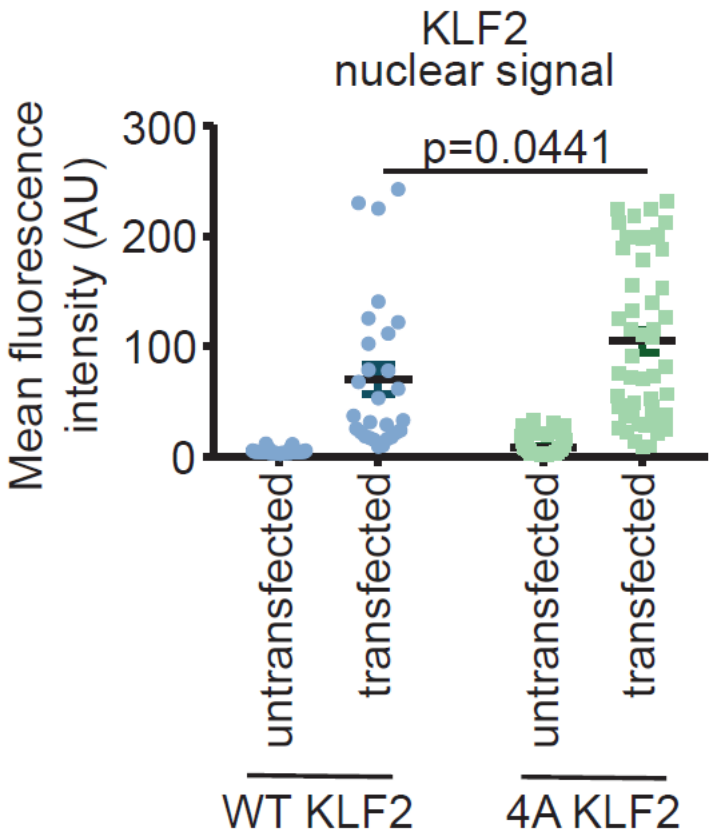

Figure 5.23: KLF2 phosphorylation results in lower nuclear expression levels. *mESCs were transfected with either empty vector control, wildtype KLF2 or 4A (T171A S175A T243A S247A) KLF2 for 24hr prior to fixing with 4% PFA. FLAG (KLF2) was visualised using an Alexafluor 488-conjugated secondary antibody. Hoechst stain was used to show nuclei. Nuclear KLF2 signal was quantified by a FIJI mask. Each data point represents KLF2 signal in one nucleus, with cells imaged from 3 biological replicates.*

The low level cytoplasmic KLF2 signal could indicate 4A KLF2 "overspill" from the nucleus due to high expression and increased expression due to increased stability, supporting the hypothesis that KLF2 phosphorylation by ERK5 leads to ubiquitylation and degradation of KLF2. Alternatively, these results could suggest that KLF2 phosphorylation is required to maintain nuclear localisation via another mechanism, such as tethering. In conclusion, ERK5 phosphorylation of KLF2 leads to ubiquitylation of KLF2 by FBW7/Cullin, followed by subsequent degradation, but does not lead to a significant change in KLF2 localisation (Figure 5.24).

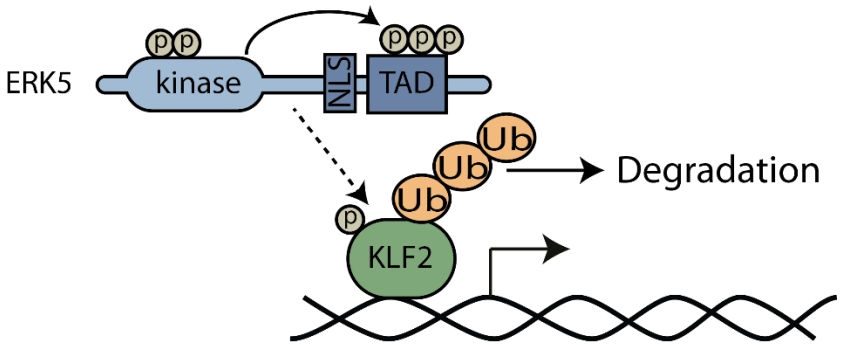

Figure 5.24: Model showing KLF2 phosphorylation by ERK5 leading to KLF2 ubiquitylation and degradation.

5.3.3 ERK5-dependent KLF2 phosphorylation and ubiquitylation inhibits ZSCAN4 expression

My data indicate that ERK5 phosphorylation of KLF2 leads to its ubiquitylation and degradation. I previously showed that ZSCAN4 and other 2C genes are regulated by ERK5 signalling via KLF2. I therefore asked whether KLF2 ubiquitylation and turnover impacts on its downstream transcriptional targets, *Zscan4* and other 2C genes. To do this, I transfected increasing amounts of wildtype and 4A *Klf2* into mESCs and analysed mRNA levels of *Zscan4*, *Tdpoz3*, and *Zfp352* by qRT-PCR. These data show that *Zscan4*, *Tdpoz3* and *Zfp352* are induced by KLF2 and mRNA levels are augmented by unphosphorylatable 4A KLF2 (Figure 5.25). This is consistent with the hypothesis 4A KLF2 is able to induce its target genes more readily due to its increased stability. This indicates that KLF2 phosphorylation by ERK5 forms a feedback loop regulating the expression of *Zscan4* and other 2C genes (Figure 5.26). In this way, ERK5 can induce KLF2 expression, leading to the induction of KLF2-dependent genes, but also phosphorylate KLF2, resulting in KLF2 turnover, inhibiting the expression of KLF2-dependent genes.

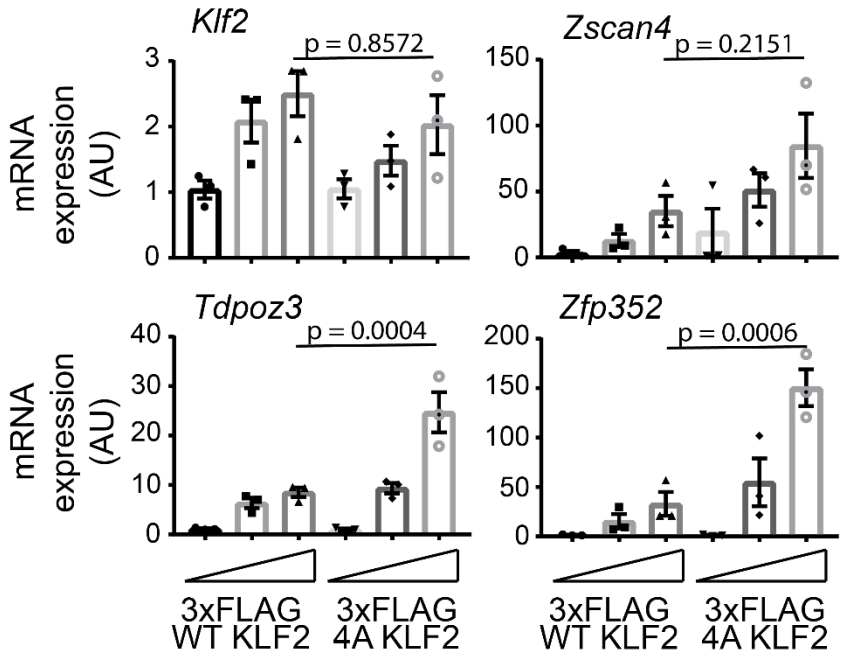

Figure 5.25: Zscan4 and other 2C gene mRNA induction is suppressed by KLF2 phosphorylation. *Wildtype KLF2 or 4A (T171A S175A T243A S247A) KLF2 was titrated into Klf2$^{\Delta/\Delta}$ mESCs. mESCs were lysed 48hr post transfection, with 24hr puromycin selection prior to lysis. RNA was extracted and subjected to qRT-PCR. Error bars indicate SEM (n=3). Significance calculated by one-way ANOVA with multiple comparisons. These results have been replicated in 3 independent Klf2$^{\Delta/\Delta}$ mESCs clones (K2, K9, K13).*

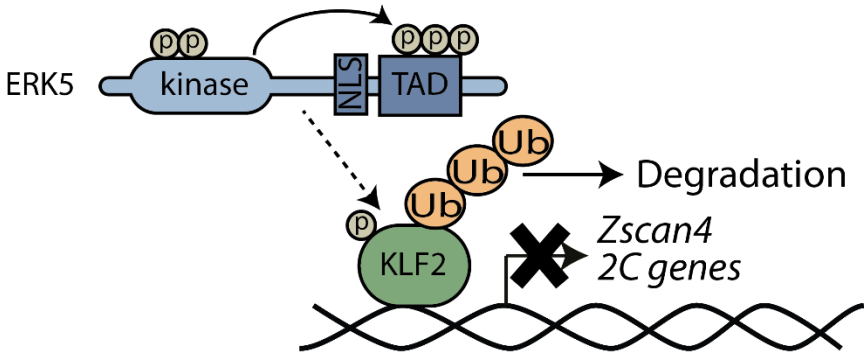

Figure 5.26: Model showing KLF2 ubiquitylation and degradation as a consequence of ERK5 phosphorylation inhibits expression of Zscan4 and 2C genes.

5.4 Discussion

ZSCAN4 is a key regulator of stem cell rejuvenation (Zalzman et al., 2010), which I have shown is regulated by ERK5 signalling. Since stem cell rejuvenation is characterised by a large transcriptional network (Eckersley-Maslin et al., 2016), it was important to

validate whether ERK5 signalling regulates ZSCAN4 alone, or with other markers of the 2C state. I have established that ERK5 signalling regulates additional 2C state markers, implicating ERK5 in the regulation of stem cell rejuvenation. This is particularly exciting as the upstream pathways regulating this process are largely uncharacterised (Storm et al., 2009).

I have also shown that ERK5 regulation of ZSCAN4 occurs through KLF2, as seen with ANNEXIN A2 and S100A10 in Chapter 4. Unlike *Anxa2* and *S100a10* however, KLF2 has not been found to ChIP to *Zscan4* gene promoters. This may be due to the highly similar nature of the members of the gene and pseudogene family, leading to underrepresentation of specific promoter sequences in ChIP-Seq screens (Falco et al., 2007). I also considered whether KLF2 might act in concert with either another transcription factor (for example DUX) or transposable element (such as *Muervl*) to regulate expression of the whole 2C gene network. While these data were inconclusive, the hypothesis would be consistent with previous data detailing a KLF-dependent mechanism of early embryonic transcriptional network regulation, where transposable elements which harbour KLF-binding sites act with KLFs to temporally coordinate transcriptional programmes during embryonic development (De Iaco et al., 2017; Hendrickson et al., 2017; Pontis et al., 2019). In this model, a KLF is directed to the promoters of its target genes through interaction with DUX or a transposable element.

ZSCAN4 is expressed in a small subpopulation (approximately 5%) of mESCs at a given time. A key question therefore remains whether ERK5 increases ZSCAN4 expression in the ZSCAN4^{+} mESC population or whether ERK5 increases the number of cells expressing ZSCAN4. Preliminary immunofluorescence data I generated suggests that the number of cells expressing ZSCAN4 does not increase, although, as with the telomere qPCR assay, samples show a high degree of biological variation. This could be due to the apparently stochastic expression of ZSCAN4.

This raises an additional question of whether ERK5 is only active in cells expressing ZSCAN4. If so, this would explain the stochastic pattern of ZSCAN4 expression, but does not explain why ERK5 is only active in those cells. There may be an external or internal trigger for ERK5 activation which has yet to be explored, which leads to the dynamic and

oscillatory pattern of ZSCAN4 expression. A possible candidate for this trigger is telomere erosion; depletion of TRF2, a protein involved in telomere end protection through formation of T loop structures, has been shown to induce ZSCAN4 expression, suggesting that ZSCAN4 is induced by telomere shortening (Markiewicz-Potoczny et al., 2020; Ruis et al., 2020). Therefore, telomere erosion may also act as an activating signal for ERK5, leading to the observed pattern of expression of ZSCAN4. Further to this, ERK5 has been implicated in stress responses, which may be consistent with this hypothesis (Widmann et al., 1999).

ZSCAN4 expression is associated with a number of cellular processes associated with zygotic genome activation, including elongated telomeres (Eckersley-Maslin et al., 2016; Nakai-Futatsugi & Niwa, 2016). I have shown that ERK5 regulates telomere length, suggesting that ERK5 can modulate biological processes associated with ZSCAN4. As telomere length is vital for genomic stability in long-term culture, this highlights a role for ERK5 in stem cell maintenance, preventing cultured mESCs from entering quiescence due to genomic instability (Zalzman et al., 2010). Furthermore, ZSCAN4 has been shown to facilitate somatic cell reprogramming during the generation of iPSCs (Jing Jiang et al., 2013). This indicates that ERK5 could be exploited to promote reprogramming of cells to a naïve state, through synergistic ERK5-dependent induction of both pluripotency genes and ZSCAN4 for stem cell rejuvenation, to support unbiased differentiation and full developmental potential (Nichols & Smith, 2009).

I have demonstrated that ERK5 signalling regulates telomere elongation, a specific ZSCAN4-dependent process (Zalzman et al., 2010). I also hypothesise that ERK5 signalling could induce the degradation of DNMT1, leading to global DNA demethylation which facilitates telomere extension (Dan et al., 2017). One of the key functions of ZSCAN4 is in UHRF1 and DNMT1 degradation (Dan et al., 2017). UHRF1 is an E3 ubiquitin ligase which is recruited by ZSCAN4 to ubiquitylate the maintenance DNA methyltransferase DNMT1, leading to the degradation of both UHRF1 and DNMT1 (Figure 5.27). This could be investigated using a TUBE pulldown for ubiquitin on UHRF1 and DNMT1 in response to expression of MEK5DD or ZSCAN4. Interestingly, other DNMTs have been identified as potentially ERK5-regulated. DNMT3A was identified by

the proteomic approach outlined in Chapter 3 to be downregulated in MEK5DD-expressing mESCs. Additionally, DNMT3B is suppressed by ERK5 (Williams et al., 2016). This indicates that ERK5 regulates global DNA methylation status. Although I have not yet tested this, bisulphite sequencing could be used to confirm this, as in previous studies examining this 2C state (Eckersley-Maslin et al., 2016).

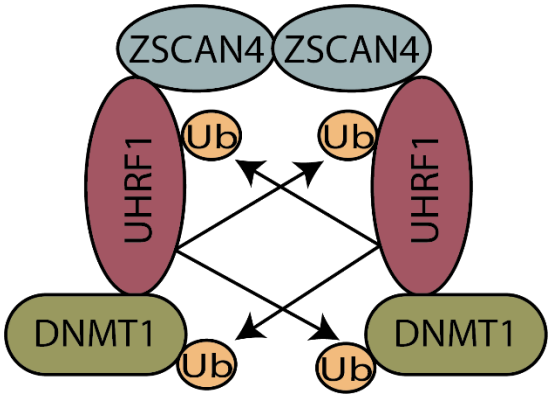

Figure 5.27: Model showing proposed mechanism for ZSCAN4-mediated turnover of UHRF1 and DNMT1. *ZSCAN4 recruits UHRF1 to DNMT1 resulting in the trans-autoubiquitylation of UHRF1 and the ubiquitylation of DNMT1. Ubiquitylation of both UHRF1 and DNMT1 leads to their degradation.*

My data indicate that KLF2 phosphorylation by ERK5 and subsequent degradation restrains ZSCAN4 expression, and by extension, the expression of the 2C transcriptional network. This can be described mathematically as an incoherent feedforward loop, where input X activates both an intermediate (Y) and the ultimate output (Z), while Y represses or inhibits Z (Figure 5.28). This points to a mechanism by which ERK5 can regulate both the cycling into the 2C state by inducing 2C gene expression through KLF2, but also out of the 2C state, as ERK5-dependent phosphorylation of KLF2 leads to KLF2 degradation and thereby removes induction of 2C genes. This is consistent with the transient nature of the rejuvenation phase (Hirata et al., 2012), and would prevent the extended expression of these genes. It would therefore be interesting to study the dynamics of ZSCAN4 expression in response to ERK5 signalling using live cell microscopy. It also raises the question of why the oscillatory expression of these genes are important. The rejuvenative phase is crucial for continual propagation of mESCs in culture, but it is unclear why it would be disadvantageous for these genes to be continually expressed. However, the

expression of early embryonic genes at later stages of development is deleterious, and therefore the expression of these genes is likely to be tightly regulated.

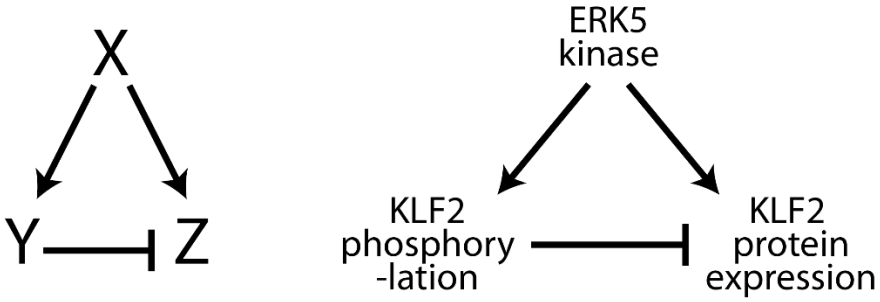

Figure 5.28: Model illustrating incoherent feedforward loop of ERK5 signalling on KLF2 levels. *An incoherent feedforward loop is one where input X activates both an intermediate (Y) and the ultimate output (Z), while Y represses or inhibits Z. In this way, ERK5 kinase activity drives KLF2 expression, but can also phosphorylate KLF2, leading to its degradation and hence reducing KLF2 levels.*

6. Discussion and Future Work

In this thesis, I have studied the functions and mechanisms of ERK5 in ESCs, using an unbiased and systematic proteomics approach. Following on from previous work, I have found that ERK5 maintains naïve pluripotency through the regulation of key pluripotency factors such as KLF2 (Williams et al., 2016), but also by inducing stem cell rejuvenation through ZSCAN4. This reverts cells to a totipotent-like state, and allows cells to retain the genomic stability to self-renew indefinitely (Hirata et al., 2012; Morikawa et al., 2016; Sunadome et al., 2011). Additionally, I have shown that ERK5 regulates membrane dynamics through induction of ANNEXIN A2 and S100A10, a function which had not be previously attributed to ERK5. Both of these novel functions present exciting relevance for ERK5 in development, regenerative medicine, and cancer.

6.1 Implications of ANNEXIN A2/S100A10 findings

I have also shown ERK5 induces expression of ANNEXIN A2 and S100A10. As ANNEXIN A2 and S100A10 modulate events at the plasma membrane such as cell adhesion and interactions with the extracellular matrix, it may be that ERK5 is activated by stimuli such as cell density, cell-cell interactions, and cell density (Lee, 2004; Madureira et al., 2011). Cell adhesion and migration are important processes in development to ensure the correct organisation of tissues within the developing organism (Matsui, 2018). Additionally, positioning within the embryo is linked to developmental potential, suggesting that the regulation of this through signalling controlling the motility of cells would be important in pluripotency in the context of development (Yamanaka et al., 2006).

6.2 Implications of ZSCAN4 findings

An outstanding question from this work is how the ERK5 pathway is activated in mESCs. Previous work has shown that ERK5 can be activated by various growth factors and stresses (Abe et al., 1996; Lennartsson et al., 2010). These stimuli would therefore be applied to all cells in a population, which does not account for the oscillatory expression pattern observed with ZSCAN4. However, cells must express the specific receptor in

order to respond to a specific stimulus. Therefore, although ERK5 may not be active in all cells in all times, growth factor receptor expression patterns may explain how ERK5 is activated in some cells and not others. Additionally, ERK5 nuclear translocation has previously been linked to the cell cycle through CDK1 phosphorylation (Iñesta-Vaquera et al., 2010). However, if this was the main driver for ERK5 induction of ZSCAN4, it might be expected that many more cells would express ZSCAN4 at any one time. It may be that an internal signal, for example telomere length approaching a critical point, is sufficient to activate ERK5 and lead to 2C gene induction. Indeed, induction of ZSCAN4 is linked to depletion of the telomere protection factor TRF2, such that without TRF2, telomeres will be eroded, leading to ZSCAN4 expression (Markiewicz-Potoczny et al., 2020; Ruis et al., 2020). Therefore, ERK5 may also be activated by telomere erosion, which could explain the oscillatory pattern of ZSCAN4 expression (Zalzman et al., 2010). An alternative explanation is that ERK5 is active in every cell, but a permissive transcriptional or epigenetic environment is required for ZSCAN4 expression. Therefore, it would be important to study other drivers of ZSCAN4 expression to understand how ERK5 functions within this framework.

6.3 Implications for ERK5 mechanisms

One of the key questions regarding the mechanisms by which ERK5 operates is whether ERK5 can regulate transcription directly as a transcription factor, given that it does not contain a DNA-binding domain. Genes such as *Klf2* are dependent on the ERK5 transcriptional activation domain, and this region also contains an interaction domain for MEF2 docking (Kato, 1997; Morikawa et al., 2016; Sunadome et al., 2011; Yan et al., 2001). Therefore it is likely that ERK5 can regulate transcription directly. However, all the ERK5 targets identified in this thesis are regulated through KLF2 transcriptional activity. As such, although ERK5 can regulate genes directly, it may be that the majority of genes regulated by ERK5 are regulated through an intermediate transcription factor such as KLF2 or MEF2. In order to disentangle the direct and indirect gene targets of ERK5, a ChIP-Seq approach should be used to identify where ERK5 binds chromatin.

ERK5 can regulate gene transcription through transcription factor substrate phosphorylation by its kinase activity. Many ERK5 substrates are positively activated when phosphorylated by ERK5; for example, MEF2A and MEF2C are phosphorylated by ERK5, leading to increased transcriptional activity (Marinissen et al., 1999). In contrast, by phosphorylating KLF2, KLF2 is targeted for proteosomal degradation, thus restricting its ability to induce target genes. This represents a negative feedback loop, through which ERK5 can both induce and repress expression of its target genes, hypothetically in an oscillatory manner. ERK5 has also been implicated in another phospho-degron-mediated feedback mechanism; ERK5 phosphorylates MEK5, which we have observed reduces MEK5 levels in cells, suggesting that ERK5 phosphorylation of MEK5 leads to its turnover (Mody et al., 2003). In this way, ERK5 can also render the ERK5 signalling pathway inactive.

6.4 Implications for ERK5 functions

ERK5 is clearly required for development, through maintenance of the pluripotent stem cell population and embryonic lethality due to defects in cardiac vasculature (Sohn et al., 2002; Williams et al., 2016). Additionally, ERK5 is implicated in diseases such as cancer (Pereira et al., 2019; Ramsay et al., 2011). However, the molecular mechanisms for ERK5 functions in pluripotent stem cells have not been explored. In this thesis, I have identified novel ERK5 targets in ZSCAN4, ANNEXIN A2 and S100A10, which could explain these phenotypes. As a stem cell rejuvenation factor, ZSCAN4 promotes the maintenance of a stem cell population through facilitation of telomere elongation (Zalzman et al., 2010). In development, this could allow ERK5 to maintain a population of naïve stem cells, capable of unbiased differentiation to any germ layer (Nichols & Smith, 2009; Williams et al., 2016). Additionally, as DNA methylation is a key barrier to somatic cell reprogramming and ZSCAN4 drives global DNA demethylation, ERK5 signalling may prove useful in improving the efficiency of iPSC generation (Dan et al., 2017; Jing Jiang et al., 2013).

Finally, ZSCAN4, ANNEXIN A2 and S100A10 can provide explanations for the importance of ERK5 in cancer. ZSCAN4 expression allows for a zygotic genome activation-like phenotype, in which developmental genes are derepressed (Eckersley-

Maslin et al., 2016). This may allow tumours to increase their proliferative capacity and heterogeneity, resulting in a more aggressive and treatment-resistant cancer, characteristic of cancers associated with ERK5 (Pavan et al., 2018; Pereira et al., 2019; Ramsay et al., 2011). Furthermore, ANNEXIN A2 and S100A10 expression equips cancer cells with the ability to migrate more, resulting in tumour metastasis (Bharadwaj et al., 2013; Heizmann et al., 2002). Again, ERK5 expression is associated with high rates of metastasis so these findings are consistent with that previously shown (Pavan et al., 2018; Pereira et al., 2019; Ramsay et al., 2011). Pluripotency factor re-expression in cancer stem cells facilitates treatment-resistance, a characteristic of ERK5-overexpressing tumours, as these factors promote efficient self-renewal and the ability to repopulate the tumour with different cell lineages, each of which may require different treatments to destroy completely (Liu et al., 2013; Prieto-Vila et al., 2017).

References

Abe, J. I., Kusuhara, M., Ulevitch, R. J., Berk, B. C., & Lee, J. D. (1996). Big mitogen-activated protein kinase 1 (BMK1) is a redox-sensitive kinase. *Journal of Biological Chemistry*. https://doi.org/10.1074/jbc.271.28.16586

Alessi, D. R., James, S. R., Downes, C. P., Holmes, A. B., Gaffney, P. R. J., Reese, C. B., & Cohen, P. (1997). Characterization of a 3-phosphoinositide-dependent protein kinase which phosphorylates and activates protein kinase Bα. *Current Biology*. https://doi.org/10.1016/s0960-9822(06)00122-9

Amano, S., Chang, Y. T., & Fukui, Y. (2015). ERK5 activation is essential for osteoclast differentiation. *PLoS ONE*. https://doi.org/10.1371/journal.pone.0125054

Amano, T., Hirata, T., Falco, G., Monti, M., Sharova, L. V., Amano, M., … Ko, M. S. H. (2013). Zscan4 restores the developmental potency of embryonic stem cells. *Nature Communications*, *4*. https://doi.org/10.1038/ncomms2966

Arman, E., Haffner-Krausz, R., Chen, Y., Heath, J. K., & Lonai, P. (1998). Targeted disruption of fibroblast growth factor (FGF) receptor 2 suggests a role for FGF signaling in pregastrulation mammalian development. *Proceedings of the National Academy of Sciences of the United States of America*. https://doi.org/10.1073/pnas.95.9.5082

Atkins, G. B., & Jain, M. K. (2007). Role of Krüppel-like transcription factors in endothelial biology. *Circulation Research*. https://doi.org/10.1161/01.RES.0000267856.00713.0a

Avilion, A. A., Nicolis, S. K., Pevny, L. H., Perez, L., Vivian, N., & Lovell-Badge, R. (2003). Multipotent cell lineages in early mouse development depend on SOX2 function. *Genes and Development*. https://doi.org/10.1101/gad.224503

Barros, J. C., & Marshall, C. J. (2005). Activation of either ERK1/2 or ERK5 MAP kinase pathways can lead to disruption of the actin cytoskeleton. *Journal of Cell Science*. https://doi.org/10.1242/jcs.02308

Ben-Porath, I., Thomson, M. W., Carey, V. J., Ge, R., Bell, G. W., Regev, A., & Weinberg, R. A. (2008). An embryonic stem cell-like gene expression signature in poorly differentiated aggressive human tumors. *Nature Genetics*. https://doi.org/10.1038/ng.127

Benjamini, Y., & Hochberg, Y. (1995). Controlling the False Discovery Rate: A Practical and Powerful Approach to Multiple Testing. *Journal of the Royal Statistical Society: Series B (Methodological)*, *57*(1), 289–300. https://doi.org/https://doi.org/10.1111/j.2517-6161.1995.tb02031.x

Bharadwaj, A., Bydoun, M., Holloway, R., & Waisman, D. (2013). Annexin A2 heterotetramer: Structure and function. *International Journal of Molecular Sciences*. https://doi.org/10.3390/ijms14036259

Bi, L., Okabe, I., Bernard, D. J., Wynshaw-Boris, A., & Nussbaum, R. L. (1999). Proliferative defect and embryonic lethality in mice homozygous for a deletion in the p110α subunit of phosphoinositide 3-kinase. *Journal of Biological Chemistry*. https://doi.org/10.1074/jbc.274.16.10963

Biswas, D., & Jiang, P. (2016). Chemically induced reprogramming of somatic cells to pluripotent stem cells and neural cells. *International Journal of Molecular Sciences*. https://doi.org/10.3390/ijms17020226

Blank, J. L., Gerwins, P., Elliott, E. M., Sather, S., & Johnson, G. L. (1996). Molecular cloning of mitogen-activated protein/ERK kinase kinases (MEKK) 2 and 3 regulation of sequential phosphorylation pathways involving mitogen-activated protein kinase and c-Jun kinase. *Journal of Biological Chemistry*. https://doi.org/10.1074/jbc.271.10.5361

Boeke, J. D., Garfinkel, D. J., Styles, C. A., & Fink, G. R. (1985). Ty elements transpose through an RNA intermediate. *Cell*, *40*(3), 491–500. https://doi.org/10.1016/0092-8674(85)90197-7

Bone, H. K., Damiano, T., Bartlett, S., Perry, A., Letchford, J., Ripoll, Y. S., … Welham, M. J. (2009). Involvement of GSK-3 in Regulation of Murine Embryonic Stem Cell Self-Renewal Revealed by a Series of Bisindolylmaleimides. *Chemistry and Biology*. https://doi.org/10.1016/j.chembiol.2008.11.003

Boulton, T. G., Nye, S. H., Robbins, D. J., Ip, N. Y., Radzlejewska, E., Morgenbesser, S. D., … Yancopoulos, G. D. (1991). ERKs: A family of protein-serine/threonine kinases that are activated and tyrosine phosphorylated in response to insulin and NGF. *Cell*, *65*(4), 663–675. https://doi.org/10.1016/0092-8674(91)90098-J

Bourillot, P. Y., Aksoy, I., Schreiber, V., Wianny, F., Schulz, H., Hummel, O., … Savatier, P. (2009). Novel STAT3 target genes exert distinct roles in the inhibition of mesoderm and endoderm differentiation in cooperation with Nanog. *Stem Cells*. https://doi.org/10.1002/stem.110

Boyer, L. A., Lee, T. I., Cole, M. F., Johnstone, S. E., Levine, S. S., Zucker, J. P., … Young, R. A. (2005). Core Transcriptional Regulatory Circuitry in Human Embryonic Stem Cells. *Cell*, *122*, 947–956. https://doi.org/10.1016/j.cell.2005.08.020

Brennand, K. J., Simone, A., Jou, J., Gelboin-Burkhart, C., Tran, N., Sangar, S., … Gage, F. H. (2011). Modelling schizophrenia using human induced pluripotent stem cells. *Nature*. https://doi.org/10.1038/nature09915

Briggs, J. A., Sun, J., Shepherd, J., Ovchinnikov, D. A., Chung, T. L., Nayler, S. P., … Wolvetang, E. J. (2013). Integration-free induced pluripotent stem cells model genetic and neural developmental features of down syndrome etiology. *Stem Cells*. https://doi.org/10.1002/stem.1297

Browne, J. A., Pearson, A. L., Zahr, R. A., Niculescu-Duvaz, I., Baines, D. L., & Dockrell, M. E. C. (2008). TGF-beta activates ERK5 in human renal epithelial cells. *Biochemical and Biophysical Research Communications*. https://doi.org/10.1016/j.bbrc.2008.06.058

Buschbeck, M., Eickhoff, J., Sommer, M. N., & Ullrich, A. (2002). Phosphotyrosine-specific phosphatase PTP-SL regulates the ERK5 signaling pathway. *Journal of Biological Chemistry*. https://doi.org/10.1074/jbc.M202149200

Buschbeck, M., & Ullrich, A. (2005). The unique C-terminal tail of the mitogen-activated protein kinase ERK5 regulates its activation and nuclear shuttling. *Journal of Biological Chemistry*, *280*(4), 2659–2667. https://doi.org/10.1074/jbc.M412599200

Callicott, R. J., & Womack, J. E. (2006). Real-time PCR assay for measurement of mouse telomeres. *Comparative Medicine*, *56*(1), 17–22. Retrieved from http://www.ingentaconnect.com/content/aalas/cm/2006/00000056/00000001/art00003

Cargnello, M., & Roux, P. P. (2011). Activation and Function of the MAPKs and Their Substrates, the MAPK-Activated Protein Kinases. *Microbiology and Molecular Biology Reviews*. https://doi.org/10.1128/mmbr.00031-10

Chambers, I., Colby, D., Robertson, M., Nichols, J., Lee, S., Tweedie, S., & Smith, A. (2003). Functional expression cloning of Nanog, a pluripotency sustaining factor in embryonic stem cells. *Cell*. https://doi.org/10.1016/S0092-8674(03)00392-1

Chambers, I., & Tomlinson, S. R. (2009). The transcriptional foundation of pluripotency. *Development*. https://doi.org/10.1242/dev.024398

Chao, T. H., Hayashi, M., Tapping, R. I., Kato, Y., & Lee, J. D. (1999). MEKK3 directly regulates MEK5 activity as part of the big mitogen- activated protein kinase 1 (BMK1) signaling pathway. *Journal of Biological Chemistry*. https://doi.org/10.1074/jbc.274.51.36035

Chen, M. J., Dixon, J. E., & Manning, G. (2017). Genomics and evolution of protein phosphatases. *Science Signaling*. https://doi.org/10.1126/scisignal.aag1796

Chen, T.-H., Chen, C.-Y., Wen, H.-C., Chang, C.-C., Wang, H.-D., Chuu, C.-P., & Chang, C.-H. (2017). YAP promotes myogenic differentiation via the MEK5-ERK5 pathway. *FASEB Journal : Official Publication of the Federation of American Societies for Experimental Biology*, *31*(7), 2963–2972. https://doi.org/10.1096/fj.201601090R

Chen, X., Xu, H., Yuan, P., Fang, F., Huss, M., Vega, V. B., … Ng, H.-H. (2008). Integration of external signaling pathways with the core transcriptional network in embryonic stem cells. *Cell*, *133*(6), 1106–1117. https://doi.org/10.1016/j.cell.2008.04.043

Cheng, A. M., Tracy, Saxton, M., Sakai, R., Kulkarni, S., Mbamalu, G., … Research, S. L. (1998). Mammalian Grb2 regulates multiple steps in embryonic development and malignant transformation. *Cell*.

Cherny, R. A., Stokes, T. M., Merei, J., Lom, L., Brandon, M. R., & Williams, R. L. (1994). Strategies for the isolation and characterization of bovine embryonic stem cells. *Reproduction, Fertility and Development*. https://doi.org/10.1071/RD9940569

Choi, B. M., Kwak, H. J., Jun, C. D., Park, S. D., Kim, K. Y., Kim, H. R., & Chung, H. T. (1996). Control of scarring in adult wounds using antisense transforming growth factor-β1 oligodeoxynucleotides. *Immunology and Cell Biology*. https://doi.org/10.1038/icb.1996.19

Choi, S. M., Kim, Y., Shim, J. S., Park, J. T., Wang, R. H., Leach, S. D., … Jang, Y. Y. (2013). Efficient drug screening and gene correction for treating liver disease using patient-specific stem cells. *Hepatology*. https://doi.org/10.1002/hep.26237

Clark, P. R., Jensen, T. J., Kluger, M. S., Morelock, M., Hanidu, A., Qi, Z., … Pober, J. S. (2011). MEK5 is Activated by Shear Stress, Activates ERK5 and Induces KLF4 to Modulate TNF Responses in Human Dermal Microvascular Endothelial Cells. *Microcirculation*. https://doi.org/10.1111/j.1549-8719.2010.00071.x

Cohen, P. (1989). The structure and regulation of protein phosphatases. *Annual Review of Biochemistry*. https://doi.org/10.1146/annurev.bi.58.070189.002321

Creutz, C. E., Pazoles, C. J., & Pollard, H. B. (1978). Identification and purification of an adrenal medullary protein (synexin) that causes calcium-dependent aggregation of isolated chromaffin granules. *Journal of Biological Chemistry*.

Creutz, Carl E., & Snyder, S. L. (2005). Interactions of annexins with the mu subunits of the clathrin assembly proteins. *Biochemistry*. https://doi.org/10.1021/bi051160w

Cross, D. A. E., Alessi, D. R., Cohen, P., Andjelkovich, M., & Hemmings, B. A. (1995). Inhibition of glycogen synthase kinase-3 by insulin mediated by protein kinase B. *Nature*. https://doi.org/10.1038/378785a0

Cuttano, R., Rudini, N., Bravi, L., Corada, M., Giampietro, C., Papa, E., … Dejana, E. (2016). KLF 4 is a key determinant in the development and progression of cerebral cavernous malformations . *EMBO Molecular Medicine*. https://doi.org/10.15252/emmm.201505433

Dale Brown, R., Kelly Ambler, S., Li, M., Sullivan, T. M., Henry, L. N., Crossno, J. T., … Stenmark, K. R. (2013). MAP kinase kinase kinase-2 (MEKK2) regulates hypertrophic remodeling of the right ventricle in hypoxia-induced pulmonary hypertension. *American Journal of Physiology - Heart and Circulatory Physiology*. https://doi.org/10.1152/ajpheart.00158.2012

Dan, J., Rousseau, P., Hardikar, S., Veland, N., Wong, J., Autexier, C., & Chen, T. (2017). Zscan4 Inhibits Maintenance DNA Methylation to Facilitate Telomere Elongation in Mouse Embryonic Stem Cells. *Cell Reports*, *20*(8), 1936–1949. https://doi.org/10.1016/j.celrep.2017.07.070

Darr, H., Mayshar, Y., & Benvenisty, N. (2006). Overexpression of NANOG in human ES cells enables feeder-free growth while inducing primitive ectoderm features. *Development*. https://doi.org/10.1242/dev.02286

Davis, S., Aldrich, T. H., Stahl, N., Pan, L., Taga, T., Kishimoto, T., … Yancopoulos, G. D. (1993). LIFRβ and gp130 as heterodimerizing signal transducers of the tripartite CNTF receptor. *Science*. https://doi.org/10.1126/science.8390097

De Iaco, A., Planet, E., Coluccio, A., Verp, S., Duc, J., & Trono, D. (2017). DUX-family transcription factors regulate zygotic genome activation in placental mammals. *Nature Genetics*, *49*(6), 941–945. https://doi.org/10.1038/ng.3858

DePasquale, J. A., & Izzard, C. S. (1991). Accumulation of talin in nodes at the edge of the lamellipodium and separate incorporation into adhesion plaques at focal contacts in fibroblasts. *Journal of Cell Biology*. https://doi.org/10.1083/jcb.113.6.1351

DeRosa, B. A., Van Baaren, J. M., Dubey, G. K., Lee, J. M., Cuccaro, M. L., Vance, J. M., … Dykxhoorn, D. M. (2012). Derivation of autism spectrum disorder-specific induced pluripotent stem cells from peripheral blood mononuclear cells. *Neuroscience Letters*. https://doi.org/10.1016/j.neulet.2012.02.086

Dunn, S. J., Martello, G., Yordanov, B., Emmott, S., & Smith, A. G. (2014). Defining an essential transcription factor program for naïve pluripotency. *Science*. https://doi.org/10.1126/science.1248882

Dutta, D., Ray, S., Home, P., Larson, M., Wolfe, M. W., & Paul, S. (2011). Self-renewal versus lineage commitment of embryonic stem cells: Protein kinase C signaling shifts the balance. *Stem Cells*. https://doi.org/10.1002/stem.605

Eckersley-Maslin, M. A., Svensson, V., Krueger, C., Stubbs, T. M., Giehr, P., Krueger, F., … Reik, W. (2016). MERVL/Zscan4 Network Activation Results in Transient Genome-wide DNA Demethylation of mESCs. *Cell Reports*, *17*(1), 179–192. https://doi.org/10.1016/j.celrep.2016.08.087

Erazo, T., Moreno, A., Ruiz-Babot, G., Rodriguez-Asiain, A., Morrice, N. A., Espadamala, J., … Lizcano, J. M. (2013). Canonical and Kinase Activity-Independent Mechanisms for Extracellular Signal-Regulated Kinase 5 (ERK5) Nuclear Translocation Require Dissociation of Hsp90 from the ERK5-Cdc37 Complex. *Molecular and Cellular Biology*. https://doi.org/10.1128/mcb.01246-12

Ernst, M., Oates, A., & Dunn, A. R. (1996). Gp130-mediated signal transduction in embryonic stem cells involves activation of Jak and Ras/mitogen-activated protein kinase pathways. *The Journal of Biological Chemistry*, *271*(47), 30136–30143. https://doi.org/10.1074/jbc.271.47.30136

Evans, M. J., & Kaufman, M. H. (1981). Establishment in culture of pluripotential cells from mouse embryos. *Nature*, *292*(5819), 154–156. https://doi.org/10.1038/292154a0

Falco, G., Lee, S. L., Stanghellini, I., Bassey, U. C., Hamatani, T., & Ko, M. S. H. (2007). Zscan4: A novel gene expressed exclusively in late 2-cell embryos and embryonic stem cells. *Developmental Biology*, *307*(2), 539–550. https://doi.org/10.1016/j.ydbio.2007.05.003

Fedorov, O., Müller, S., & Knapp, S. (2010). The (un)targeted cancer kinome. *Nature Chemical Biology*. https://doi.org/10.1038/nchembio.297

Feighery, R., Maguire, P., Ryan, M. P., & McMorrow, T. (2008). A proteomic approach to immune-mediated epithelial-mesenchymal transition. *Proteomics - Clinical Applications*. https://doi.org/10.1002/prca.200780148

Feldman, B., Poueymirou, W., Papaioannou, V. E., DeChiara, T. M., & Goldfarb, M. (1995). Requirement of FGF-4 for postimplantatior mouse development. *Science*. https://doi.org/10.1126/science.7809630

Feng, B., Jiang, J., Kraus, P., Ng, J. H., Heng, J. C. D., Chan, Y. S., … Ng, H. H. (2009). Reprogramming of fibroblasts into induced pluripotent stem cells with orphan nuclear receptor Esrrb. *Nature Cell Biology*. https://doi.org/10.1038/ncb1827

Fernandez-Alonso, R., Bustos, F., Budzyk, M., Kumar, P., Helbig, A. O., Hukelmann, J., … Findlay, G. M. (2020). Phosphoproteomics identifies a bimodal EPHA2 receptor switch that promotes embryonic stem cell differentiation. *Nature Communications*. https://doi.org/10.1038/s41467-020-15173-4

Fernandez-Alonso, R., Davidson, L., Hukelmann, J., Zengerle, M., Prescott, A. R., Lamond, A., … Findlay, G. M. (2017). Brd4-Brd2 isoform switching coordinates pluripotent exit and Smad2-dependent lineage specification. *EMBO Reports*. https://doi.org/10.15252/embr.201643534

Feske, S. (2007). Calcium signalling in lymphocyte activation and disease. *Nature Reviews*

Immunology. https://doi.org/10.1038/nri2152

Ficz, G., Branco, M. R., Seisenberger, S., Santos, F., Krueger, F., Hore, T. A., … Reik, W. (2011). Dynamic regulation of 5-hydroxymethylcytosine in mouse ES cells and during differentiation. *Nature*, *473*(7347), 398–404. https://doi.org/10.1038/nature10008

Finegan, K. G., Wang, X., Lee, E. J., Robinson, A. C., & Tournier, C. (2009). Regulation of neuronal survival by the extracellular signal-regulated protein kinase 5. *Cell Death and Differentiation*. https://doi.org/10.1038/cdd.2008.193

FISCHER, E. H., & KREBS, E. G. (1955). Conversion of phosphorylase b to phosphorylase a in muscle extracts. *The Journal of Biological Chemistry*. https://doi.org/10.1016/s0021-9258(19)52289-x

Flaherty, K. T., Robert, C., Hersey, P., Nathan, P., Garbe, C., Milhem, M., … Schadendorf, D. (2012). Improved Survival with MEK Inhibition in BRAF-Mutated Melanoma. *New England Journal of Medicine*. https://doi.org/10.1056/nejmoa1203421

Gashaw, I., Ellinghaus, P., Sommer, A., & Asadullah, K. (2011). What makes a good drug target? *Drug Discovery Today*. https://doi.org/10.1016/j.drudis.2011.09.007

Genetos, D. C., Wong, A., Watari, S., & Yellowley, C. E. (2010). Hypoxia increases Annexin A2 expression in osteoblastic cells via VEGF and ERK. *Bone*. https://doi.org/10.1016/j.bone.2010.08.024

Gerke, V., & Moss, S. E. (2002). Annexins: From structure to function. *Physiological Reviews*. https://doi.org/10.1152/physrev.00030.2001

Giles, J. R., Yang, X., Mark, W., & Foote, R. H. (1993). Pluripotency of cultured rabbit inner cell mass cells detected by isozyme analysis and eye pigmentation of fetuses following injection into blastocysts or morulae. *Molecular Reproduction and Development*. https://doi.org/10.1002/mrd.1080360203

Gírio, A., Montero, J. C., Pandiella, A., & Chatterjee, S. (2007). Erk5 is activated and acts as a survival factor in mitosis. *Cellular Signalling*. https://doi.org/10.1016/j.cellsig.2007.05.005

Giurisato, E., Lonardi, S., Telfer, B., Lussoso, S., Risa-Ebrí, B., Zhang, J., … Tournier, C. (2020). Extracellular-regulated protein kinase 5-mediated control of p21 expression promotes macrophage proliferation associated with tumor growth and metastasis. *Cancer Research*. https://doi.org/10.1158/0008-5472.CAN-19-2416

Glenney, J. (1986). Phospholipid-dependent Ca2+ binding by the 36-kDa tyrosine kinase substrate (calpactin) and its 33-kDa core. *Journal of Biological Chemistry*, *261*(16), 7247–7252. https://doi.org/https://doi.org/10.1016/S0021-9258(17)38382-5

Gomez, N., Erazo, T., & Lizcano, J. M. (2016). ERK5 and cell proliferation: Nuclear localization is what matters. *Frontiers in Cell and Developmental Biology*. https://doi.org/10.3389/fcell.2016.00105

Gómez, N., Erazo, T., & Lizcano, J. M. (2016). ERK5 and Cell Proliferation: Nuclear Localization Is What Matters. *Frontiers in Cell and Developmental Biology*. https://doi.org/10.3389/fcell.2016.00105

Gontan, C., Achame, E. M., Demmers, J., Barakat, T. S., Rentmeester, E., Van Ijcken, W., … Gribnau, J. (2012). RNF12 initiates X-chromosome inactivation by targeting REX1 for degradation. *Nature*. https://doi.org/10.1038/nature11070

Grindheim, A. K., Saraste, J., & Vedeler, A. (2017). Protein phosphorylation and its role in the regulation of Annexin A2 function. *Biochimica et Biophysica Acta - General Subjects*. https://doi.org/10.1016/j.bbagen.2017.08.024

Guo, R., Ye, X., Yang, J., Zhou, Z., Tian, C., Wang, H., … Liu, L. (2018). Feeders facilitate telomere maintenance and chromosomal stability of embryonic stem cells. *Nature Communications*. https://doi.org/10.1038/s41467-018-05038-2

Guschin, D., Rogers, N., Briscoe, J., Witthuhn, B., Watling, D., Horn, F., … Stark, G. R. (1995). A major role for the protein tyrosine kinase JAK1 in the JAK/STAT signal transduction pathway in response to interleukin-6. *The EMBO Journal*, *14*(7), 1421–1429.

Handyside, A., Hooper, M. L., Kaufman, M. H., & Wilmut, I. (1987). Towards the isolation of embryonal stem cell lines from the sheep. *Roux's Archives of Developmental Biology*. https://doi.org/10.1007/BF00376313

Hansen, M. D. H., Ehrlich, J. S., & Nelson, W. J. (2002). Molecular mechanism for orienting membrane and actin dynamics to nascent cell-cell contacts in epithelial cells. *Journal of Biological Chemistry*. https://doi.org/10.1074/jbc.M207747200

Harrington, L. S., Findlay, G. M., Gray, A., Tolkacheva, T., Wigfield, S., Rebholz, H., … Lamb, R. F. (2004). The TSC1-2 tumor suppressor controls insulin-PI3K signaling via regulation of IRS proteins. *Journal of Cell Biology*. https://doi.org/10.1083/jcb.200403069

Hayashi, M., Kim, S.-W., Imanaka-Yoshida, K., Yoshida, T., Abel, E. D., Eliceiri, B., … Lee, J.-D. (2004). Targeted deletion of BMK1/ERK5 in adult mice perturbs vascular integrity and leads to endothelial failure. *The Journal of Clinical Investigation*, *113*(8), 1138–1148. https://doi.org/10.1172/JCI19890

Hayashi, M., & Lee, J. D. (2004). Role of the BMK1/ERK5 signaling pathway: Lessons from knockout mice. *Journal of Molecular Medicine*. https://doi.org/10.1007/s00109-004-0602-8

Hayes, M. J., Shao, D., Bailly, M., & Moss, S. E. (2006). Regulation of actin dynamics by annexin 2. *EMBO Journal*. https://doi.org/10.1038/sj.emboj.7601078

He, K. L., Deora, A. B., Xiong, H., Ling, Q., Weksler, B. B., Niesvizky, R., & Hajjar, K. A. (2008). Endothelial cell annexin A2 regulates polyubiquitination and degradation of its binding partner S100A10/p11. *Journal of Biological Chemistry*, *283*(28), 19192–19200. https://doi.org/10.1074/jbc.M800100200

Heinrich, P. C., Behrmann, I., Müller-Newen, G., Schaper, F., & Graeve, L. (1998). Interleukin-6-type cytokine signalling through the gp130/Jak/STAT pathway. *Biochemical Journal*. https://doi.org/10.1042/bj3340297

Heizmann, C. W., Fritz, G., & Schäfer, B. W. (2002). S100 proteins: structure, functions and pathology. *Frontiers in Bioscience : A Journal and Virtual Library*. https://doi.org/10.2741/heizmann

Hendrickson, P. G., Doráis, J. A., Grow, E. J., Whiddon, J. L., Lim, J. W., Wike, C. L., … Cairns, B. R. (2017). Conserved roles of mouse DUX and human DUX4 in activating cleavage-stage genes and MERVL/HERVL retrotransposons. *Nature Genetics*, *49*(6), 925–934. https://doi.org/10.1038/ng.3844

Hikasa, H., Ezan, J., Itoh, K., Li, X., Klymkowsky, M. W., & Sokol, S. Y. (2010). Regulation of TCF3 by Wnt-dependent phosphorylation during vertebrate axis specification. *Developmental Cell*. https://doi.org/10.1016/j.devcel.2010.09.005

Hirata, T., Amano, T., Nakatake, Y., Amano, M., Piao, Y., Hoang, H. G., & Ko, M. S. H. (2012). Zscan4 transiently reactivates early embryonic genes during the generation of induced pluripotent stem cells. *Scientific Reports*, *2*. https://doi.org/10.1038/srep00208

Hishida, T., Nakachi, Y., Mizuno, Y., Katano, M., Okazaki, Y., Ema, M., … Okuda, A. (2015). Functional compensation between Myc and PI3K signaling supports self-renewal of embryonic stem cells. *Stem Cells*. https://doi.org/10.1002/stem.1893

Holmes, K., Roberts, O. L., Thomas, A. M., & Cross, M. J. (2007). Vascular endothelial growth factor receptor-2: Structure, function, intracellular signalling and therapeutic inhibition. *Cellular Signalling*. https://doi.org/10.1016/j.cellsig.2007.05.013

Hou, P., Li, Y., Zhang, X., Liu, C., Guan, J., Li, H., … Deng, H. (2013). Pluripotent stem cells induced from mouse somatic cells by small-molecule compounds. *Science*. https://doi.org/10.1126/science.1239278

Huse, M., & Kuriyan, J. (2002). The conformational plasticity of protein kinases. *Cell*. https://doi.org/10.1016/S0092-8674(02)00741-9

Identification of the regulatory phosphorylation sites in pp42/mitogen-activated protein kinase (MAP kinase). (1991). *EMBO Journal /*, *10*(4), 885–892.

Ikebuchi, N. W., & Waisman, D. M. (1990). Calcium-dependent regulation of actin filament bundling by lipocortin-85. *Journal of Biological Chemistry*.

Iñesta-Vaquera, F. A., Campbell, D. G., Tournier, C., Gómez, N., Lizcano, J. M., & Cuenda, A. (2010a). Alternative ERK5 regulation by phosphorylation during the cell cycle. *Cellular Signalling*. https://doi.org/10.1016/j.cellsig.2010.07.010

Iñesta-Vaquera, F. A., Campbell, D. G., Tournier, C., Gómez, N., Lizcano, J. M., & Cuenda, A. (2010b). Alternative ERK5 regulation by phosphorylation during the cell cycle. *Cellular Signalling*. https://doi.org/10.1016/j.cellsig.2010.07.010

Ivanova, N., Dobrin, R., Lu, R., Kotenko, I., Levorse, J., DeCoste, C., … Lemischka, I. R. (2006). Dissecting self-renewal in stem cells with RNA interference. *Nature*. https://doi.org/10.1038/nature04915

Jiang, Jianming, Chan, Y. S., Loh, Y. H., Cai, J., Tong, G. Q., Lim, C. A., … Ng, H. H. (2008). A core Klf circuitry regulates self-renewal of embryonic stem cells. *Nature Cell Biology*. https://doi.org/10.1038/ncb1698

Jiang, Jing, Lv, W., Ye, X., Wang, L., Zhang, M., Yang, H., … Li, J. (2013). Zscan4 promotes genomic stability during reprogramming and dramatically improves the quality of iPS cells as demonstrated by tetraploid complementation. *Cell Research*, *23*(1), 92–106.

https://doi.org/10.1038/cr.2012.157

Johnson, M. H., & Ziomek, C. A. (1981). The foundation of two distinct cell lineages within the mouse morula. *Cell*. https://doi.org/10.1016/0092-8674(81)90502-X

Julio, M. K. de, Alvarez, M. J., Galli, A., Chu, J., Price, S. M., Califano, A., & Shen, M. M. (2011). Regulation of extra-embryonic endoderm stem cell differentiation by Nodal and Cripto signaling. *Development*. https://doi.org/10.1242/dev.065656

Kadoya, K., Togo, S., Tulafu, M., Namba, Y., Iwai, M., Watanabe, J., … Takahashi, K. (2019). Specific Features of Fibrotic Lung Fibroblasts Highly Sensitive to Fibrotic Processes Mediated via TGF-β-ERK5 Interaction. *Cellular Physiology and Biochemistry : International Journal of Experimental Cellular Physiology, Biochemistry, and Pharmacology*, *52*(4), 822–837. https://doi.org/10.33594/000000057

Kalkan, T., Olova, N., Roode, M., Mulas, C., Lee, H. J., Nett, I., … Smith, A. (2017). Tracking the embryonic stem cell transition from ground state pluripotency. *Development (Cambridge)*. https://doi.org/10.1242/dev.142711

Kalkan, T., & Smith, A. (2014). Mapping the route from naive pluripotency to lineage specification. *Philosophical Transactions of the Royal Society B: Biological Sciences*. https://doi.org/10.1098/rstb.2013.0540

Kalluri, R., & Neilson, E. G. (2003). Epithelial-mesenchymal transition and its implications for fibrosis. *Journal of Clinical Investigation*. https://doi.org/10.1172/JCI200320530

Kalluri, R., & Weinberg, R. A. (2009). The basics of epithelial-mesenchymal transition. *Journal of Clinical Investigation*. https://doi.org/10.1172/JCI39104

Kasler, H G, Victoria, J., Duramad, O., & Winoto, A. (2000). ERK5 is a novel type of mitogen-activated protein kinase containing a transcriptional activation domain. *Molecular and Cellular Biology*, *20*(22), 8382–8389. https://doi.org/10.1128/MCB.20.22.8382-8389.2000

Kasler, Herbert G., Victoria, J., Duramad, O., & Winoto, A. (2000). ERK5 Is a Novel Type of Mitogen-Activated Protein Kinase Containing a Transcriptional Activation Domain. *Molecular and Cellular Biology*. https://doi.org/10.1128/mcb.20.22.8382-8389.2000

Kato, Y. (1997). BMK1/ERK5 regulates serum-induced early gene expression through transcription factor MEF2C. *The EMBO Journal*, *16*(23), 7054–7066. https://doi.org/10.1093/emboj/16.23.7054

Kato, Y, Tapping, R., Huang, S., & Watson, M. (1998). Bmk1/Erk5 is required for cell proliferation induced by epidermal growth factor. *Nature*, *395*(October), 713–716. https://doi.org/10.1038/27234

Kato, Yutaka, Zhao, M., Morikawa, A., Sugiyama, T., Chakravortty, D., Koide, N., … Lee, J. D. (2000). Big mitogen-activated kinase regulates multiple members of the MEF2 protein family. *Journal of Biological Chemistry*, *275*(24), 18534–18540. https://doi.org/10.1074/jbc.M001573200

Keutzer, J. C., & Hirschhorn, R. R. (1990). The growth-regulated gene 1B6 is identified as the heavy chain of calpactin I. *Experimental Cell Research*. https://doi.org/10.1016/0014-4827(90)90291-H

Kondoh, K., Terasawa, K., Morimoto, H., & Nishida, E. (2006). Regulation of Nuclear Translocation of Extracellular Signal-Regulated Kinase 5 by Active Nuclear Import and Export Mechanisms. *Society*, *26*(5), 1679–1690. https://doi.org/10.1128/MCB.26.5.1679

Koressaar, T., & Remm, M. (2007). Enhancements and modifications of primer design program Primer3. *Bioinformatics*. https://doi.org/10.1093/bioinformatics/btm091

Krugmann, S., Jordens, I., Gevaert, K., Driessens, M., Vandekerckhove, J., & Hall, A. (2001). Cdc42 induces filopodia by promoting the formation of an IRSp53:Mena complex. *Current Biology*, *11*(21), 1645–1655. https://doi.org/https://doi.org/10.1016/S0960-9822(01)00506-1

Kunath, T., Saba-El-Leil, M. K., Almousailleakh, M., Wray, J., Meloche, S., & Smith, A. (2007). FGF stimulation of the Erk1/2 signalling cascade triggers transition of pluripotent embryonic stem cells from self-renewal to lineage commitment. *Development*. https://doi.org/10.1242/dev.02880

Kuo, C. T., Veselits, M. L., Barton, K. P., Lu, M. M., Clendenin, C., & Leiden, J. M. (1997). The LKLF transcription factor is required for normal tunica media formation and blood vessel stabilization during murine embryogenesis. *Genes and Development*. https://doi.org/10.1101/gad.11.22.2996

Lanier, L. L., Chang, C., Azuma, M., Ruitenberg, J. J., Hemperly, J. J., & Phillips, J. H. (1991). Molecular and functional analysis of human natural killer cell-associated neural cell adhesion molecule (N-CAM/CD56). *Journal of Immunology*.

Lanner, F., & Rossant, J. (2010). The role of FGF/Erk signaling in pluripotent cells. *Development*, *137*(20), 3351–3360. https://doi.org/10.1242/dev.050146

Lee, D. B. N. (2004). Annexin A2 heterotetramer: role in tight junction assembly. *AJP: Renal Physiology*, *287*(3), F481–F491. https://doi.org/10.1152/ajprenal.00175.2003

Lee, E. S., Boldo, L. S., Fernandez, B. O., Feelisch, M., & Harmsen, M. C. (2017). Suppression of TAK1 pathway by shear stress counteracts the inflammatory endothelial cell phenotype induced by oxidative stress and TGF-β1. *Scientific Reports*. https://doi.org/10.1038/srep42487

Lee, J. D., Ulevitch, R. J., & Han, J. (1995). Primary structure of BMK1: A new mammalian MAP kinase. *Biochemical and Biophysical Research Communications*. https://doi.org/10.1006/bbrc.1995.2189

Lemmon, M. A., & Schlessinger, J. (2010). Cell signaling by receptor tyrosine kinases. *Cell*. https://doi.org/10.1016/j.cell.2010.06.011

Lennartsson, J., Burovic, F., Witek, B., Jurek, A., & Heldin, C. H. (2010). Erk 5 is necessary for sustained PDGF-induced Akt phosphorylation and inhibition of apoptosis. *Cellular Signalling*. https://doi.org/10.1016/j.cellsig.2010.01.020

Li, J., Yen, C., Liaw, D., Podsypanina, K., Bose, S., Wang, S. I., … Parsons, R. (1997). PTEN, a putative protein tyrosine phosphatase gene mutated in human brain, breast, and prostate cancer. *Science*. https://doi.org/10.1126/science.275.5308.1943

Li, M., Zhang, D., Hou, Y., Jiao, L., Zheng, X., & Wang, W. H. (2003). Isolation and culture of

embryonic stem cells from porcine blastocysts. *Molecular Reproduction and Development*. https://doi.org/10.1002/mrd.10301

Li, P., Tong, C., Mehrian-Shai, R., Jia, L., Wu, N., Yan, Y., … Ying, Q. L. (2008). Germline Competent Embryonic Stem Cells Derived from Rat Blastocysts. *Cell*. https://doi.org/10.1016/j.cell.2008.12.006

Li, R., Liang, J., Ni, S., Zhou, T., Qing, X., Li, H., … Pei, D. (2010). A mesenchymal-to-Epithelial transition initiates and is required for the nuclear reprogramming of mouse fibroblasts. *Cell Stem Cell*. https://doi.org/10.1016/j.stem.2010.04.014

Li, X., Zhu, L., Yang, A., Lin, J., Tang, F., Jin, S., … Jin, Y. (2011). Calcineurin-NFAT signaling critically regulates early lineage specification in mouse embryonic stem cells and embryos. *Cell Stem Cell*. https://doi.org/10.1016/j.stem.2010.11.027

Liang, P., Lan, F., Lee, A. S., Gong, T., Sanchez-Freire, V., Wang, Y., … Wu, J. C. (2013). Drug screening using a library of human induced pluripotent stem cell-derived cardiomyocytes reveals disease-specific patterns of cardiotoxicity. *Circulation*. https://doi.org/10.1161/CIRCULATIONAHA.113.001883

Lin, E. C. K., Amantea, C. M., Nomanbhoy, T. K., Weissig, H., Ishiyama, J., Hu, Y., … Rosenblum, J. S. (2016). ERK5 kinase activity is dispensable for cellular immune response and proliferation. *Proceedings of the National Academy of Sciences*, *113*(42), 11865–11870. https://doi.org/10.1073/pnas.1609019113

Lin, Q., Schwarz, J., Bucana, C., & Olson, E. N. (1997). Control of mouse cardiac morphogenesis and myogenesis by transcription factor MEF2C. *Science*. https://doi.org/10.1126/science.276.5317.1404

Lin, T., Ambasudhan, R., Yuan, X., Li, W., Hilcove, S., Abujarour, R., … Ding, S. (2009). A chemical platform for improved induction of human iPSCs. *Nature Methods*, *6*(11), 805–808. https://doi.org/10.1038/nmeth.1393

Liu, A., Yu, X., & Liu, S. (2013). Pluripotency transcription factors and cancer stem cells: Small genes make a big difference. *Chinese Journal of Cancer*. https://doi.org/10.5732/cjc.012.10282

Liu, H., Kim, Y., Sharkis, S., Marchionni, L., & Jang, Y. Y. (2011). In vivo liver regeneration potential of human induced pluripotent stem cells from diverse origins. *Science Translational Medicine*. https://doi.org/10.1126/scitranslmed.3002376

Liu, S., Cong, Y., Wang, D., Sun, Y., Deng, L., Liu, Y., … Wicha, M. S. (2014). Breast cancer stem cells transition between epithelial and mesenchymal states reflective of their normal counterparts. *Stem Cell Reports*. https://doi.org/10.1016/j.stemcr.2013.11.009

Liu, Y., Myrvang, H. K., & Dekker, L. V. (2014). Annexin A2 complexes with S100 proteins: structure, function and pharmacological manipulation. *British Journal of Pharmacology*, 1–35. https://doi.org/10.1111/bph.12978

Loh, Y. H., Wu, Q., Chew, J. L., Vega, V. B., Zhang, W., Chen, X., … Ng, H. H. (2006). The Oct4 and Nanog transcription network regulates pluripotency in mouse embryonic stem cells. *Nature Genetics*. https://doi.org/10.1038/ng1760

Luiz, J. P. M., Toller-Kawahisa, J. E., Viacava, P. R., Nascimento, D. C., Pereira, P. T., Saraiva, A. L., … Alves-Filho, J. C. (2020). MEK5/ERK5 signaling mediates IL-4-induced M2 macrophage differentiation through regulation of c-Myc expression. *Journal of Leukocyte Biology*, *108*(4), 1215–1223. https://doi.org/10.1002/JLB.1MA0520-016R

Macfarlan, T. S., Gifford, W. D., Driscoll, S., Lettieri, K., Rowe, H. M., Bonanomi, D., … Pfaff, S. L. (2012). Embryonic stem cell potency fluctuates with endogenous retrovirus activity. *Nature*, *487*(7405), 57–63. https://doi.org/10.1038/nature11244

Madak-Erdogan, Z., Ventrella, R., Petry, L., & Katzenellenbogen, B. S. (2014). Novel roles for ERK5 and cofilin as critical mediators linking ERα-driven transcription, actin reorganization, and invasiveness in breast cancer. *Molecular Cancer Research*. https://doi.org/10.1158/1541-7786.MCR-13-0588

Madureira, P. A., O'Connell, P. A., Surette, A. P., Miller, V. A., & Waisman, D. M. (2012). The biochemistry and regulation of S100A10: A multifunctional plasminogen receptor involved in oncogenesis. *Journal of Biomedicine and Biotechnology*. https://doi.org/10.1155/2012/353687

Madureira, P. A., Surette, A. P., Phipps, K. D., Taboski, M. A. S., Miller, V. A., & Waisman, D. M. (2011). The role of the annexin A2 heterotetramer in vascular fibrinolysis. *Blood*. https://doi.org/10.1182/blood-2011-06-334672

Maguire, C. T., Demarest, B. L., Hill, J. T., Palmer, J. D., Brothman, A. R., Yost, H. J., & Condic, M. L. (2013). Genome-Wide Analysis Reveals the Unique Stem Cell Identity of Human Amniocytes. *PLoS ONE*. https://doi.org/10.1371/journal.pone.0053372

Marenholz, I., Heizmann, C. W., & Fritz, G. (2004). S100 proteins in mouse and man: From evolution to function and pathology (including an update of the nomenclature). *Biochemical and Biophysical Research Communications*. https://doi.org/10.1016/j.bbrc.2004.07.096

Marinissen, M. J., Chiariello, M., Pallante, M., & Gutkind, J. S. (1999). A Network of Mitogen-Activated Protein Kinases Links G Protein-Coupled Receptors to the c-jun Promoter: a Role for c-Jun NH2-Terminal Kinase, p38s, and Extracellular Signal-Regulated Kinase 5. *Molecular and Cellular Biology*. https://doi.org/10.1128/mcb.19.6.4289

Markiewicz-Potoczny, M., Lobanova, A., Loeb, A. M., Kirak, O., Olbrich, T., Ruiz, S., & Lazzerini Denchi, E. (2020). TRF2-mediated telomere protection is dispensable in pluripotent stem cells. *Nature*. https://doi.org/10.1038/s41586-020-2959-4

Masui, S., Ohtsuka, S., Yagi, R., Takahashi, K., Ko, M. S. H., & Niwa, H. (2008). Rex1/Zfp42 is dispensable for pluripotency in mouse ES cells. *BMC Developmental Biology*. https://doi.org/10.1186/1471-213X-8-45

Matsui, T. (2018). Editorial: Cell Adhesion and Migration in the Development of Multicellular Organisms . *Frontiers in Cell and Developmental Biology* . Retrieved from https://www.frontiersin.org/article/10.3389/fcell.2018.00142

Matthews, D. J., & Gerritsen, M. E. (2010). *Targeting Protein Kinases for Cancer Therapy*. *Targeting Protein Kinases for Cancer Therapy*. https://doi.org/10.1002/9780470555293

Mattila, P. K., & Lappalainen, P. (2008). Filopodia: Molecular architecture and cellular

functions. *Nature Reviews Molecular Cell Biology*. https://doi.org/10.1038/nrm2406

McCracken, S. R. C., Ramsay, A., Heer, R., Mathers, M. E., Jenkins, B. L., Edwards, J., … Leung, H. Y. (2008). Aberrant expression of extracellular signal-regulated kinase 5 in human prostate cancer. *Oncogene*. https://doi.org/10.1038/sj.onc.1210963

Miao, H., Gale, N. W., Guo, H., Qian, J., Petty, A., Kaspar, J., … Wang, B. (2015). EphA2 promotes infiltrative invasion of glioma stem cells in vivo through cross-talk with Akt and regulates stem cell properties. *Oncogene*, *34*(5), 558–567. https://doi.org/10.1038/onc.2013.590

Miyazono, K., Kamiya, Y., & Morikawa, M. (2010). Bone morphogenetic protein receptors and signal transduction. *Journal of Biochemistry*, *147*(1), 35–51. https://doi.org/10.1093/jb/mvp148

Mody, N., Campbell, D. G., Morrice, N., Peggie, M., & Cohen, P. (2003). An analysis of the phosphorylation and activation of extracellular-signal-regulated protein kinase 5 (ERK5) by mitogen-activated protein kinase kinase 5 (MKK5) in vitro. *Biochemical Journal*. https://doi.org/10.1042/BJ20030193

MODY, N., CAMPBELL, D. G., MORRICE, N., PEGGIE, M., & COHEN, P. (2003). An analysis of the phosphorylation and activation of extracellular-signal-regulated protein kinase 5 (ERK5) by mitogen-activated protein kinase kinase 5 (MKK5) in vitro. *Biochemical Journal*, *372*(2), 567–575. https://doi.org/10.1042/bj20030193

Montero, J. C., Ocaña, A., Abad, M., Ortiz-Ruiz, M. J., Pandiella, A., & Esparís-Ogando, A. (2009). Expression of Erk5 in early stage breast cancer and association with disease free survival identifies this kinase as potential therapeutic target. *PLoS ONE*. https://doi.org/10.1371/journal.pone.0005565

Morel, E., & Gruenberg, J. (2007). The p11/S100A10 light chain of annexin A2 is dispensable for annexin A2 association to endosomes and functions in endosomal transport. *PLoS ONE*, *2*(10). https://doi.org/10.1371/journal.pone.0001118

Morikawa, M., Koinuma, D., Mizutani, A., Kawasaki, N., Holmborn, K., Sundqvist, A., … Miyazono, K. (2016). BMP Sustains Embryonic Stem Cell Self-Renewal through Distinct Functions of Different Krüppel-like Factors. *Stem Cell Reports*. https://doi.org/10.1016/j.stemcr.2015.12.004

Morimoto, H., Kondoh, K., Nishimoto, S., Terasawa, K., & Nishida, E. (2007). Activation of a C-terminal transcriptional activation domain of ERK5 by autophosphorylation. *Journal of Biological Chemistry*. https://doi.org/10.1074/jbc.M704079200

Murakami, M., Ichisaka, T., Maeda, M., Oshiro, N., Hara, K., Edenhofer, F., … Yamanaka, S. (2004). mTOR Is Essential for Growth and Proliferation in Early Mouse Embryos and Embryonic Stem Cells. *Molecular and Cellular Biology*. https://doi.org/10.1128/mcb.24.15.6710-6718.2004

Nakai-Futatsugi, Y., & Niwa, H. (2016). Zscan4 Is Activated after Telomere Shortening in Mouse Embryonic Stem Cells. *Stem Cell Reports*, *6*(4), 483–495. https://doi.org/10.1016/j.stemcr.2016.02.010

Nakamura, K., & Johnson, G. L. (2003). PB1 domains of MEKK2 and MEKK3 interact with the

MEK5 PB1 domain for activation of the ERK5 pathway. *Journal of Biological Chemistry*. https://doi.org/10.1074/jbc.C300313200

Nakamura, K., & Johnson, G. L. (2007). Noncanonical Function of MEKK2 and MEK5 PB1 Domains for Coordinated Extracellular Signal-Regulated Kinase 5 and c-Jun N-Terminal Kinase Signaling. *Molecular and Cellular Biology*. https://doi.org/10.1128/mcb.00125-07

Naya, F. J., Black, B. L., Wu, H., Bassel-Duby, R., Richardson, J. A., Hill, J. A., & Olson, E. N. (2002). Mitochondrial deficiency and cardiac sudden death in mice lacking the MEF2A transcription factor. *Nature Medicine*. https://doi.org/10.1038/nm789

Newbern, J., Zhong, J., Wickramasinghe, S. R., Li, X., Wu, Y., Samuels, I., … Landreth, G. E. (2008). Mouse and human phenotypes indicate a critical conserved role for ERK2 signaling in neural crest development. *Proceedings of the National Academy of Sciences of the United States of America*. https://doi.org/10.1073/pnas.0805239105

Nichols, J., & Smith, A. (2009). Naive and Primed Pluripotent States. *Cell Stem Cell*. https://doi.org/10.1016/j.stem.2009.05.015

Nichols, J., Zevnik, B., Anastassiadis, K., Niwa, H., Klewe-Nebenius, D., Chambers, I., … Smith, A. (1998). Formation of pluripotent stem cells in the mammalian embryo depends on the POU transcription factor Oct4. *Cell*. https://doi.org/10.1016/S0092-8674(00)81769-9

Niwa, H., Burdon, T., Chambers, I., & Smith, A. (1998). Self-renewal of pluripotent embryonic stem cells is mediated via activation of STAT3. *Genes and Development*. https://doi.org/10.1101/gad.12.13.2048

Nori, S., Okada, Y., Yasuda, A., Tsuji, O., Takahashi, Y., Kobayashi, Y., … Okano, H. (2011). Grafted human-induced pluripotent stem-cell-derived neurospheres promote motor functional recovery after spinal cord injury in mice. *Proceedings of the National Academy of Sciences of the United States of America*. https://doi.org/10.1073/pnas.1108077108

Ohnesorge, N., Viemann, D., Schmidt, N., Czymai, T., Spiering, D., Schmolke, M., … Schmidt, M. (2010). Erk5 activation elicits a vasoprotective endothelial phenotype via induction of Krüppel-like factor 4 (KLF4). *Journal of Biological Chemistry*. https://doi.org/10.1074/jbc.M110.103127

Onishi, K., & Zandstra, P. W. (2015). LIF signaling in stem cells and development. *Development (Cambridge)*. https://doi.org/10.1242/dev.117598

Ozaki, T., & Sakiyama, S. (1993). Molecular cloning of rat calpactin I heavy-chain cDNA whose expression is induced in v-src-transformed rat culture cell lines. *Oncogene*. https://doi.org/10.1016/0928-4680(94)90377-8

PANSKY, B. (1982). *Review of MEDICAL EMBRYOLOGY*. *McGraw-Hill,*.

Papaioannou, V. E., Mcburney, M. W., Gardner, R. L., & Evans, M. J. (1975). Fate of teratocarcinoma cells injected into early mouse embryos. *Nature*. https://doi.org/10.1038/258070a0

Pavan, S., Meyer-Schaller, N., Diepenbruck, M., Kalathur, R. K. R., Saxena, M., & Christofori, G. (2018). A kinome-wide high-content siRNA screen identifies MEK5–ERK5 signaling as critical for breast cancer cell EMT and metastasis. *Oncogene*.

https://doi.org/10.1038/s41388-018-0270-8

Pearson, A. J., Fullwood, P., Tapia, G. T., Prise, I., Smith, M. P., Xu, Q., … Tournier, C. (2020). Discovery of a gatekeeper residue in the C-terminal tail of the extracellular signal-regulated protein kinase 5 (ERK5). *International Journal of Molecular Sciences*. https://doi.org/10.3390/ijms21030929

Peng, X. ding, Xu, P. Z., Chen, M. L., Hahn-Windgassen, A., Skeen, J., Jacobs, J., … Hay, N. (2003). Dwarfism, impaired skin development, skeletal muscle atrophy, delayed bone development, and impeded adipogenesis in mice lacking Akt1 and Akt2. *Genes and Development*. https://doi.org/10.1101/gad.1089403

Pereira, D. M., Gomes, S. E., Borralho, P. M., & Rodrigues, C. M. P. (2019). MEK5/ERK5 activation regulates colon cancer stem-like cell properties. *Cell Death Discovery*. https://doi.org/10.1038/s41420-019-0150-1

Pfaffl, M. W. (2001). A new mathematical model for relative quantification in real-time RT-PCR. *Nucleic Acids Research*. https://doi.org/10.1093/nar/29.9.e45

Pontis, J., Planet, E., Offner, S., Turelli, P., Duc, J., Coudray, A., … Trono, D. (2019). Hominoid-Specific Transposable Elements and KZFPs Facilitate Human Embryonic Genome Activation and Control Transcription in Naive Human ESCs. *Cell Stem Cell*. https://doi.org/10.1016/j.stem.2019.03.012

Prieto-Vila, M., Takahashi, R. U., Usuba, W., Kohama, I., & Ochiya, T. (2017). Drug resistance driven by cancer stem cells and their niche. *International Journal of Molecular Sciences*. https://doi.org/10.3390/ijms18122574

Qi, M., & Elion, E. A. (2005). Formin-induced actin cables are required for polarized recruitment of the Ste5 scaffold and high level activation of MAPK Fus3. *Journal of Cell Science*. https://doi.org/10.1242/jcs.02418

Qualmann, B., & Kelly, R. B. (2000). Syndapin isoforms participate in receptor-mediated endocytosis and actin organization. *Journal of Cell Biology*. https://doi.org/10.1083/jcb.148.5.1047

Rajinder, S. S., Wensheng, L., & Michael, G. B. (2009). A novel role of ERK5 in integrin-mediated cell adhesion and motility in cancer cells via Fak signaling. *Journal of Cellular Physiology*.

Ramsay, A. K., McCracken, S. R. C., Soofi, M., Fleming, J., Yu, A. X., Ahmad, I., … Leung, H. Y. (2011). ERK5 signalling in prostate cancer promotes an invasive phenotype. *British Journal of Cancer*. https://doi.org/10.1038/sj.bjc.6606062

Razumovskaya, E., Sun, J., & Rönnstrand, L. (2011). Inhibition of MEK5 by BIX02188 induces apoptosis in cells expressing the oncogenic mutant FLT3-ITD. *Biochemical and Biophysical Research Communications*. https://doi.org/10.1016/j.bbrc.2011.07.089

Redmer, T., Diecke, S., Grigoryan, T., Quiroga-Negreira, A., Birchmeier, W., & Besser, D. (2011). E-cadherin is crucial for embryonic stem cell pluripotency and can replace OCT4 during somatic cell reprogramming. *EMBO Reports*. https://doi.org/10.1038/embor.2011.88

Regan, C. P., Li, W., Boucher, D. M., Spatz, S., Su, M. S., & Kuida, K. (2002). Erk5 null mice display multiple extraembryonic vascular and embryonic cardiovascular defects.

Proceedings of the National Academy of Sciences of the United States of America. https://doi.org/10.1073/pnas.142293999

Réty, S., Sopkova, J., Renouard, M., Osterloh, D., Gerke, V., Tabaries, S., … Lewit-Bentley, A. (1999). The crystal structure of a complex of p11 with the annexin II N-terminal peptide. *Nature Structural Biology*. https://doi.org/10.1038/4965

Rintala-Dempsey, A. C., Rezvanpour, A., & Shaw, G. S. (2008). S100-annexin complexes - Structural insights. *FEBS Journal*. https://doi.org/10.1111/j.1742-4658.2008.06654.x

Roberts, O. L., Holmes, K., Müller, J., Cross, D. A. E., & Cross, M. J. (2010). ERK5 is required for VEGF-mediated survival and tubular morphogenesis of primary human microvascular endothelial cells. *Journal of Cell Science*. https://doi.org/10.1242/jcs.072801

Roberts, O. L., Holmes, K., Müller, J., Cross, D. a E., & Cross, M. J. (2009). ERK5 and the regulation of endothelial cell function. *Biochemical Society Transactions*. https://doi.org/10.1042/BST0371254

Rodda, D. J., Chew, J. L., Lim, L. H., Loh, Y. H., Wang, B., Ng, H. H., & Robson, P. (2005). Transcriptional regulation of Nanog by OCT4 and SOX2. *Journal of Biological Chemistry*. https://doi.org/10.1074/jbc.M502573200

Rossant, J., & Lis, W. T. (1979). Potential of isolated mouse inner cell masses to form trophectoderm derivatives in vivo. *Developmental Biology*. https://doi.org/10.1016/0012-1606(79)90022-8

Ruis, P., Van Ly, D., Borel, V., Kafer, G. R., McCarthy, A., Howell, S., … Boulton, S. J. (2020). TRF2-independent chromosome end protection during pluripotency. *Nature*. https://doi.org/10.1038/s41586-020-2960-y

Ruzinova, M. B., & Benezra, R. (2003). Id proteins in development, cell cycle and cancer. *Trends in Cell Biology*. https://doi.org/10.1016/S0962-8924(03)00147-8

Samavarchi-Tehrani, P., Golipour, A., David, L., Sung, H. K., Beyer, T. A., Datti, A., … Wrana, J. L. (2010). Functional genomics reveals a BMP-Driven mesenchymal-to-Epithelial transition in the initiation of somatic cell reprogramming. *Cell Stem Cell*. https://doi.org/10.1016/j.stem.2010.04.015

Samuels, I. S., Karlo, J. C., Faruzzi, A. N., Pickering, K., Herrup, K., Sweatt, J. D., … Landreth, G. E. (2008). Deletion of ERK2 mitogen-activated protein kinase identifies its key roles in cortical neurogenesis and cognitive function. *Journal of Neuroscience*. https://doi.org/10.1523/JNEUROSCI.0679-08.2008

Sarbassov, D. D., Guertin, D. A., Ali, S. M., & Sabatini, D. M. (2005). Phosphorylation and regulation of Akt/PKB by the rictor-mTOR complex. *Science*. https://doi.org/10.1126/science.1106148

Schramp, M., Ying, O., Tai, Y. K., & Martin, G. S. (2008). ERK5 promotes Src-induced podosome formation by limiting Rho activation. *Journal of Cell Biology*. https://doi.org/10.1083/jcb.200801078

Scotland, K. B., Chen, S., Sylvester, R., & Gudas, L. J. (2008). Analysis of Rex1 (Zfp42) function in embryonic stem cell differentiation. *Developmental Dynamics*.

https://doi.org/10.1002/dvdy.22037

Sehgal, S. N. (1998). Rapamune® (RAPA, rapamycin, sirolimus): Mechanism of action immunosuppressive effect results from blockade of signal transduction and inhibition of cell cycle progression. In *Clinical Biochemistry*. https://doi.org/10.1016/S0009-9120(98)00045-9

Serhal, L., & Edwards, C. J. (2019). Upadacitinib for the treatment of rheumatoid arthritis. *Expert Review of Clinical Immunology*. https://doi.org/10.1080/1744666X.2019.1544892

Shi, Y., & Massagué, J. (2003). Mechanisms of TGF-β signaling from cell membrane to the nucleus. *Cell*. https://doi.org/10.1016/S0092-8674(03)00432-X

Smith, A. (2006). A glossary for stem-cell biology. *Nature*. https://doi.org/10.1038/nature04954

Smith, A. (2017). Formative pluripotency: The executive phase in a developmental continuum. *Development (Cambridge)*. https://doi.org/10.1242/dev.142679

Sohn, S. J., Li, D., Lee, L. K., & Winoto, A. (2005). Transcriptional Regulation of Tissue-Specific Genes by the ERK5 Mitogen-Activated Protein Kinase. *Molecular and Cellular Biology*. https://doi.org/10.1128/mcb.25.19.8553-8566.2005

Sohn, S. J., Sarvis, B. K., Cado, D., & Winoto, A. (2002). ERK5 MAPK regulates embryonic angiogenesis and acts as a hypoxia-sensitive repressor of vascular endothelial growth factor expression. *Journal of Biological Chemistry*, *277*(45), 43344–43351. https://doi.org/10.1074/jbc.M207573200

Sokol, S. Y. (2011). Maintaining embryonic stem cell pluripotency with Wnt signaling. *Development*. https://doi.org/10.1242/dev.066209

Speakman, C. M., Domke, T. C. E., Wongpaiboonwattana, W., Sanders, K., Mudaliar, M., Van Aalten, D. M. F., … Stavridis, M. P. (2014). Elevated O-GlcNAc levels activate epigenetically repressed genes and delay mouse ESC differentiation without affecting naïve to primed cell transition. *Stem Cells*. https://doi.org/10.1002/stem.1761

Stahl, N, Farruggella, T. J., Boulton, T. G., Zhong, Z., Darnell, J. E. J., & Yancopoulos, G. D. (1995). Choice of STATs and other substrates specified by modular tyrosine-based motifs in cytokine receptors. *Science (New York, N.Y.)*, *267*(5202), 1349–1353. https://doi.org/10.1126/science.7871433

Stahl, Neil, Boulton, T. G., Farruggella, T., Ip, N. Y., Davis, S., Witthuhn, B. A., … Yancopoulos, G. D. (1994). Association and activation of Jak-Tyk kinases by CNTF-LIF-OSM-IL-6 β receptor components. *Science*. https://doi.org/10.1126/science.8272873

Stevens, L. C., & Little, C. C. (1954). Spontaneous Testicular Teratomas in an Inbred Strain of Mice. In *Proc. Natl. Acad. Sci. USA* (pp. 1080–1087). https://doi.org/10.1073/pnas.40.11.1080

Storm, M. P., Kumpfmueller, B., Bone, H. K., Buchholz, M., Sanchez Ripoll, Y., Chaudhuri, J. B., … Welham, M. J. (2014). Zscan4 is regulated by PI3-kinase and DNA-damaging agents and directly interacts with the transcriptional repressors LSD1 and CtBP2 in mouse embryonic stem cells. *PLoS ONE*, *9*(3). https://doi.org/10.1371/journal.pone.0089821

Storm, M. P., Kumpfmueller, B., Thompson, B., Kolde, R., Vilo, J., Hummel, O., … Welham, M. J. (2009). Characterization of the phosphoinositide 3-kinase-dependent transcriptome in murine embryonic stem cells: Identification of novel regulators of pluripotency. *Stem Cells*, *27*(4), 764–775. https://doi.org/10.1002/stem.3

Stradal, T., Courtney, K. D., Rottner, K., Hahne, P., Small, J. V., & Pendergast, A. M. (2001). The Abl interactor proteins localize to sites of actin polymerization at the tips of lamellipodia and filopodia. *Current Biology*. https://doi.org/10.1016/S0960-9822(01)00239-1

Sun, W., Kesavan, K., Schaefer, B. C., Garrington, T. P., Ware, M., Johnson, N. L., … Johnson, G. L. (2001). MEKK2 Associates with the Adapter Protein Lad/RIBP and Regulates the MEK5-BMK1/ERK5 Pathway. *Journal of Biological Chemistry*. https://doi.org/10.1074/jbc.M003719200

Sunadome, K., Yamamoto, T., Ebisuya, M., Kondoh, K., Sehara-Fujisawa, A., & Nishida, E. (2011a). ERK5 Regulates Muscle Cell Fusion through Klf Transcription Factors. *Developmental Cell*. https://doi.org/10.1016/j.devcel.2010.12.005

Sutherland, E. W., & Wosilait, W. D. (1955). Inactivation and activation of liver phosphorylase [8]. *Nature*. https://doi.org/10.1038/175169a0

Suzuki, N., Yamazaki, S., Yamaguchi, T., Okabe, M., Masaki, H., Takaki, S., … Nakauchi, H. (2013). Generation of engraftable hematopoietic stem cells from induced pluripotent stem cells by way of teratoma formation. *Molecular Therapy*. https://doi.org/10.1038/mt.2013.71

Takahashi, K., & Yamanaka, S. (2006). Induction of Pluripotent Stem Cells from Mouse Embryonic and Adult Fibroblast Cultures by Defined Factors. *Cell*. https://doi.org/10.1016/j.cell.2006.07.024

Tan, Q., Lui, P. P. Y., Rui, Y. F., & Wong, Y. M. (2012). Comparison of potentials of stem cells isolated from tendon and bone marrow for musculoskeletal tissue engineering. *Tissue Engineering - Part A*. https://doi.org/10.1089/ten.tea.2011.0362

Terasawa, K., Okazaki, K., & Nishida, E. (2003). Regulation of c-Fos and Fra-1 by the MEK5-ERK5 pathway. *Genes to Cells*, *8*(3), 263–273. https://doi.org/10.1046/j.1365-2443.2003.00631.x

Tesar, P. J., Chenoweth, J. G., Brook, F. A., Davies, T. J., Evans, E. P., Mack, D. L., … McKay, R. D. G. (2007). New cell lines from mouse epiblast share defining features with human embryonic stem cells. *Nature*. https://doi.org/10.1038/nature05972

Thomson, J. a, Itskovitz-Eldor, J., Shapiro, S. S., Waknitz, M. a, Swiergiel, J. J., Marshall, V. S., & Jones, J. M. (1998). Embryonic stem cell lines derived from human blastocysts [see comments] [published erratum appears in Science 1998 Dec 4;282(5395):1827]. *Science*. https://doi.org/10.1126/science.282.5391.1145

Tomlinson, F. H., Houser, O. W., Scheithauer, B. W., Sundt, T. M., Okazaki, H., & Parisi, J. E. (1994). Angiographically occult vascular malformations: A correlative study of features on magnetic resonance imaging and histological examination. *Neurosurgery*. https://doi.org/10.1227/00006123-199405000-00002

Tusa, I., Gagliardi, S., Tubita, A., Pandolfi, S., Urso, C., Borgognoni, L., … Rovida, E. (2018). ERK5

is activated by oncogenic BRAF and promotes melanoma growth. *Oncogene*. https://doi.org/10.1038/s41388-018-0164-9

Ucar, D., Matossian, M., Hoang-Barnes, V., Hossain, F., Gupta, M., Burks, H., … Miele, L. (2019). Abstract P2-03-04: A novel druggable target upstream of Notch: MEK5/ERK5 signaling regulates Jagged-1 and Notch1 expression in triple negative breast cancer stem cells. https://doi.org/10.1158/1538-7445.sabcs18-p2-03-04

Ulloa, L., & Tabibzadeh, S. (2001). Lefty Inhibits Receptor-regulated Smad Phosphorylation Induced by the Activated Transforming Growth Factor-β Receptor. *Journal of Biological Chemistry*, *276*(24), 21397–21404. https://doi.org/10.1074/jbc.M010783200

Urbach, A. (2004). Modeling for Lesch-Nyhan Disease by Gene Targeting in Human Embryonic Stem Cells. *Stem Cells*. https://doi.org/10.1634/stemcells.22-4-635

Urbach, Achia, & Benvenisty, N. (2009). Studying early lethality of 45,XO (Turner's syndrome) embryos using human embryonic stem cells. *PLoS ONE*. https://doi.org/10.1371/journal.pone.0004175

Verstreken, C. M., Labouesse, C., Agley, C. C., & Chalut, K. J. (2019). Embryonic stem cells become mechanoresponsive upon exit from ground state of pluripotency. *Open Biology*. https://doi.org/10.1098/rsob.180203

Wang, J., Erazo, T., Ferguson, F. M., Buckley, D. L., Gomez, N., Muñoz-Guardiola, P., … Gray, N. S. (2018). Structural and Atropisomeric Factors Governing the Selectivity of Pyrimido-benzodiazipinones as Inhibitors of Kinases and Bromodomains. *ACS Chemical Biology*. https://doi.org/10.1021/acschembio.7b00638

Wang, R., Wang, Y., Liu, N., Ren, C., Jiang, C., Zhang, K., … Wang, P. (2013). FBW7 regulates endothelial functions by targeting KLF2 for ubiquitination and degradation. *Cell Research*, *23*(6), 803–819. https://doi.org/10.1038/cr.2013.42

Welcker, M., & Clurman, B. E. (2008). FBW7 ubiquitin ligase: A tumour suppressor at the crossroads of cell division, growth and differentiation. *Nature Reviews Cancer*. https://doi.org/10.1038/nrc2290

Westmoreland, J. J., Takahashi, S., & Wright, C. V. E. (2007). Xenopus lefty requires proprotein cleavage but not N-linked glycosylation to inhibit nodal signaling. *Developmental Dynamics*. https://doi.org/10.1002/dvdy.21210

Widmann, C., Gibson, S., Jarpe, M. B., & Johnson, G. L. (1999). Mitogen-Activated Protein Kinase: Conservation of a Three-Kinase Module From Yeast to Human. *Physiol Rev*, *79*(1), 143–180. https://doi.org/10.1074/jbc.271.28.16586

Williams, C. A. C., Fernandez-Alonso, R., Wang, J., Toth, R., Gray, N. S., & Findlay, G. M. (2016). Erk5 Is a Key Regulator of Naive-Primed Transition and Embryonic Stem Cell Identity. *Cell Reports*. https://doi.org/10.1016/j.celrep.2016.07.033

Wiśniewski, J. R., Hein, M. Y., Cox, J., & Mann, M. (2014). A "proteomic ruler" for protein copy number and concentration estimation without spike-in standards. *Molecular & Cellular Proteomics : MCP*, *13*(12), 3497–3506. https://doi.org/10.1074/mcp.M113.037309

Wolanin, P. M., Thomason, P. A., & Stock, J. B. (2002). Histidine protein kinases: Key signal

transducers outside the animal kingdom. *Genome Biology*. https://doi.org/10.1186/gb-2002-3-10-reviews3013

Wrana, J. L., Attisano, L., Cárcamo, J., Zentella, A., Doody, J., Laiho, M., … Massague, J. (1992). TGFβ signals through a heteromeric protein kinase receptor complex. *Cell*. https://doi.org/10.1016/0092-8674(92)90395-S

Wrana, J. L., Attisano, L., Wieser, R., Ventura, F., & Massagué, J. (1994). Mechanism of activation of the TGF-β receptor. *Nature*. https://doi.org/10.1038/370341a0

Yamanaka, Y., Ralston, A., Stephenson, R. O., & Rossant, J. (2006). Cell and molecular regulation of the mouse blastocyst. *Developmental Dynamics*, *235*(9), 2301–2314. https://doi.org/https://doi.org/10.1002/dvdy.20844

Yan, C., Luo, H., Lee, J. D., Abe, J. ichi, & Berk, B. C. (2001a). Molecular Cloning of Mouse ERK5/BMK1 Splice Variants and Characterization of ERK5 Functional Domains. *Journal of Biological Chemistry*, *276*(14), 10870–10878. https://doi.org/10.1074/jbc.M009286200

Yan, C., Luo, H., Lee, J. D., Abe, J. ichi, & Berk, B. C. (2001b). Molecular Cloning of Mouse ERK5/BMK1 Splice Variants and Characterization of ERK5 Functional Domains. *Journal of Biological Chemistry*. https://doi.org/10.1074/jbc.M009286200

Yang, C. C., Ornatsky, O. I., McDermott, J. C., Cruz, T. F., & Prody, C. A. (1998). Interaction of myocyte enhancer factor 2 (MEF2) with a mitogen-activated protein kinase, ERK5/BMK1. *Nucleic Acids Research*, *26*(20), 4771–4777. https://doi.org/10.1093/nar/26.20.4771

Yang, J., Boerm, M., McCarty, M., Bucana, C., Fidler, I. J., Zhuang, Y., & Su, B. (2000). Mekk3 is essential for early embryonic cardiovascular development. *Nature Genetics*. https://doi.org/10.1038/73550

Yang, S. H., Sharrocks, A. D., & Whitmarsh, A. J. (2003). Transcriptional regulation by the MAP kinase signaling cascades. *Gene*. https://doi.org/10.1016/S0378-1119(03)00816-3

Yeo, J. C., Jiang, J., Tan, Z. Y., Yim, G. R., Ng, J. H., Göke, J., … Ng, H. H. (2014). Klf2 is an essential factor that sustains ground state pluripotency. *Cell Stem Cell*, *14*(6), 864–872. https://doi.org/10.1016/j.stem.2014.04.015

Ying, Q. L., Nichols, J., Chambers, I., & Smith, A. (2003). BMP induction of Id proteins suppresses differentiation and sustains embryonic stem cell self-renewal in collaboration with STAT3. *Cell*. https://doi.org/10.1016/S0092-8674(03)00847-X

Ying, Q. L., Wray, J., Nichols, J., Batlle-Morera, L., Doble, B., Woodgett, J., … Smith, A. (2008). The ground state of embryonic stem cell self-renewal. *Nature*. https://doi.org/10.1038/nature06968

Yokota, Y. (2001). Id and development. *Oncogene*. https://doi.org/10.1038/sj/onc/1205090

Yost, C., Torres, M., Miller, J. R., Huang, E., Kimelman, D., & Moon, R. T. (1996). The axis-inducing activity, stability, and subcellular distribution of β-catenin is regulated in Xenopus embryos by glycogen synthase kinase 3. *Genes and Development*. https://doi.org/10.1101/gad.10.12.1443

Younai, S., Nichter, L. S., Wellisz, T., Reinisch, J., Nimni, M. E., Tuan -, T. L., & Tredget, E. E.

(1994). Modulation of collagen synthesis by transforming growth factor-β in keloid and hypertrophic scar fibroblasts. *Annals of Plastic Surgery*. https://doi.org/10.1097/00000637-199408000-00005

Yu, J., Vodyanik, M. A., Smuga-Otto, K., Antosiewicz-Bourget, J., Frane, J. L., Tian, S., … Thomson, J. A. (2007). Induced pluripotent stem cell lines derived from human somatic cells. *Science*. https://doi.org/10.1126/science.1151526

Zalzman, M., Falco, G., Sharova, L. V., Nishiyama, A., Thomas, M., Lee, S. L., … Ko, M. S. H. (2010). Zscan4 regulates telomere elongation and genomic stability in ES cells. *Nature*, *464*(7290), 858–863. https://doi.org/10.1038/nature08882

Zhang, J., Zhang, F., Ebert, D., Cobb, M. H., & Goldsmith, E. J. (1995). Activity of the MAP kinase ERK2 is controlled by a flexible surface loop. *Structure*. https://doi.org/10.1016/S0969-2126(01)00160-5

Zhang, X., Zhang, J., Wang, T., Esteban, M. A., & Pei, D. (2008). Esrrb activates Oct4 transcription and sustains self-renewal and pluripotency in embryonic stem cells. *Journal of Biological Chemistry*. https://doi.org/10.1074/jbc.M803481200

Zhao, S. H., Huang, L. N., Wu, J. H., Zhang, Y., Pan, D. Y., & Liu, X. (2009). Vascular endothelial growth factor upregulates expression of annexin A2 in vitro and in a mouse model of ischemic retinopathy. *Molecular Vision*.

Zhou, G., Bao, Z. Q., & Dixon, J. E. (1995). Components of a new human protein kinase signal transduction pathway. *The Journal of Biological Chemistry*, *270*(21), 12665–12669. https://doi.org/10.1074/jbc.270.21.12665

Zhou, H., Li, W., Zhu, S., Joo, J. Y., Do, J. T., Xiong, W., … Ding, S. (2010). Conversion of mouse epiblast stem cells to an earlier pluripotency state by small molecules. *The Journal of Biological Chemistry*, *285*(39), 29676–29680. https://doi.org/10.1074/jbc.C110.150599

Zhou, Z., Rawnsley, D. R., Goddard, L. M., Pan, W., Cao, X. J., Jakus, Z., … Kahn, M. L. (2015). The Cerebral Cavernous Malformation Pathway Controls Cardiac Development via Regulation of Endocardial MEKK3 Signaling and KLF Expression. *Developmental Cell*. https://doi.org/10.1016/j.devcel.2014.12.009

Zobiack, N., Rescher, U., Ludwig, C., Zeuschner, D., & Gerke, V. (2003). The annexin 2/S100A10 complex controls the distribution of transferrin receptor-containing recycling endosomes. *Molecular Biology of the Cell*, *14*(12), 4896–4908. https://doi.org/10.1091/mbc.E03-06-0387

Appendix A – Generation of CRISPR/Cas9 Knockout Cell Lines

The Clustered Regularly Interspaced Short Palindromic Repeat (CRISPR)/Cas9 system was used for genome editing by Charles Williams to generate *Erk5*$^{-/-}$ and *Klf2*$^{\Delta/\Delta}$ mESCs. Paired guide RNAs were expressed from two plasmids; the sense plasmid (in pX335 vector) contains a puromycin resistance cassette and the antisense plasmid (in pKN7 vector) also expresses Cas9 D10A nuclease. The guide RNA pairs used to generate the CRISPR lines used in this thesis are found in Table A.1 (Williams et al., 2016).

Table A.1: CRISPR/Cas9 Constructs.

TARGET	CRISPR PROJECT NO.	TARGET EXON	DU NUMBER	SENSE/ ANTI-SENSE	SEQUENCE
ERK5	CR80	Ex3	DU48907	Antisense	GTCACCACA TCAAAAGCA TTAGG
			DU48901	Sense	GCAATGCCA AACGGACCC TCAGGG
KLF2	CR517	Ex2	DU57062	Antisense	GCCCGCCTC GGGTTCATTT CG
			DU57060	Sense	GTGAGGACC TAAACAACG TGT

Multiple clones from each CRISPR/Cas9 edit were clonally expanded and propagated. These were selected based on validation of gene deletion by sequencing and immunoblot analysis, as well as mESC morphology phenotype in the case of *Erk5*$^{-/-}$ mESCs. Unless otherwise stated, the clone lines presented in this thesis were K2 (*Klf2*$^{\Delta/\Delta}$) and UD3 (*Erk5*$^{-/-}$).

Appendix B – Optimisation of qPCR approaches

To ensure that the qPCR approaches captured relevant changes in gene expression for *Zscan4*, *Anxa2*, and *S100a10* mRNA, I performed time courses for this assay. This showed that although 24hrs post transfection was optimal for observing changed in *Klf2* mRNA, 48hrs was more optimal for *Zscan4*, *Anxa2* and *S100a10* mRNA in both wildtype mESCs (Figure B1) and *Erk5*$^{-/-}$ mESCs (Figure B2). This could suggest a hierarchical system of gene regulation where *Klf2* is induced first, followed by a second wave of transcriptional induction for other ERK5 target genes.

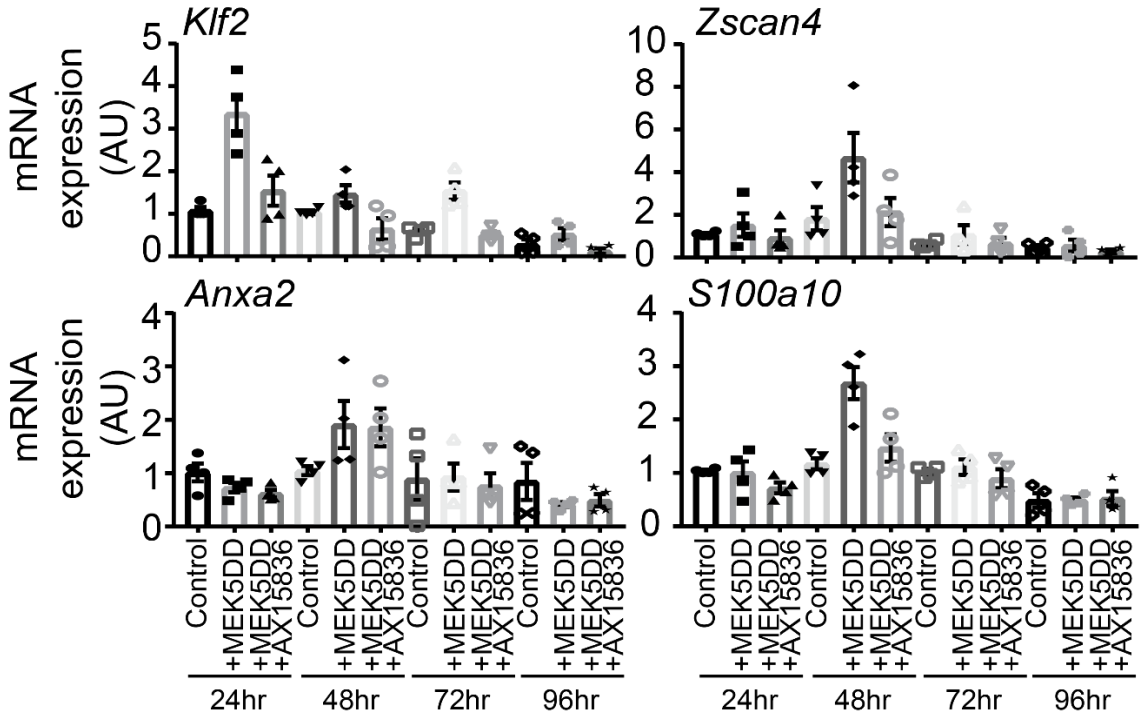

Figure B.1:Optimisation of qPCR approach in wildtype mESCs. *Wildtype mESCs were transfected with either empty vector or MEK5DD, and AX15836 (10 μM, 24 hr) was used to inhibit the ERK5 pathway. mESCs were lysed at indicated time post transfection, with 24hr puromycin selection prior to lysis. Error bars indicate SEM (n=4).*

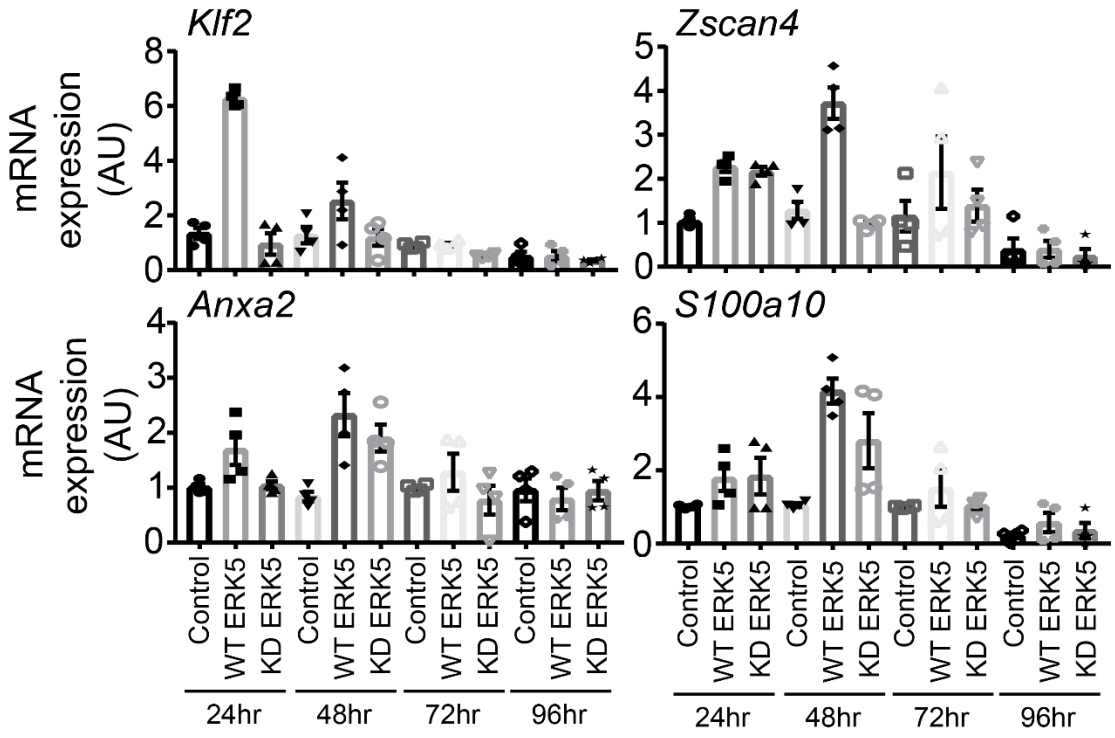

Figure B.2: Optimisation of qPCR approach in Erk5$^{-/-}$ mESCs. *Erk5$^{-/-}$ mESCs were transfected with MEK5DD and either empty vector, wildtype ERK5 or kinase dead (D200A) ERK5. mESCs were lysed at indicated time post transfection, with 24hr puromycin selection prior to lysis. Error bars indicate SEM (n=4).*